

Final Report

Technical and Financial

Hypoxia, Monitoring, and Mitigation System

Contract Number: N00014-13-C-0323

Prepared for

Office of Naval Research (ONR) Code 342

For the Period

July 24, 2013 to May 31, 2014

Submitted By

S. J. Mahoney, Principle Investigator

Athena GTX, Inc.

Des Moines, IA

Document Title: HAMS Final Report (Technical and Financial)

REPORT DOCUMENTATION PAGE				Form Approved OMB No. 0704-0188	
<p>The public reporting burden for this collection of information is estimated to average 1 hour per response, including the time for reviewing instructions, searching existing data sources, gathering and maintaining the data needed, and completing and reviewing the collection of information. Send comments regarding this burden estimate or any other aspect of this collection of information, including suggestions for reducing the burden, to Department of Defense, Washington Headquarters Services, Directorate for Information Operations and Reports (0704-0188), 1215 Jefferson Davis Highway, Suite 1204, Arlington, VA 22202-4302. Respondents should be aware that notwithstanding any other provision of law, no person shall be subject to any penalty for failing to comply with a collection of information if it does not display a currently valid OMB control number. PLEASE DO NOT RETURN YOUR FORM TO THE ABOVE ADDRESS.</p>					
1. REPORT DATE (DD-MM-YYYY) 05/30/2014		2. REPORT TYPE Final Report		3. DATES COVERED (From - To) 24 Jul 2013 to 31 May 2014	
4. TITLE AND SUBTITLE Final Report Technical and Financial Hypoxia, Monitoring, and Mitigation System			5a. CONTRACT NUMBER N00014-13-C-0323		
			5b. GRANT NUMBER NA		
			5c. PROGRAM ELEMENT NUMBER NA		
6. AUTHOR(S) Mahoney, Sean, J			5d. PROJECT NUMBER NA		
			5e. TASK NUMBER NA		
			5f. WORK UNIT NUMBER NA		
7. PERFORMING ORGANIZATION NAME(S) AND ADDRESS(ES) Athena GTX, Inc. 2200 Gannett Avenue Des Moines, IA 50321			8. PERFORMING ORGANIZATION REPORT NUMBER CDRL A002		
9. SPONSORING/MONITORING AGENCY NAME(S) AND ADDRESS(ES) Steele, Christopher Office of Naval Research (ONR) Code 342			10. SPONSOR/MONITOR'S ACRONYM(S) ONR		
			11. SPONSOR/MONITOR'S REPORT NUMBER(S) NA		
12. DISTRIBUTION/AVAILABILITY STATEMENT Approved for public release, distribution unlimited					
13. SUPPLEMENTARY NOTES None					
14. ABSTRACT The HAMS baseline program has been completed on time, within budget . The baseline parametric algorithm to predict % O2 saturation and aircrew state and the modification of the USN Consciousness Model to predict LOC due to altitude induced hypoxia remain as viable approaches moving into the next phase of development.					
15. SUBJECT TERMS Hypoxia, Cognitive State, Oxygen Saturation, Altitude, Software Algorithms, Models					
16. SECURITY CLASSIFICATION OF:			17. LIMITATION OF ABSTRACT	18. NUMBER OF PAGES	19a. NAME OF RESPONSIBLE PERSON
a. REPORT	b. ABSTRACT	c. THIS PAGE			Mahoney, Sean, J
U	U	U	UU		19b. TELEPHONE NUMBER (Include area code) 515-288-3360 x103

Table of Contents

1.0	Summary	7
2.0	Introduction	8
3.0	Methods, Assumptions, and Procedures	9
3.1	Task 1 – Preliminary Research and Documentation	9
3.2	Task 2 – Develop Parametric Predictive Models.....	9
3.3	Task 3 – Algorithm Development and Refinement.....	10
3.4	Task 3a – Update the USN Consciousness Model Implementation.....	10
3.5	Task 3b – Determine Model Deficiencies for Hypoxia	10
3.6	Task 3c – Determine Model Deficiencies – Other.....	10
3.7	Task 4 – BETA Model Software Development/Definition	10
3.8	Task 5 – (Option) – Concept System Refinement	11
3.9	Task 6 – Documentation and Deliverables	11
4.0	Results and Discussion	11
4.1	Task 1 – Preliminary Research and Documentation	11
4.1.1	Significantly Relevant Literature Research Results	12
4.1.2	Correlations between ANS and Hypoxia	16
4.1.3	Relevant Aspects of USN Annotated Bibliography	19
4.1.4	Additional Relevant Literature Search Results.....	19
4.1.5	Data Provided by ONR.....	21
4.1.6	File Transfer Protocol Site	23
4.2	Task 2 – Develop Parametric Predictive Models.....	23
4.3	Task 3 – Algorithm Development and Refinement.....	28
4.3.1	Task 3a – Update the USN Consciousness Model Implementation.....	28
4.3.2	Task 3b – Determine Model Deficiencies for Hypoxia	37
4.3.3	Task 3c – Determine Model Deficiencies - Other	56
4.4	Task 4 – BETA Model Software Development/Definition	56
4.4.1	Parametric Model	57
4.4.2	Unconsciousness Model	67

4.5	Task 5 – (Option) – Concept System Refinement	73
4.6	Task 6 - Deliverables	73
5.0	Financial Results	73
5.1	FY2013 Funding (\$170K)	74
5.2	Benchmarks for FY2014 Funding (\$286K).....	74
6.0	Schedule and Deliverables	75
6.1	Schedule.....	75
6.2	Deliverables.....	75
6.2.1	Monthly Updates	75
6.2.2	Quarterly Reports	75
6.2.3	Final Report.....	75
6.2.4	BETA Software.....	75
6.2.5	Option – Trade-off Analysis and Preliminary Specification	76
7.0	Conclusion.....	76
8.0	Recommendations.....	77
9.0	References.....	77
10.0	Appendix.....	78
10.1	Task 1: Preliminary Research and Documentation.....	78
10.1.1	Additional Literature Search Results – Abstracts Only	78
10.1.2	Hams File Sharing Management System.....	89
10.2	Task 4: BETA Model.....	92
10.2.1	Subject Hypoxia Simulation Runs–Parametric Model	92
10.2.2	Subject Hypoxia Simulation Runs – Unconsciousness Model.....	98
10.3	Detailed Financial Spreadsheets (PDF)	121
11.0	List of Symbols, Abbreviations and Acronyms	122
12.0	Distribution List.....	123

Table of Figures

Figure 1 Oxygen Saturation for King-Devick Test Study.....	12
Figure 2 Human Performance Decrements by Oxygen Saturation and Altitude.....	13
Figure 3. Wolf, 2014 TUC Compilation and Depressurization profile to 35K feet.....	15
Figure 4 ROBD composite experimental data graphs.....	22
Figure 5. TAILSS Hypoxia Prediction Block Diagram (Initial Model in Simulink).....	23
Figure 6. Example Output from the Baseline TAILSS Hypoxia Prediction Algorithm.....	24
Figure 7. Step Response Estimation 0 to 10K Feet.....	27
Figure 8. Step Response Estimation 10K to 18K Feet.....	28
Figure 9. Step Response Estimation 10K to 25K Feet.....	28
Figure 10 USN Consciousness Model in ExcelVBA.....	29
Figure 11 Matrix formulation of USN Consciousness Model.....	30
Figure 12 Retinal oxygen utilization.....	32
Figure 13 Comparison of Original and Modified VBA Algorithms.....	35
Figure 14 Comparison of Simulation Results from Algorithm Modification.....	36
Figure 15 Model response at 0.5 threshold.....	39
Figure 16 Model response at 0.6 threshold.....	40
Figure 17 Model response at 0.7 threshold.....	41
Figure 18 Model response at 0.8 threshold.....	42
Figure 19 Combination of altitude and acceleration exposures.....	43
Figure 20 Subject 7 exposure to 18,000 simulated with the USN Consciousness Model.....	45
Figure 21 LOC threshold at 0% Connectivity for Subject 7 at 18,000 feet.....	46
Figure 22 LOC threshold at 20% Connectivity for Subject 7 at 18,000 feet.....	46
Figure 23 Subject 7 exposure to 25,000 simulated with the USN Consciousness Model.....	48
Figure 24 LOC threshold at 0% Connectivity for Subject 7 at 25,000 feet.....	49
Figure 25 LOC threshold at 20% Connectivity for Subject 7 at 25,000 feet.....	49
Figure 26 Subject 7 SaO ₂ values at 18,000 feet. (Horizontal axis – time (sec)).....	51
Figure 27 Simulation output values, active and cluster mass, compared to SaO ₂	55
Figure 28. Integrated BETA Model Block Diagram.....	57
Figure 29. Altitude Dependent Exponent Evaluation - Constant.....	58
Figure 30. Altitude Dependent Exponent Evaluation – Linear Equation.....	58
Figure 31. Altitude Dependent Exponent Evaluation - Exponential Equation.....	59
Figure 32. Updated Model for SpO ₂ Calculations.....	60
Figure 33. Parametric Transient Time Dependent Output.....	62
Figure 34. "C" Code Verification - Transient Output.....	63
Figure 35. Parametric Model Initial Verification Analysis.....	65
Figure 36. Example of Parametric Model Verification Data Plot.....	66
Figure 37 Wolf Paper Figure.....	69

Figure 38 Simulation of the Hoffman Altitude Exposure with arbitrary recovery period 71

Table of Tables

Table 1. Stages of Hypoxia (from DeHart (1985)) 14
Table 2. Baseline Algorithm State and %O2 Saturation 25
Table 3: Comparison of physiological outputs calculated with the initial model and the current model . 26
Table 4. Model R² Results 27
Table 5 Consciousness Model Current Variable Storage Requirements 31
Table 6 Consciousness Model Current Variable Storage Requirements 34
Table 7 Summary Simulation Results 38
Table 8 Experimental Subjective Response for Subject 7 at 18,000 feet 47
Table 9 Experimental Subjective Response for Subject 7 at 25,000 feet 50
Table 10 Decision value variations for the Neurological State Model 52
Table 11 "C" Code Output Verification – Steady State Output 63
Table 12 Inputs and Outputs of the Customizable Energy Expenditure 67
Table 13 Result summary compared to Hoffman 70
Table 14 Result summary compared to Hoffman 72

1.0 Summary

This final report discusses the technical and financial program status for the period of July 2013 through May 2014.

The program consists of four baseline tasks and one optional task:

1. Preliminary Research and Documentation
2. Develop Parametric Predictive Models
3. Algorithm Development and Refinement
4. BETA Model Software Development/Definition
5. *Concept System Refinement (Option)*

Work has been completed on Tasks 1, 2, 3 and 4. The Task 5 option has been exercised and begins in June 2014. Separate documentation and CDRL deliverable will address the results of these efforts and are due in July 2014.

The concentrated effort on the literature search activity (Task 1) has been completed. A File Transfer Protocol (FTP) site has been created to share references and data among the team members and Office of Naval Research (ONR).

The baseline parametric hypoxia modeling effort (Task 2) has been completed. A model to predict %O₂ saturation, aircrew state, alveolar pressure of oxygen (PaO₂) and alveolar pressure of carbon dioxide (PaCO₂) has been converted over to the C programming language. This will allow the algorithm to eventually run on a micro-controller. Additionally the time based algorithms have been adjusted to better represent the physiological response of the human to high altitude hypoxic events.

The conversion of the United States Navy (USN) Consciousness Model (Task 3) has been completed. Initial verification and sensitivity analysis has shown positive results and the code has been reduced to a size and complexity that will run on a modest microcontroller. The addition of a hypoxia component to the acceleration component of the model has demonstrated good results.

The final baseline task (BETA Model Software Development/Definition – Task 4) has been completed. Software algorithms have been developed and progressively refined to predict hypoxia and near-hypoxia conditions. The focus on implementation in a memory-limited, bit-constrained microcontroller has remained a top priority. Existing data has been used as an initial verification tool and the positive results are included in this report.

The baseline parametric algorithm to predict %O₂ saturation and aircrew state and the modification of the USN Consciousness Model to predict LOC due to altitude induced hypoxia remain as viable approaches moving into the next phase of development.

2.0 Introduction

Special Notice 13-SN-0003 outlined a research thrust entitled “Hypoxia Monitoring, Alert and Mitigation System” (HAMS) that was launched under the Long Range Broad Agency Announcement (BAA) for Navy and Marine Corps Science and Technology: ONRBAA13-001. The desired features of the Hypoxia Monitoring, Alert, and Mitigation System were to predict/detect/warn warfighters of impending hypoxic events based on individual physiological, environmental, and cognitive monitoring. The stated goal was to provide optimal protection of military personnel and equipment through intelligent monitoring and adaptive modeling that accounted for individual differences in tolerance and provided timely notification/warning aids so personnel could take corrective action before compromise or loss. The team of Athena GTX (Athena) and Criterion Analysis Incorporated (CAI) collaborated, proposed and won an award under this effort.

This final report discusses the technical and financial program status for the period of July 2013 through May 2014. It is intended to inform the Program Officer and Administrative Contracting Officer of the technical and financial results of the HAMS program.

This algorithm development effort and the approach taken under this project is within the context that the algorithms developed will eventually need to run on a “fieldable” solution. Consequently the focus was on algorithms that can run on micro-controller based platforms. As technology evolves from the laboratory into actual high altitude environments and is then coupled to stress of military operations the complexity of the issues this program addresses can be realized.

This initial phase of the larger HAMS project vision was focused on algorithm development only. As this team has developed the current algorithms there has been an eye towards sensor availability for the future. Previous efforts to date have showed that attempting to reliably peer into the brain from the scalp surface through the skull with EEG and f-NIRS is neither comfortable nor feasible in a dynamic laboratory/simulator environment much less in an aircraft; and hence, in our experience, remains suspect for operational use. Perhaps this program will deliver such a solution; perhaps it is not feasible with today’s technology. This by no means concludes that the technologies are not innovative or interesting or that they do not show promise, but the distance between a quiet, sedentary (perhaps anesthetized subject) and an aviator in flight or ground troops involves a tremendous leap of “technical courage”. We believe the technology and processing abilities today will allow for a total change in focus from trying to integrate a comprehensive sensing solution into a flight or ground helmet to one where the needed solution is not actually near the head or helmet. This insight changes algorithm design. A small, lightweight, and comfortable monitoring system might eventually be designed to continuously measure multiple physiological parameters in an effort to track operator state and hypoxia, e.g., from the arm alone. Sensors which detect SpO2, pulse/pulse rate, ECG, and skin temperature will be researched and evaluated for integration feasibility with a tactile vibrator for alerting the user to the suspicion of growing hypoxia. Novel and non-traditional sensor locations and technologies will be investigated as they impact

data and algorithm design issues, and advanced signal processing techniques applied, and compared in this program for extensive technology leveraging. However, all of this will be directly applicable to effective algorithm design. Each of the different measurements will be entered into a multi-parameter evolutionary prediction algorithm which outputs a numerical score that correlates to how prevalent any effects of hypoxia are to the user and to perhaps suggest or anticipate the onset of hypoxia based on trend data. Depending on the hypoxia algorithm's output, a signal potentially will be sent wirelessly to an alarming device integrated into the sensing platform wirelessly, or located in a key area of the users life support to vibrate which will alert the user if preventative action needs to be taken. No sensing system is infallible so key iteration rate considerations will need to be established in the algorithm design earlier than thought necessary to maximize hypoxia code output characteristics and iteration rates needed.

3.0 Methods, Assumptions, and Procedures

This section summarizes the Task descriptions for this project.

3.1 Task 1 – Preliminary Research and Documentation

The primary efforts are to review/document cognitive and psychomotor decline with hypoxia. A literature search will be conducted in the area of cognitive and psychomotor effects of hypoxic hypoxia and acceleration-induced hypoxia with the purpose of documenting potential experimental results that could be used to develop parametric models predicting decrement in cognitive and psychomotor performance and unconsciousness. Validated sensor technology, criteria for measurement, digital signal processing techniques and codes and state assessment models which outline physiological trends and normal ranges which can be used to identify and quantify hypoxia or near –hypoxia states as part of an overall physiological state assessment tool will be identified. Additionally, the potential for detecting or modeling “hypoxia-like” symptoms will be explored. Areas to explore include, but are not limited to, the effects of: toxins, spatial disorientation, fatigue and dehydration. In order to facilitate the most efficient use of time and resources across all performers on this project, Athena will coordinate with ONR on the areas of the initial literature search and sources found before they are obtained and reviewed. This will reduce the potential for duplication of effort. It is expected that ONR will share literature and data as appropriate to reduce duplication of effort on this task.

3.2 Task 2 – Develop Parametric Predictive Models

Based on Task 1, a subset of criteria and models will be selected for use in conceptualization of a directly applicable approach and trade study rationale. Parametric models will be developed to predict decrement in cognitive and psychomotor performance and unconsciousness. Particular emphasis will be placed on model approaches that would work on small, low power computing devices such as microcontrollers.

3.3 Task 3 – Algorithm Development and Refinement

Task 3 has an overall basic approach and three specific subtasks. First pass I/O requirements of the evolving algorithm will be identified and evolved into a solid first pass hypoxia model which could integrate the preliminary physiological sensors in a pseudo-concept demonstration. Theoretical sensor placements and I/O requirements that drive model input, outputs, and iteration rates for all three identified applications will be determined such that the required signals are attained with minimum intrusiveness to the operators. Emphasis shall be placed on making the software compatible with a TBD sensor system that is small, lightweight, and comfortable for the end user.

3.4 Task 3a – Update the USN Consciousness Model Implementation

Under US Navy RDT&E funds an acceleration-induced loss of consciousness model was developed and implemented using Microsoft Visual Basic 5.0. This approach was subsequently updated to include actual oxygen saturation measures. This model will be converted into an implementation to allow investigation of model limitations, possible correlation to literature search results of Task 1-2 and embedded software definition requirements identified in Task 3.

3.5 Task 3b – Determine Model Deficiencies for Hypoxia

The USN Consciousness model was developed for acceleration-induced unconsciousness but with the addition of actual oxygen saturation values hypoxic hypoxia effects could also be predicted. This task will document predictive deficiencies for hypoxic hypoxia and acceleration-induced hypoxia and modification required to improve predictions.

3.6 Task 3c – Determine Model Deficiencies – Other

A series of models are leveraged over from current and previously sponsored programs: Automated Combat Casualty System (ACCS) state assessment, Hammerhead™ and mini-Medic®. The existing models and algorithms will be assessed for their applicability to this project and a determination of what can and cannot be leveraged will be made. This task will then identify predictive and assessment deficiencies and the modifications needed to improve prediction, detection, mitigation assurance and avoidance.

3.7 Task 4 – BETA Model Software Development/Definition

We will develop, through sequential iterations, a progressively more refined prediction algorithm for hypoxia and near-hypoxia conditions. This will be based on the contractor approach used to develop the multi-parameter assessment prediction, assessment, assurance of state, and the USN Model within the embedded design vision of this Special Notice. Parameters and conditions will be tailored to recognize and alert the user of complications specifically due to hypoxia. The necessary design features to convert a Windows® based implementation to a memory-limited, bit-constrained microcontroller implementation will be documented for possible realization in an optional task project. For each iteration the algorithms

and software will be evaluated using existing data and data provided by ONR as it becomes available and as it relates to this project.

3.8 Task 5 – (Option) – Concept System Refinement

This option continues to refine the approach to meet the Special Notice Objectives and goals with the USN in an evolving hardware approach platform(s). This is preliminary integration of prospective hardware approaches in Task 3-4 and the software developed in Task 4 into a preliminary specification. As the USN or other contractor's efforts are finalized and selected for possible integration, the contractor will assist the USN in understanding the trade-offs of integration to hardware platforms, alarm options, mitigation strategies.

3.9 Task 6 – Documentation and Deliverables

- [1] Quarterly Reports - Two quarterly progress reports (CDRL A001)
- [2] Final Report - (CDRL A002)
- [3] BETA software - Software developed in Task 4 will be provided (CDRL A003)
- [4] Option – Trade-off Analyses and Preliminary Specification (CDRL A004)
- [5] Monthly Updates - Monthly email updates in Contractor format will be provided

4.0 Results and Discussion

4.1 Task 1 – Preliminary Research and Documentation

The primary literature review effort has been completed. Research included internal online searches as well as utilizing research and data provided by Dr. Shender on behalf of the ONR. We have also created a secure online-site (File Transfer Protocol (FTP) site) for collaboration of documents and data specifically for those involved with this program. Dr. Shender subsequently uploaded additional data to the FTP site that included smaller time steps between data points for algorithm development and evaluation.

Tangible validation data or definitive cognitive endpoints for the modeling and algorithm development efforts are still a need for the program and we have not been overly successful in finding this information in the literature. Interesting correlations for Autonomic Nervous System (ANS) system analysis and hypoxia predictions have been explored and could provide a path for prediction for the onset of hypoxia and are discussed in detail below. Summaries and abstracts of relevant literature search results are also included below. The literature has information available for directly measuring cerebral oxygen levels but these do not seem to be well suited to a product design for the HAMS applications. The abstracts of the remaining literature search results are included in Section 10.1.1 for completeness.

4.1.1 Significantly Relevant Literature Research Results

Stepanek J, Cocco D, Pradhan GN, Smith BE, Bartlett J, Studer M, Kuhn F, Cevette MJ. Early detection of hypoxia-induced cognitive impairment using the King-Devick test. *Aviat Space Environ Med* 2013; 84:1017 – 22.

The King-Devick test is cognitive screening test based on sequential rapid number reading aloud with performance based on a task performance time and errors. Subjects read a series of numbers from test cards, one demonstration and 3 test cards, lasting less than 2 minutes. The sum of the test cards times and the number of errors in reading the numbers constitutes the data. Twenty-five subjects were exposed for three minutes to hypoxic conditions via a gas mixture equivalent to 23,000 feet altitude whereupon they performed the test. Pre- and post-hypoxia exposure test controls were performed. Significant differences were found during the hypoxia exposure compared to pre- and post-hypoxia controls which indicated that the test was sensitive to the stressor. Figure 1 below is from the paper (paper Figure 5) which shows the change in Oxygen saturation over the exposure averaged over all subjects. Oxygen saturation decreased from $98 \pm 0.9\%$ to $80 \pm 7.8\%$ after 3 minutes on hypoxic gas and continued to decline during the cognitive test $75.8 \pm 8.3\%$ at test completion. This study only indicates that the cognitive test is sensitive to hypoxia. Given the number of subjects and the standard deviations on oxygen saturation and test performance, some stratification of results based on oxygen saturation would have been useful to this project to help determine thresholds for hypoxia onset prediction.

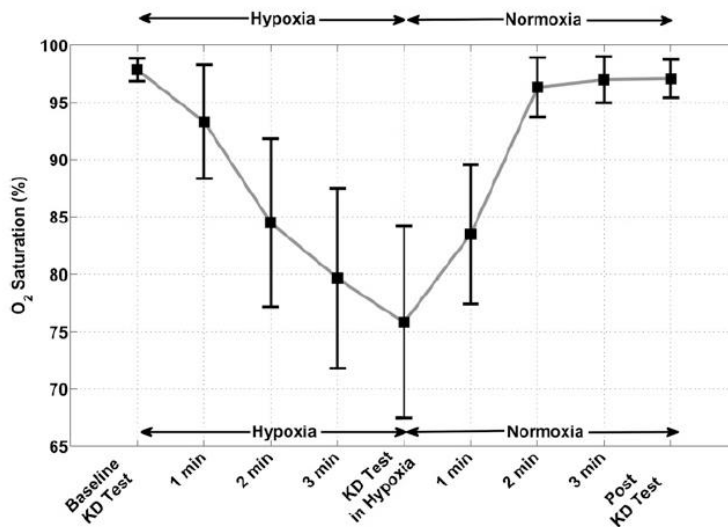


Figure 1 Oxygen Saturation for King-Devick Test Study

This recently published paper is like the majority of papers that put the subjects into a hypoxic state to measure performance decrement but don't correlate a measure like oxygen saturation to onset of cognitive decline.

Thresholds for hypoxia-induced psychomotor and cognitive decrement are needed to serve as warning indicators based on measured and predicted data. Given the beat-to-beat method in which oxygen saturation is measured via a pulse oximeter, a certain degree of "inexactness" exists. So it is unlikely that small differences in SaO2 will matter once a higher level threshold has been crossed. After an operationally relevant point further impairment thresholds would seem unnecessary. Fulco et al (1988) summarized the known data on the decrement in human performance in graphical form.

Fulco, C.S. & Cymerman, A. Human performance and acute hypoxia. In: Human Performance Physiology and Environmental Medicine at Terrestrial Extremes. (Chap 12), K.B. Pandolf, M.N. Sawka, and R.R. Gonzalez (Eds.) Benchmark Press, Indianapolis, IN: pp 467-495, 1988.

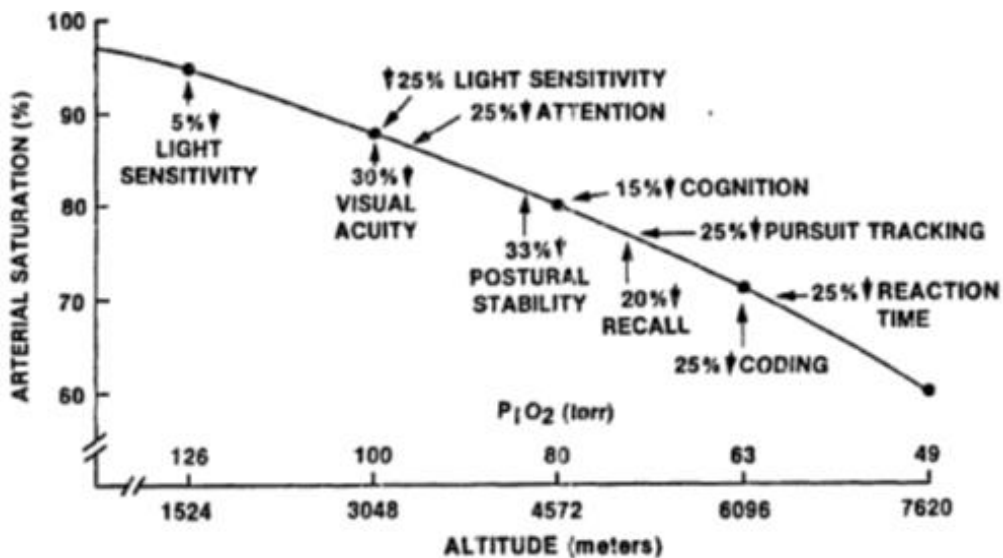


Figure 2 Human Performance Decrements by Oxygen Saturation and Altitude

Figure 2 (ref. Figure 6 in the publication from Fulco et al (1988)) indicates published decrements in human performance versus altitude and arterial saturation one of which may serve as a preliminary threshold for the measured pulse oximetry value. Loss of attention and visual acuity at arterial saturation of less than 90% but greater than 85% would be critical initial factors for the pilot or the ground soldier. This graph can be digitized to get more exact numbers where the original papers may be more difficult to obtain.

This paper also correlates to the discussion in Fundamentals of Aerospace Medicine (DeHart, 1985 page 98) where visual acuity is affected at 3048 meters and SpO2 is between 87% and 98% at altitudes between

0 and 3048 meters (10,000 feet). Above this altitude more serious detrimental conditions begin to emerge. The table below is from Table 5-13 in DeHart (1985).

Table 1. Stages of Hypoxia (from DeHart (1985))

Stage	Altitude Breathing Air (m)	%O2 Saturation
Indifferent	0 – 3048	98 – 87
Compensatory	3048 – 4572	87 – 80
Disturbance	4572 – 6072	80 – 65
Critical	6092 – 7010	65 – 60

ASMARO D, MAYALL J, FERGUSON S. Cognition at altitude: impairment in executive and memory processes under hypoxic conditions. *Aviat Space Environ Med* 2013; 84: 1159 – 65.

Authors measured short-term and working memory capacity using Digit Span tasks, cognitive flexibility and selective attention using the Word-Color Stroop Task, executive functioning using Trailmaking A and B tests at baseline and simulated altitudes equal to 17,500 ft. and 25,000 ft. to study the affect of altitude exposure on cognitive tasks. While this study pertains to the aviation exposure some implications of ground operations are evident. Cognitive performance decrements were observed at both altitudes compared to control but the 17,500 ft. score differences with respect to control were not as large as those at 24,000 ft. In several conditions the control versus 17,500 ft. results was not significantly different. Unfortunately for our purposes this study did not report any physiological data, not even SaO₂, which one would have considered necessary for safety. One might imply an oxygen saturation level, but that is not useful or appropriate. The implication for lower altitude operations is that embedding some cognitive test parameter in an interaction will not likely be helpful in indicating loss of cognitive performance. Once again leading to the conclusion that a tripwire parameters like SaO₂ at a predetermined level such as 85 to 80% may be sufficient to start corrective action. One interesting aspect of this work was that the authors reported that the subjects were largely unaware of their impairment and some actually thought they were performing well when in fact not performing well. Since the function of the ultimate device is to warn and advise, convincing the user that the device is correct and they are impaired may be a challenge.

Wolf M. Physiological consequences of rapid or prolonged aircraft decompression: evaluation using a human respiratory model. *Aviat. Space Environ. Med.* 2014; 85: 466–72.

Wolf (2014) published a new paper on a human respiratory model describing the effects of rapid and prolonged aircraft decompression. This is further work concerning the use of a model this author has

reported on for many years. Wolf proposes using the SaO₂ of 70% as a critical value. He provides a data curve that can be used for validation (see Figure 3) plus a time of useful consciousness model output based on several studies and the requisite background information.

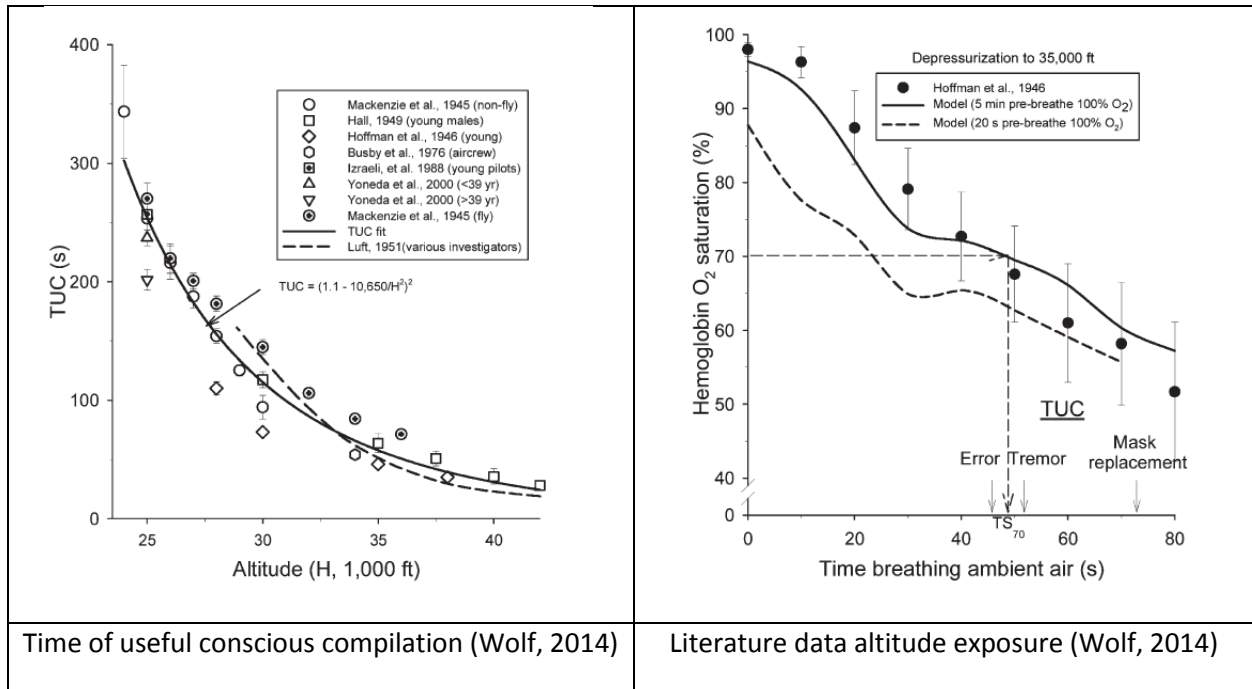


Figure 3. Wolf, 2014 TUC Compilation and Depressurization profile to 35K feet

The information is primarily applicable to the aviation hypobaric decompression scenario, but should also prove to be applicable to sustained operations (at least with respect to the lower altitudes – up to 25K feet before the onset of possible neurological damage). In the literature data graph above, at 35K feet, the time before imminent unconsciousness was 72 seconds (mask replacement). The 35K feet SaO₂ data presented in this paper will be digitized, interpolated and run through the model to examine predictions compared to the literature data.

Self DA et al. Physiological Determinants of Human Acute Hypoxia Tolerance. Report DOT/FAA/AM-13/22, November 2013.

These FAA researchers looked at 5 minute normobaric exposures to 25,000 feet where the physiological tolerance was defined by SaO₂. They measured heart rate variability (HRV), total hemoglobin, VO₂ max and resting oxygen consumption prior to exposure. They measured cerebral oximetry, ECG, middle cerebral artery blood flow velocity, noninvasive beat-to-beat arterial pressure and its first derivative, cardiac output, and left ventricular stroke volume, cerebral pulse oximetry, hemoglobin oxygen saturation, tidal volume and respiratory rate, breath-by-breath inhalation and end-tidal O₂, CO₂, and N₂

tensions. They computed VO₂, mixed venous PO₂ (DLO₂) and alveolar-capillary O₂ gradient. They also looked in blood samples for serum S100b which is considered a marker for cerebral hypoxic insult. They found that seven variables could be combined in a multivariate linear regression to predict the decline in SpO₂ with an r² of 0.706. The equation is pasted as an image below:

$$\text{SpO}_2 = [-18.73 - (0.2 \dot{V} \text{O}_2 \text{max}) + (.383 \text{HRV}) + (2.68 \text{End } \dot{V} \text{O}_2 - \text{Resting } \dot{V} \text{O}_2) + (2.38 \text{PAO}_2) + (.414 \text{DLO}_2) - (.309 \text{PAO}_2\text{-MVO}_2 \text{ gradient}) - (.528 \text{rSO}_2)]$$

Serum S100b levels were statistically different between pre and post exposure but the differences appear small.

This report may give us some insight on personalization parameters for our model.

Self DA et al. Physiological Equivalence of Normobaric and Hypobaric Exposures of Humans to 25,000 Feet. Report DOT/FAA/AM-10/20, December 2010.

Subjects were exposed to 25,000 feet in The CAMI hypobaric altitude training chamber and the normobaric Portable Reduced Oxygen Training Enclosure (a commercially available portable altitude training system developed by Colorado Altitude Training; Louisville, CO). The report describes that PaCO₂ values appear to be lower in hypobaric vs. normobaric exposures. This would indicate that an expected pH shift in the oxygen disassociation to the left at higher altitudes would be subsequently reduced and consequently affect the SpO₂ prediction of a model based on hypobaric conditions when comparing expected results to normobaric test conditions.

4.1.2 Correlations between ANS and Hypoxia

Often the referenced literature focuses on one physiological measure to determine hypoxic state. However, the medical state of all individuals all the time usually mandates a multi-parameter assessment. Similarly one sensor cannot logically produce multiple measures without other sensors to produce “balance and reasonableness” to the output. Multiple physiological parameters that are used to quantify user conditions can be ascertained from SpO₂, ECG, and temperature/humidity measurements. Heart rate, cardiac complexity, heart rate variability, pulse-wave transit time, shock index, modified shock index, and pulse integrity have been found to be good indicators of some health conditions, including hypoxia and hypovolemia, but a multi-parameter model need not differentiate between types of hypoxia (hypoxic, hypemic stagnant, histotoxic (DeHart, 1985)).

A multi-variable input and an adaptive scaling code will provide a single numerical value which corresponds to the urgency of state the subject as well as any trending of state apparent. Specifically, the diagnosis or reason for that state we express is not as important as the knowledge of the deterioration of that state as a combined score. Although the common baseline many feel is pulse oximetry we submit that the difficulty of obtaining a clean pulse oximetry signal in motion is extremely difficult. Similarly, obtaining a clean cerebral tissue measurement through the scalp is at best highly motion suspect. The effort cannot therefore overly focus on pulse oximetry and will attempt to derive measurement techniques centered at early ANS insult leading to hypoxia if uncorrected. But can we understand the role of the cardiovascular system and ANS relative to generation and management of hypoxia? The review completed to date has addressed this.

The time course changes in both cardiovascular and autonomic nervous system (ANS) function during acclimatization to altitude and hypoxia has been widely studied (e.g., Kawaguchi, et. al, 2003; Favret and Richalet, 2008; Barak, et. al, 2008; Hansen and Sander, 2002; Benoit, et.al., 1997, Iiyori, et. al., 2007/2008 (on line publications); Pellet, et. al., 1997, and Agostoni, et.al, 2000). The bulk of these studies suggest that the ANS insult defined as a notable change in activity is seen before the cardiovascular change is seen in many cases and many different trial designs. One might argue that this makes sense since the ANS drives the vascular response. Although obvious, this is a more difficult measure to take and much harder to interpret across any individual much less a population. But further, this suggests that looking for a physiological change in a vital sign recognized by the FDA in HAMS, may suggest that the event has already occurred and not that it is “going to” occur, i.e., that measure is not considered to be “anticipative” but “reactive to the event”. In addition, the volatility of data seems to be demographically driven; i.e., the impact of age, sex and weight are clear. Finally, often the volatility of data is environmentally driven; i.e., the effect of cold and heat on the vascular response.

Consider the following, Barak, et.al. (2008) showed, for example, that the tolerance of a group of test subjects to hypoxia varies substantially among healthy subjects which supported earlier work that some individuals are simply *better* performers than others in the hypoxic environment (Stobdan, 2007). Similarly, the issue of exercise performance and ventilation control and the stimuli driving ventilation as well as the mechanism of that control in hypoxia, drove a new research trend as much as ten years ago (Sheel, 2008, Longhurst, 2003). Longhurst’s work neatly outlined the areas of compensation associated with a subject during progressive ascent to higher altitudes. Although we are not looking at progressive ascent, it proves a baseline consideration for the mechanisms expected to be seen in HAMS. Longhurst’s work as well as Sheel’s suggest that the HAMS must be reactively able to detect this compensation dynamically. As the human ascends, changes in cardiovascular parameters of heart rate (tachycardia), increased cardiac output and changes in flow distribution occur not only at minimal workloads but certainly at higher levels of stress and performance. In fact, Thompson, et al. (2004) showed that workload in acute hypoxia further exacerbates the issues of change locally since reduced gas tensions alters not only skeletal muscle performance, but heart rhythm and in other selected vascular beds such as the pulmonary arteries and lung tissues. This may lead to leakage, edema and dysfunction (Thompson, et. al,

2004). This in turn will impact gas exchange progressively, hence respiratory quotients, tissue oxygenation and carbon dioxide exhalation. Subsequently, subject acid base balance is progressively changed, progressive tissue toxicity may occur, and the overall result is that the subject's performance is expected to be spiraling downward. The changes or trends therefore become critical to track and measure as they may provide a better insight to prediction than the values alone.

From the perspective of the cardiovascular system, interactive response neural-hormonal mechanisms respond quickly during progressive hypoxia including local cardiac and direct vascular control. For example: studies in normally active subjects produced a three-fold increase in limb blood flow in hypoxia even in the presence of decreased ventricular stroke volumes (Kennedy, et. al, 2008). In normotensive environments, local responses are a direct result of autonomic outflow from the brainstem. Hypoxemia elicits the chemoreceptors, particularly those in the carotid bodies and the medulla, which can essentially oppose the changes driven by autonomic outflow (Guyton, 1976). Likely in the acute stages of hypoxia conflicting autonomic drives result in what one subject may manifest as normal ANS activity now progressively being disrupted. Heart Rate Variability (HRV) and cardiac complexity analysis of ECG RR-intervals provide measures of ANS tone (Barak, 2008). We know for example that higher workloads enhance the sympathetic and reduce the parasympathetic responses to the heart. Barak also showed over five years ago that higher workloads in hypoxemia hinder the typical response and the ratio as described above. Although the exact mechanisms of control and actions in higher workloads under the presence or absence of hypoxia are not fully delineated at this point in the literature since then (and likely not specifically agreed upon by researchers), we feel the near real time tracking of ANS integrity in the subject, while tracking subject movement or lack of movement via accelerometers, and heart rate complexity may provide an interesting insight as to the possibility of progressive hypoxia even in the simplest form without having a measure of blood or cerebral oxygen levels at all. To make this claim would also reap some disagreement from peers. However, what if this is true? Interestingly, this also suggests that when peripheral shutdown occurs due to increased sympathetic influences, and pulse oximetry begins to damp out, this ANS complexity may prove to be even more insightful. The linear stochastic HRV methods are more commonly known and understood and have been used in hypoxia assessment (Sugimura, et. al. (2008)). One key thought from Wadhwa, et.al, (2008) however suggests that there is even an undefined stimulus not currently understood that is absent in normoxia subject states. If correct, this elicits the subject's ANS to increase oxygen delivery to the tissues during hypoxia. These stimuli may also be different in males versus females (Wadhwa, et. al., 2008) Hence, measuring hypoxia via blood oxygen levels alone or only at the cerebral level may not provide insight as to subjects impending hypoxic condition or state.

We conclude from the research done to date that measurement of autonomic activity, specifically using novel high speed DSP techniques to separate parasympathetic and sympathetic tone and looking for near real time changes in the activity as well as trends are clearly a step forward in assessing the progression of a clinically defined and progressive hypoxic condition well before the hypoxia is seen in any pulse oximetry system. Our literature support for this hypothesis is present but not overwhelming. However, as

a projected product, the HAMS solution approaches should consider this option moving forward into HAMS II.

4.1.3 Relevant Aspects of USN Annotated Bibliography

- Increased age reduces the time before hypoxia appeared, therefore susceptibility to hypoxia increases with age
- Cerebral blood flow velocity was not a good indicator of mental stress during hypoxia
- Altitude dependent SaO₂ values can be used to predict AMS susceptibility
- It took six days of acclimatization for balance to improve over sea-level base value.
- Hypoxia leads to a depressed cough reflex
- The effects of altitude may be specific to particular cognitive tasks; exercise during altitude results in decreased mental performance
- Hypoxic brain injury is reduce by administration of EPO
- Drugs such as alcohol and tobacco can worsen the effects of hypoxia on aviators
- Nicergoline offers protective properties against hypoxia-induced injury
- Low levels of taurine are associated with a higher susceptibility to hypoxia
- Hypobaric hypoxia causes a decrease in olfactory function
- HSP70 induced via GGA pretreatment significantly improved tolerance to acute hypoxia

4.1.4 Additional Relevant Literature Search Results

Abraini, J.H., Bouquet, C., Joulia, F., Nicolas, M., & Kriem, B. (1998). Cognitive performance during simulated climb of Mount Everest: implications for brain function and central adaptive processes under chronic hypoxic stress. *European Journal of Physiology*, 463(4), 553-559.

- Even though this is a slow ascent, it is controlled, not dynamic in impact and may serve as a corroborating study for establishing thresholds for risk of hypoxia and performance degradation.
- Put eight male climbers in a decompression chamber and gradually decompressed them to the altitude of Mount Everest over 31 days. Throughout the 31 days cognitive tests were performed. They found that test subjects performed similar to control subjects up until 5,500 m to 6,500 m, where test subjects performance began to get worse compared to the control subjects.
- Limitations: Reasonably the limitations of this work are major. The eight subjects were all experienced climbers. The ascent was gradual rather than fast which would occur in an aircraft. Three subjects had transient strokes during the experiments.

Burtscher, Martin, et. al., (2012). Short-term exposure to hypoxia for work and leisure activities in health and disease: which level of hypoxia is safe? *Sleep Breath, 16*, 435-442.

- May serve as a corroborating study for establishing thresholds for risk of hypoxia and performance degradation.
- Looked to determine a safe altitude for people to be at for a “short” amount of time. Found that most high altitude conditions occur above 3000 m, and therefore that altitude is safe for most people. Exceptions include, women who are pregnant, people with diabetes or COPD, and children under 6 weeks.
- Limitations: does not ever specify “short” and “extended” periods of time and the exceptions are common sense. Also, Journal is not commonly seen. Peer review is not established.

Golja, P., Kacin, A., Tipton, M.J., Eiken, O., & Mekjavic, I.B. (Jun 2004). Hypoxia increases the cutaneous threshold for the sensation of cold. *European Journal of Applied Physiology, 92 (1-2)*, 62-68.

- This may lead to looking at additional sensor modalities as part of HAMS to further refine and eliminate false positive/negative indications.
- Tested 13 male subjects ability to perceive a temperature change on their toe while breathing a hypoxic gas mixture. They found that a greater difference in temperature was required before a cold sensation was perceived while the test subjects were breathing either a hypobaric or a normobaric hypoxic mixture versus ambient air. There was no significant difference in temperature required to sense a warm sensation.
- Allows conclusions that environment impacts sensor performance and perception of the user.
- Other thoughts: If temperature perception is hindered, what about other touch sensations such as pressure, like the controls required to drive the air craft? (Depression in smell sensation during hypobaric hypoxia was shown in a different study).

King, Allen B., and Robinson, Summer M. (1972) Ventilation Response to Hypoxia and Acute Mountain Sickness. *Aerospace Medicine, 43(4)*, 419-421.

- Information from this study may be used for a subject evaluation algorithm
- The study found that subjects who experienced the most severe symptoms of Acute Mountain Sickness, also shows a significant increase in minute ventilation during the first six hours of a 31 hours simulated decompression at 14,000 ft.
- Acute mountain sickness may also have an effect on cognitive ability, especially if symptoms are severe enough.

Martin, Russell L., et. al., (2000). Effect of Normobaric Hypoxia on Sound Localization. *Aviation, Space, and Environmental Medicine*, 71, 991-995.

- Study found that sound localization was not affected by hypoxia.
- May be contrary to other published papers
- Have found in numerous studies that some sensations are affected, and some are not, what causes this differences, and how can we use this to test or evaluate if someone is starting to become hypoxic.

Tauboll, Erik, et. al., (1997). Cerebral Artery Blood Velocity in Normal Subjects During Acute Decreases in Barometric Pressure. *Aviation, Space, and Environmental Medicine*, 70, 692-697.

- This may be used to more accurately model the effects of hypoxia
- Found that there is an increase in cerebral artery blood velocity due to a decrease in blood oxygen content rather than the decreased pressure, while studying patients in a hypobaric chamber with and without supplemental oxygen.
- Thoughts: Though a decrease in blood oxygen levels has a similar physiological response at sea level as when at low air pressure, would the introduction of supplemental oxygen cause the same physiological response at the same environments?

Yoneda, Ikuo, Tomoda, Masami, Tokumaru, Osamu, Sato, Tetsuo, and Watanabe, Yasuhiro. (2000). Time of Useful Consciousness Determination in Aircrew Members with Reference to Prior Altitude Chamber Experience and Age. *Aviation, Space, and Environmental Medicine*, 71, 72-76.

- This may be used to evaluate tolerance to hypoxia based on age
- This study compared the time of useful consciousness to the subject's age, and found that the younger subjects had a longer time of useful consciousness (TUC) and were more able to tolerate significantly lower SaO₂ levels.
- While decompressed to 25,000 ft. TUC of ages 39 and less was 237 seconds, and for those 40 and older was 202 seconds.

4.1.5 Data Provided by ONR

In addition literature research, we also received data from ONR (Dr. Shender) which examined cognitive ability while utilizing a ROBD to simulate different altitudes. This data was of tremendous value during the evaluation phase of this program. A sample of this data is show in Figure 4.

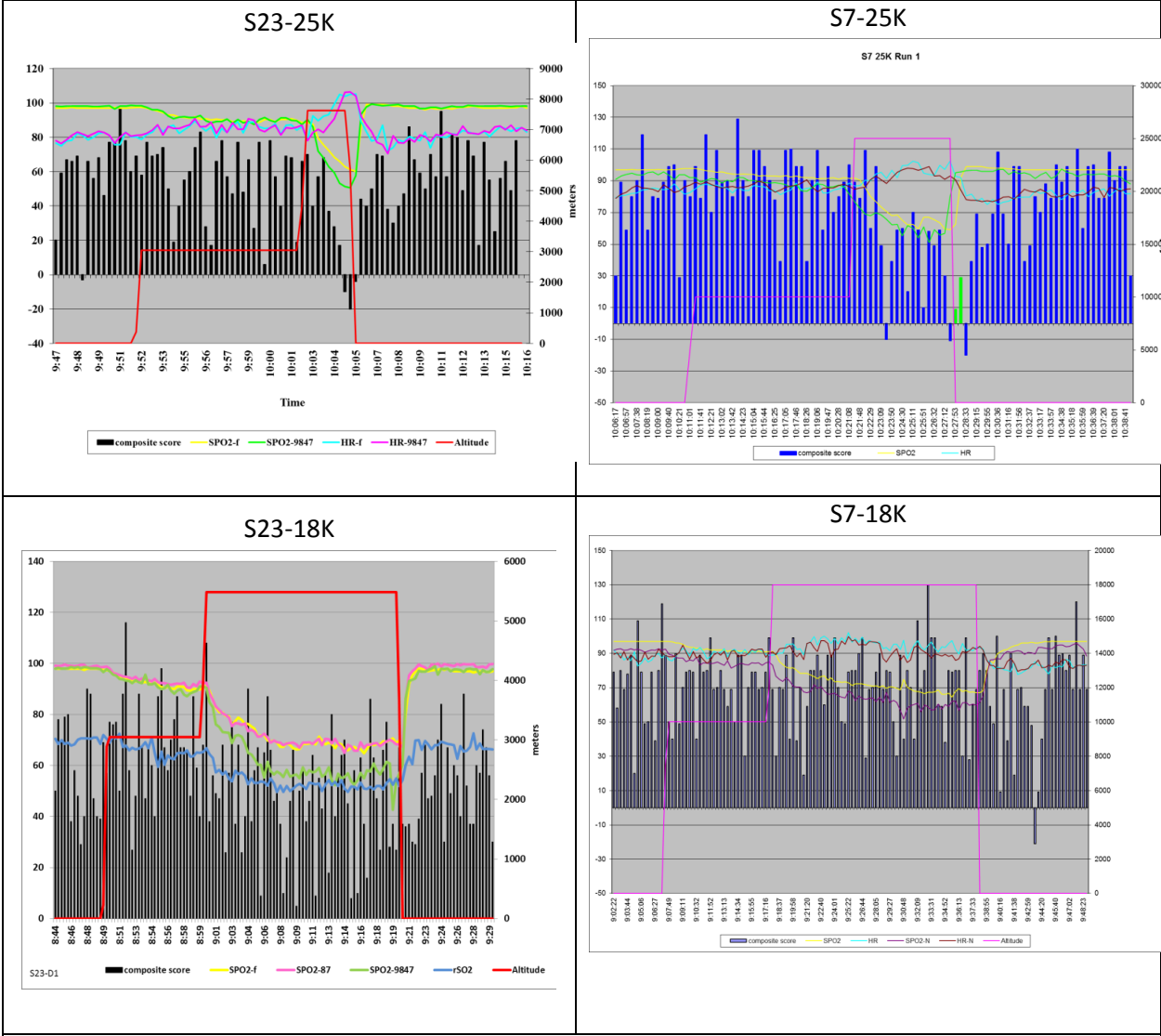


Figure 4 ROBD composite experimental data graphs

One key consideration of the ROBD data is the neuro-hormonal impacts of the device as compared to altitude chamber insult to the subject producing results. In turn the data produced will need special consideration as to the source. In reference, the data from lower negative body pressure chambers as opposed to hemorrhage has lent itself to some interesting debate with respect to the ANS triggers. In this case we will plan on examining the data and the device more closely as it applies to model development.

4.1.6 File Transfer Protocol Site

To facilitate collaborative research, the Athena GTX team has created a login protected FTP site where documents and data can be uploaded. New accounts for each user can be created as necessary and additional documents and data may be shared using this tool. The procedure for obtaining a user account and brief instructions on how to use the site are provided in Section 10.1.2.

4.2 Task 2 - Develop Parametric Predictive Models

The baseline for this effort is the hypoxia modeling and prediction work done under the Tactical Aircrew Integrated Life Support System (TAILSS) program. We were successful in recovering the original MATLAB/SIMULINK files that were utilized in creating the final deliverables to the USN. The initial model, seen in Figure 5, predicts %O₂ saturation, aircrew state, PaO₂ and PaCO₂ based on Altitude and the oxygen concentration of the breathing gas (See block diagram below). The code was implemented in SIMULINK for this project due to coordination with Carlton Technologies efforts for utilization of pulse dosing with ceramic oxygen generation in tactical aircraft. This implementation is not suitable for the HAMS implementation on an embedded system and therefore has been converted to C so that it is able to be embedded in a microcontroller/microprocessor.

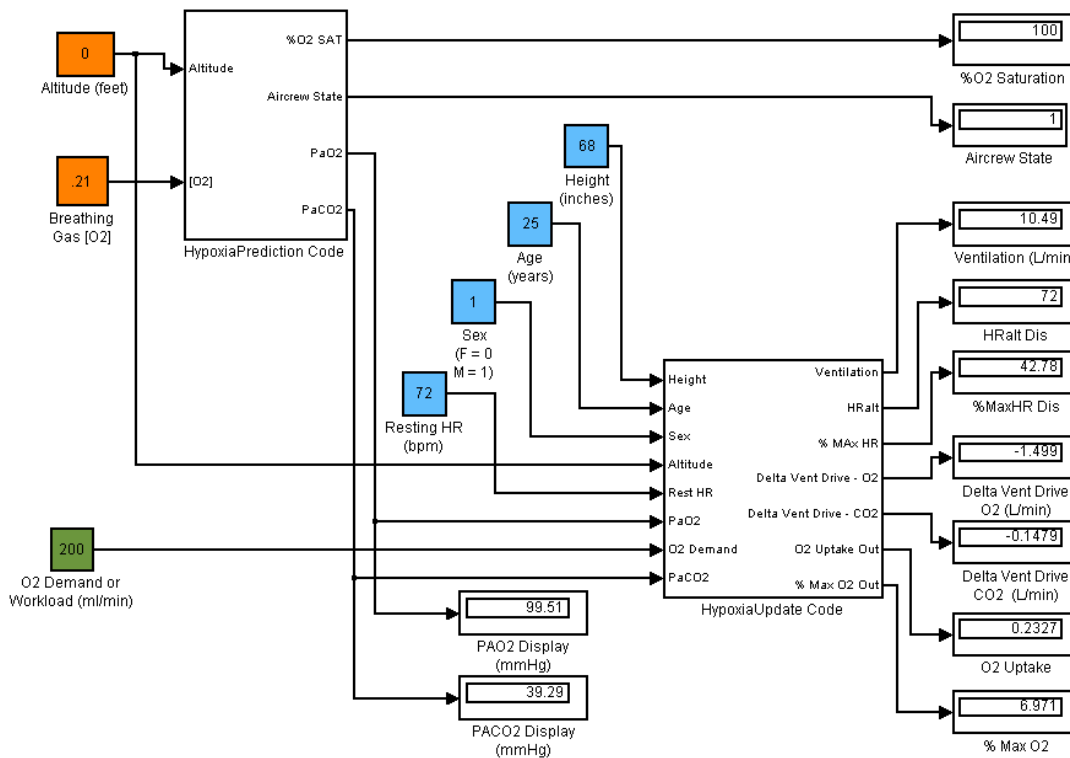


Figure 5. TAILSS Hypoxia Prediction Block Diagram (Initial Model in Simulink)

The below figure shows an example of the baseline hypoxia prediction algorithm output from the TAILSS program. The model produces an estimate of %SpO₂ as a function of altitude (cabin) and breathing gas oxygen concentration. It also takes into account pH shifts based on a PaCO₂ estimate. The final output incorporates the following:

- Bounds for the SpO₂ (0 to 100%),
- a delay function and
- a transfer function

in order to produce a realistic response to changes in altitude. Although this can be used as a systems engineering design tool it is not biofidelic enough for HAMS. For the HAMS project further verification and validation to more closely predict individual physiological responses was undertaken.

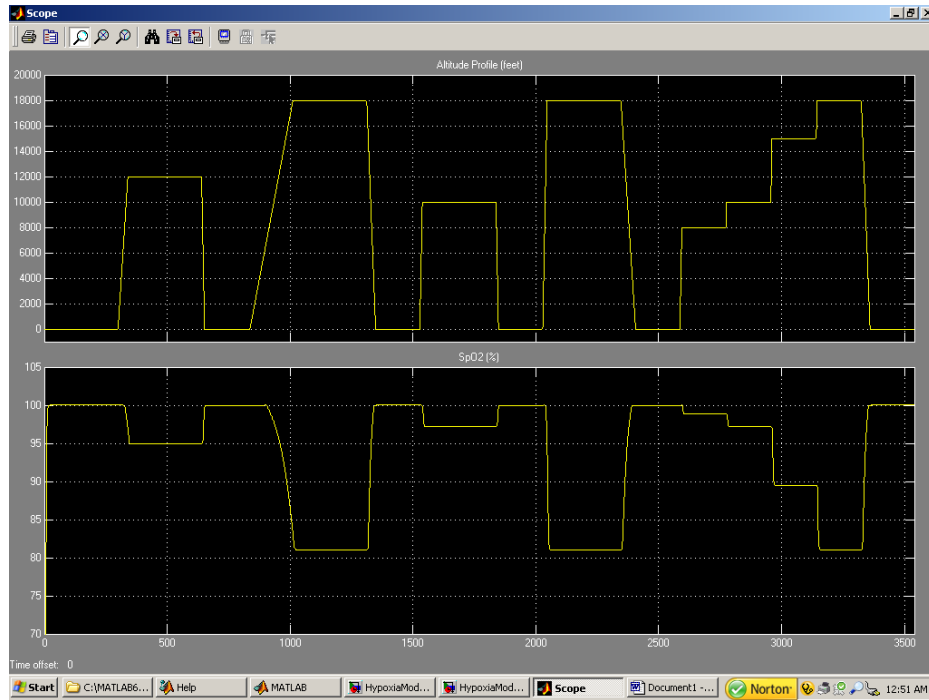


Figure 6. Example Output from the Baseline TAILSS Hypoxia Prediction Algorithm

A summary of the calculations is included below.

- Cabin pressure is derived by utilizing the 1976 COESA-extended US standard atmosphere model equations. Presently the constants for altitudes below 65,000 feet are included in the algorithm. This calculation can be eliminated in the future if a direct measurement of cabin pressure is available – leaving only a unit conversion to mmHg as applicable.
- PaCo₂ is predicted as a functions of Cabin Pressure and then adjusted based on Altitude and [O₂].
- Respiratory Exchange Ratio (RER) is also calculated based on Cabin Pressure.
- PaO₂ is then predicted as a function of Cabin Pressure, [O₂], RER and PaCO₂.
- The PaCO₂ prediction is then used to derive a pH adjustment factor to account for the shift in the O₂ disassociation curve due to pH of the blood.
- The final %SpO₂ is calculated as a function of PaO₂ and the pH adjustment factor.
- The final time dependent %SpO₂ output incorporates a time delay and transfer function.
- State is a simple function of SpO₂ derived from Table 5-13 in DeHart (1985). (See Table below).

Table 2. Baseline Algorithm State and %O₂ Saturation

State	%O ₂ Saturation	Stage
1	98 ≤ SpO ₂ ≤ 100	Normal
2	87 ≤ SpO ₂ < 98	Indifferent
3	80 ≤ SpO ₂ < 87	Compensatory
4	65 ≤ SpO ₂ < 80	Disturbance
5	0 ≤ SpO ₂ < 65	Critical

Based on the ROBD data provided, the time dependent functions of the algorithm needed to be adjusted. The baseline model included a 4 second delay and about a 15 second response time to an altitude stressor. Review of the ROBD data and literature review articles suggests that the response time is minutes and not tens of seconds.

Verification of the converted C code implementation was completed comparing the results of the initial SIMULINK model to the converted C code model for a number a test cases. The results shown in Table 3 indicate that the two models are equivalent, and any difference which may have been calculated is due to rounding and is not physiologically significant.

Table 3: Comparison of physiological outputs calculated with the initial model and the current model

		Former Model			Current Model			Difference		
		O2 SAT	PAO2	PACO2	O2 SAT	PAO2	PACO2	O2 SAT	PAO2	PACO2
0.21	0	100	99.5	39.3	100	99.5	39.1	0	0	0.2
0.21	10000	97	60	35	97	60	34	0	0	1
0.21	20000	74	34	29	74	34	29	0	0	0
0.21	30000	29	15	25	29	15	24	0	0	1
0.21	40000	3	2	21	3	2	21	0	0	0
0.4	10000	100	152	40	100	151	40	0	1	0
0.6	20000	100	152	40	100	152	40	0	0	0
0.8	30000	100	119	40	100	119	40	0	0	0
1	0	100	671	40	100	671	40	0	0	0
1	10000	100	440	40	100	440	40	0	0	0
1	20000	100	272	40	100	272	40	0	0	0
1	30000	100	154	40	100	154	40	0	0	0
1	40000	97	61	35	97	61	34	0	0	1

The final piece of the planned effort under this task was to refine the time dependent functions of the baseline algorithm. By analyzing the SpO2 data from Subjects 7 and 23 the following time depend functions have been added to the baseline algorithm:

- Time delay on the order of 40 seconds and a
- Decaying exponential of the form

$$K_1 + K_2 e^{-at}$$

Where,

- $K_1 + K_2$ is the initial value,
- K_1 is the steady state value and
- $1/a$ is the time constant of the decaying exponential and is on the order of 1 to 4 minutes.

The a term is altitude (or at least altitude change) dependent and will be discussed in Section 4.4.1 of this report. The K terms is found using the existing baseline model output.

Figures 7, 8 and 9 show the step responses for Subject 7 and Subject 23 along with the model that uses the above time dependent functions. The same time constant (3.7 minutes) was used in Figures 7 and 8, but a significantly shorter time constant (66 sec) was needed in Figure 9. The model results compare reasonably well to the Subject response data. The average response for the subjects was calculated and then an R^2 correlation was computed to evaluate the Model with the following results:

Table 4. Model R² Results

Step Response (feet)	R ² (Model compared to Subject 7 & 23 Average)
0 to 10K	0.989
10K to 18K	0.970
10K to 25K	0.978

This approach was promising for use as the time dependent functions in the baseline model and was incorporated.

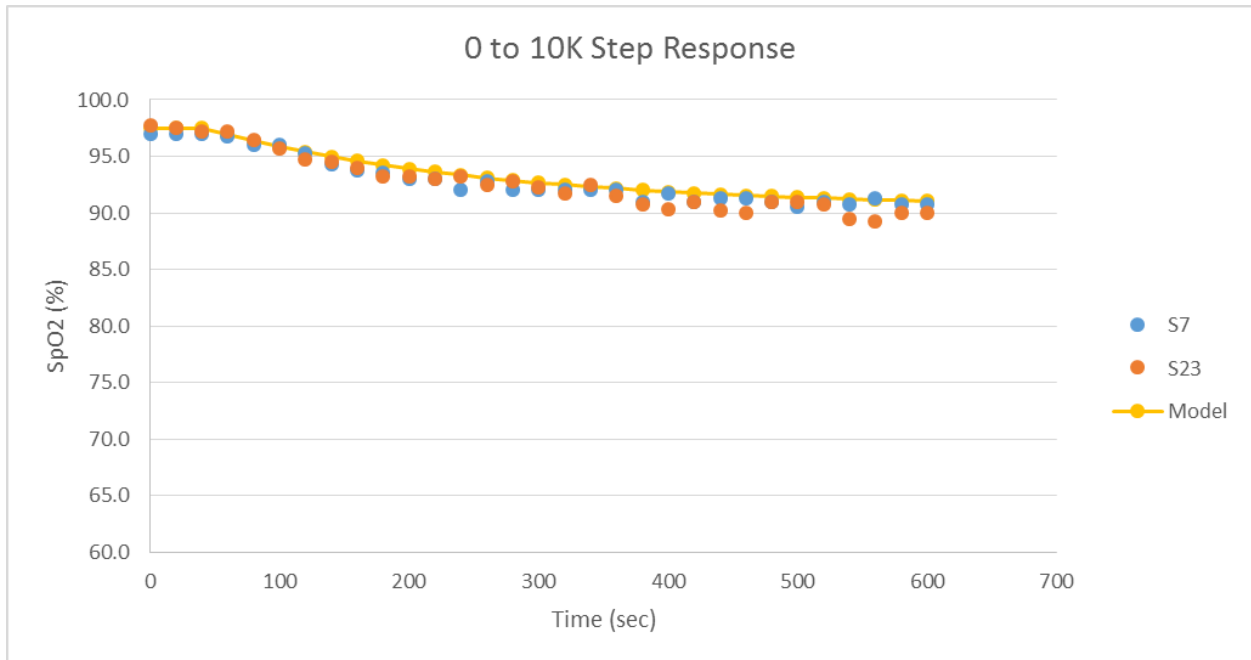


Figure 7. Step Response Estimation 0 to 10K Feet

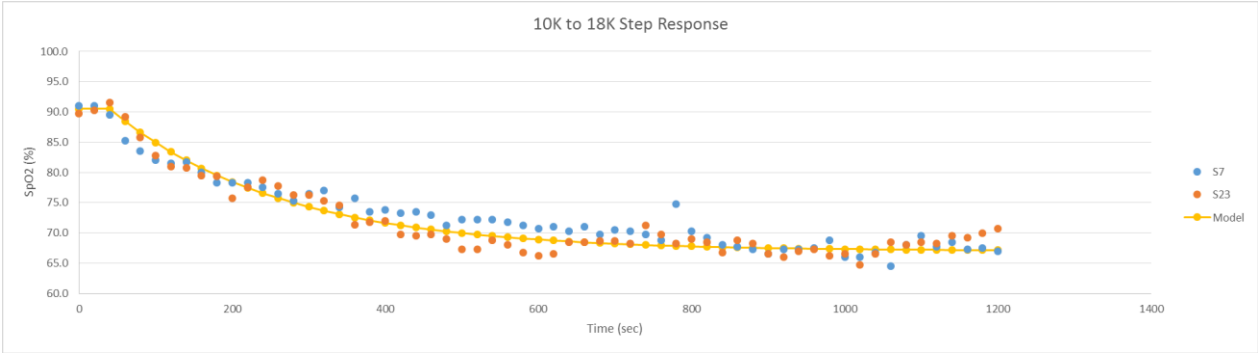


Figure 8. Step Response Estimation 10K to 18K Feet

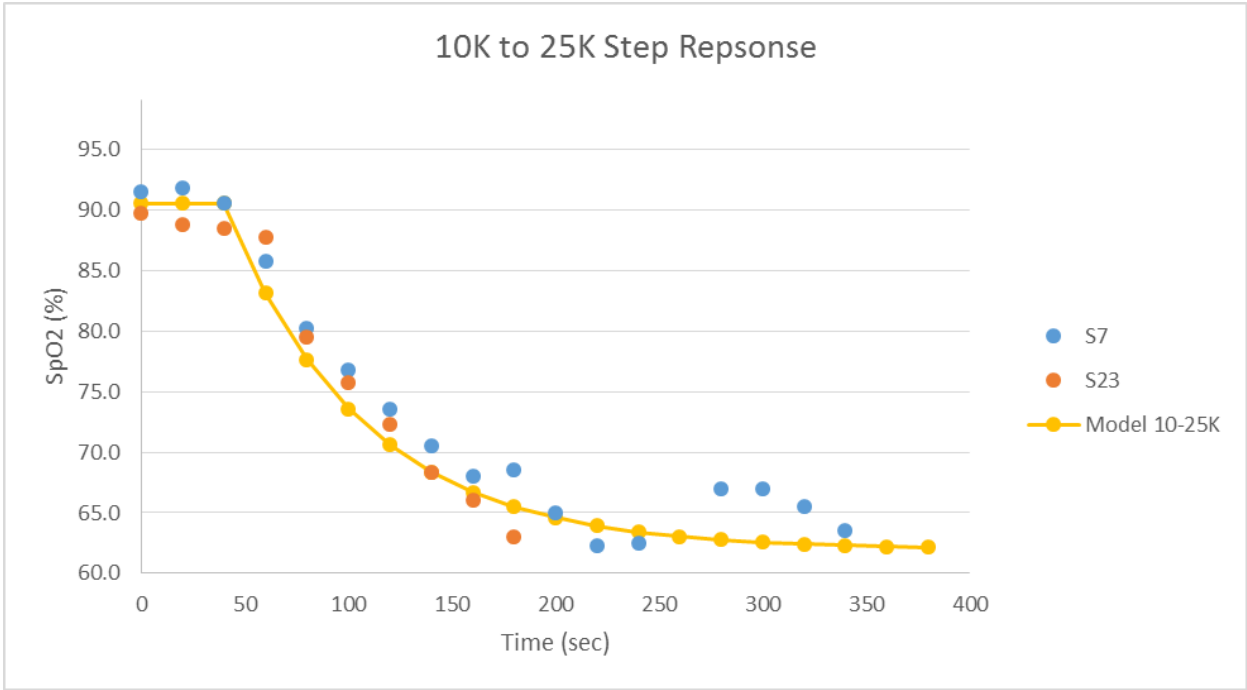


Figure 9. Step Response Estimation 10K to 25K Feet

4.3 Task 3 - Algorithm Development and Refinement

4.3.1 Task 3a - Update the USN Consciousness Model Implementation

The USN Consciousness Model was written originally in Visual Basic 5.0 which is no longer supported and not easily converted to more modern languages since Microsoft evolved to the .net framework. The

original code was stripped of Visual Basic 5.0 components and reconfigured for ExcelVBA under Excel 2010. Initial tests showed comparability to the earlier model. This capability allowed for rapid modification and testing to facilitate development of a smaller package.

A screen shot of the user interface page is shown in Figure 10.

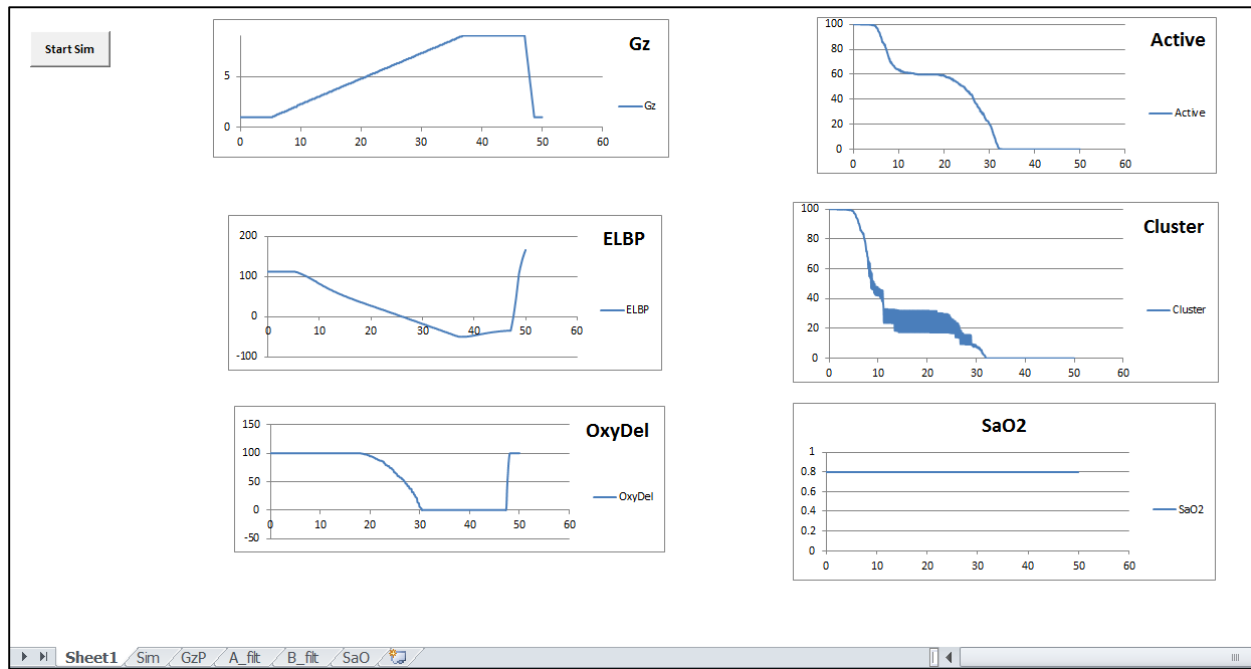


Figure 10 USN Consciousness Model in ExcelVBA

The simulation results are stored in the “Sim” tab, the input acceleration is stored in the “GzP” tab, the two oxygen utilization filters, A_fit and B_fit, are stored in their respective tabs, and the input SaO2 is stored in the “SaO” tab. The results have been compared to the original model running under Windows virtual XP mode either as the executable or under Visual Basic 5 where the same results are predicted, while not the exact same numbers calculated due to the intentional statistical variability imposed in the model. This new version, while not yet ready for dissemination pending further testing, will allow rapid modification of the code to shrink it to a smaller executable and storage memory footprint.

Since this effort is focused on developing algorithms that must run in an embedded environment (small, low power microcontroller/microprocessor), we explored the possibilities of reducing the original code and memory requirements. Some reduction in memory requirements are evident through cleaning up code and modification of computational methods. These have been further explored using the ExcelVBA model and are discussed below.

The USN Consciousness model has a matrix-based formulation where the connectivity of the Reticular Activating System was mapped as grid of nodes as shown in Figure 11.

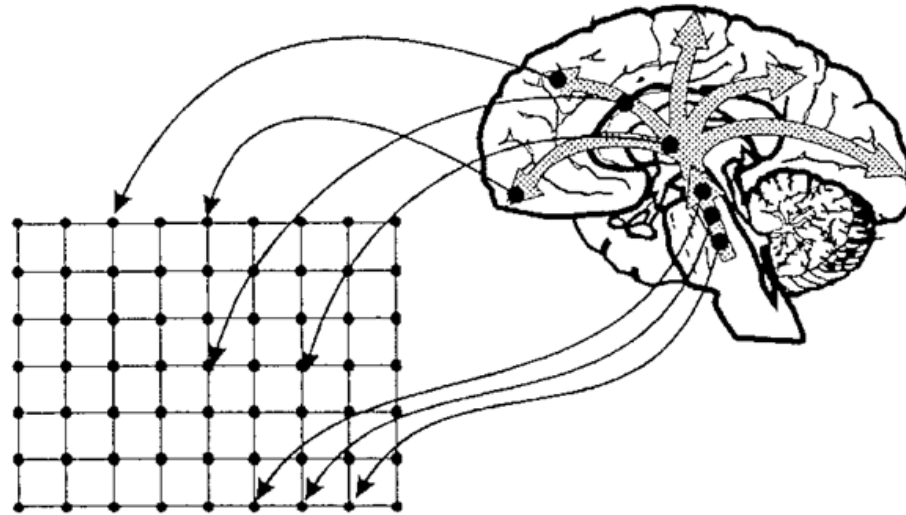


Figure 11 Matrix formulation of USN Consciousness Model

These nodes were active and connected when adequately perfused and oxygenated. These nodes were inactive and connection was lost when perfusion and oxygenation decreased. The model predicted reduction in “state” and unconsciousness when the connectivity in the grid from bottom to top was reduced or lost, respectively.

The grid of nodes formed the basis for 2 and 3 dimensional matrix formulation. A 20x20 element square matrix formed the basic grid and calculations were made based on matrix manipulation.

In considering the microcontroller storage requirements and where economies may be found only these matrix variables will be considered moving forward.

Table 5 Consciousness Model Current Variable Storage Requirements

Variable	Elements	Precision	Bytes	Total	Program Usage
z0(42, 42)	1764	Single	4	7056	Percolation calculation
OxySat(5, 42, 42)	8820	Single	4	35280	O2 utilization calculation
OxyDel(5, 42, 42)	8820	Single	4	35280	O2 delivery calculation
FilterNum(42, 42)	1764	Single	4	7056	Index into O2 utilization filter coefficient normal distribution
OxyOffThresh(42, 42)	1764	Single	4	7056	Randomized node on
OxyOnThresh(42, 42)	1764	Single	4	7056	Randomized node off
AOxy(100, 5)	500	Double	8	4000	O2 utilization filter coefficients
BOxy(100, 5)	500	Double	8	4000	O2 utilization filter coefficients
ACV(3)	3	Single	4	12	Eye level BP calc
BCV(3)	3	Single	4	12	Eye level BP calc
Gz(2000)	2000	Single	4	8000	Data-could be in a buffer
EyeBP(3)	3	Single	4	12	
Sa(2000)	2000	Single	4	8000	Data-could be in a buffer
GStress(3)	3	Single	4	12	
hScale(42, 42)	1764	Single	4	7056	Hydrostatic column distribution

Total of 129,888 bytes

Possible areas of reduction are the input data for Gz and SaO2 since these will be likely 2-byte values but computationally as read in as an array into a program may expand. The matrix sizes are all allocated as 42 x 42 but in the code the actual size of the node matrix is 20 x 20. If this was just a convenience left in while determining the optimum node matrix size, the size can henceforth be easily adjusted. The

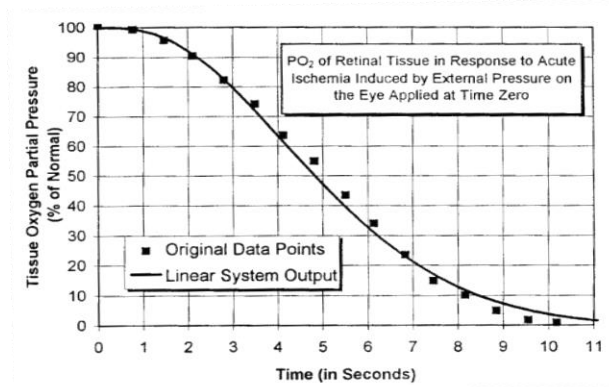
calculations for oxygen delivery and saturation (level), indicated as highlighted in yellow, have been identified as having the best chance for memory requirements reduction. The matrix format of these calculations relate to the node matrix and introduction of statistical variability but some of this may be calculated as needed and statistical process applied then. Understanding of the oxygen utilization filter calculation is essential before making any modifications. This is discussed in the next section.

Oxygen Utilization Filter

Examining the model code the oxygen utilization filter A and B coefficients are look-up tables which hold four coefficients for this calculation. These coefficients are “hard wired” into the code so that they must take up space of any program code which is at a premium for small, low power processors. The actual number values from the original software contain a significant number of significant digits. The B coefficients are quite small, on the order of 10^{-4} , and the A coefficients are more reasonable in terms of number representation. To be able to reduce or eliminate the memory overhead, one must understand what is being calculated.

Cammarota, in his original thesis, utilized the retinal oxygen depletion represented characteristically in

Figure 12 which he represented as the system response to a step function (step pressure to stop blood flow to the eye) in the H(s) equation indicated below.



$$H(s) = \frac{1}{(s + 6.667)(s + 0.4)(s + 0.4 \pm j0.4)}$$

Figure 12 Retinal oxygen utilization

This s-domain equation cannot be used to operate on data in the time domain. The H(s) system response was expanded in SciLab (version 5.4.1) to give a polynomial denominator and then converted into the z domain using the bilinear transformation tool in SciLab to derive the equation below:

$$H(z) = \frac{0.0000044 + 0.0000177z^{-1} + 0.0000265z^{-2} + 0.0000177z^{-3} + 0.0000044z^{-4}}{0.44345 - 2.27083z^{-1} + 4.20826z^{-2} - 3.38083z^{-3} + z^{-4}}$$

Examining the coefficients in the A and B filter matrices, those values correspond exactly in characteristic (sign) and magnitude (not the exact number but close) to the denominator for A and the numerator for B. The z domain equation directly becomes a difference equation whereby the time history data values can be operated on. The 3 dimensional matrices for OxySat and OxyDel are basically holding the result and intermediate values for the filter calculation. The essential flow of the program is that the eye level blood pressure is changed by the Gz(n) value which changes the oxygen delivery (the input) which the output (oxygen saturation) can be computed with the filter. Oxygen delivery will be the result of an offset SGN function based on eye level blood pressure and normal blood pressure. The representative blood pressures at the nodes are randomized based on values of the hScale matrix. The z0 matrix will be either set to 0 or 1 based on the threshold to turn on and off and then the percolation calculation through the matrix will occur resulting in a determination of connectivity. Some reduction in memory requirements may be possible by using the mean filter coefficients to calculate an oxygen saturation value and then applying statistical process to the result by node location. This modification would eliminate storing the filter coefficients in a matrix and also the filter number index matrix. The OxySat and OxyDel matrices may reduce to 20 x 20 and just hold the result at the node matrix size with no intermediate results needed. There is no indication that a time series average is being processed, just access to the filter coefficients.

As discussed above the algorithm matrix formulations used are a 20x20 element square matrix and the original storage dimensions were changed based on that reduction as indicated in Table 6. Reducing the matrix sizes to the correct value resulted in a 77% reduction of space requirements for those matrices. The model formulation used oxygen utilization filter coefficients generated in a statistically varied way with respect to standard deviation and then selected the filter coefficient set through a table of statistically generated filter numbers. Eliminating the three matrices associated with the oxygen utilization filter resulted in close to a 15,000 byte reduction in storage requirements. Overall the storage requirements were reduced to a quarter of the original calculation to approximately 34,000 bytes as seen in Table 6.

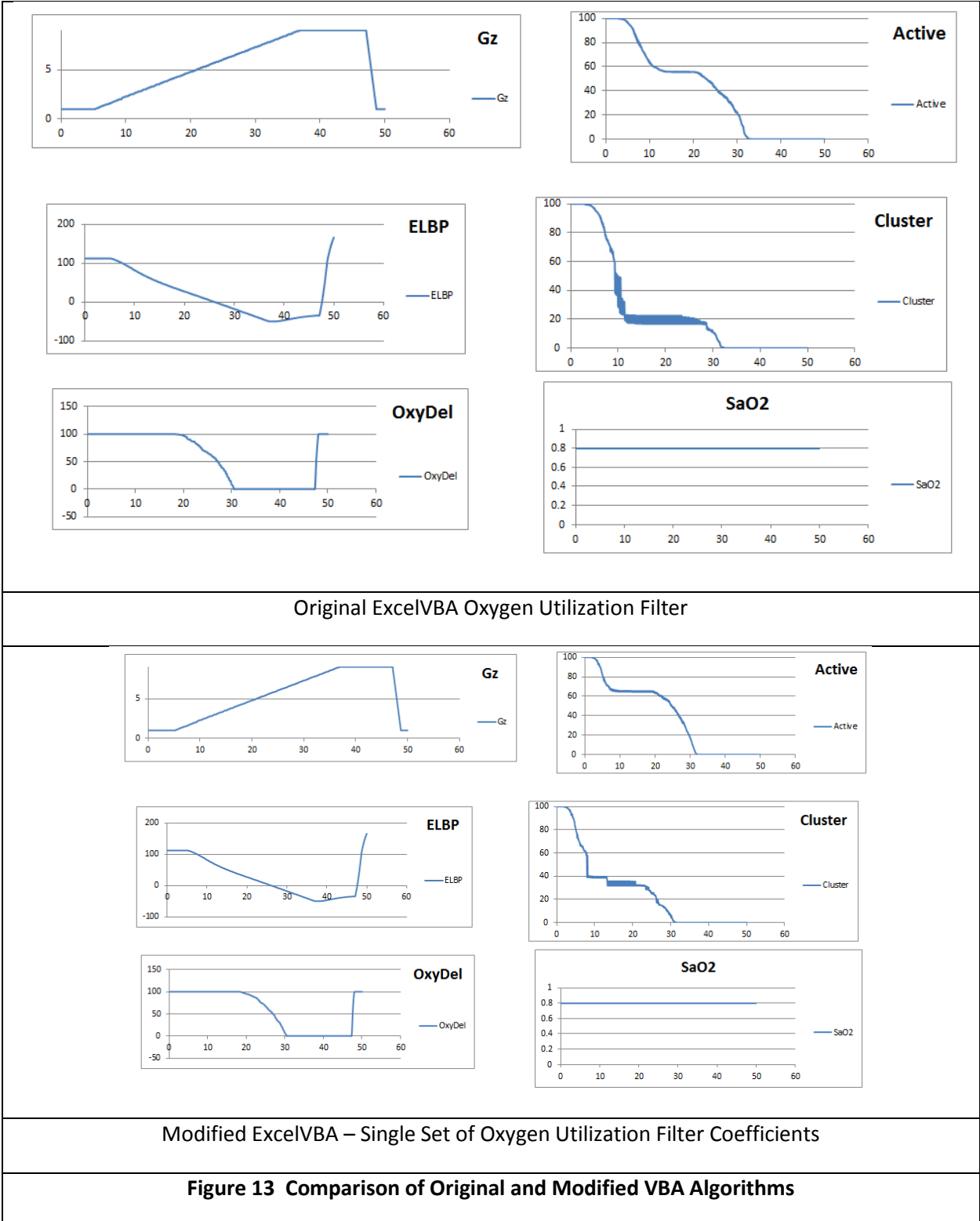
Table 6 Consciousness Model Current Variable Storage Requirements

Variable	Elements	Precision	Bytes	Total Bytes	Variable	New Total Bytes	Reduction
z0(42, 42)	1764	Single	4	7056	z0(20, 20)	1600	77%
OxySat(5, 42, 42)	8820	Single	4	35280	OxySat(5, 20, 20)	8000	77%
OxyDel(5, 42, 42)	8820	Single	4	35280	OxyDel(5, 20, 20)	8000	77%
FilterNum(42, 42)	1764	Single	4	7056	eliminated	0	-
OxyOffThresh(42, 42)	1764	Single	4	7056	OxyOffThresh(20, 20)	7056	0%
OxyOnThresh(42, 42)	1764	Single	4	7056	OxyOnThresh(20, 20)	7056	0%
AOxy(100, 5)	500	Double	8	4000	eliminated	40	99%
BOxy(100, 5)	500	Double	8	4000	eliminated	40	99%
ACV(3)	3	Single	4	12	ACV(3)	-	-
BCV(3)	3	Single	4	12	BCV(3)	-	-
Gz(2000)	2000	Single	4	8000	Gz(2000)	Buffer	TBD
EyeBP(3)	3	Single	4	12	EyeBP(3)	-	-
Sa(2000)	2000	Single	4	8000	Sa(2000)	Buffer	TBD
GStress(3)	3	Single	4	12	GStress(3)	-	-
hScale(42, 42)	1764	Single	4	7056	hScale(20, 20)	1600	77%

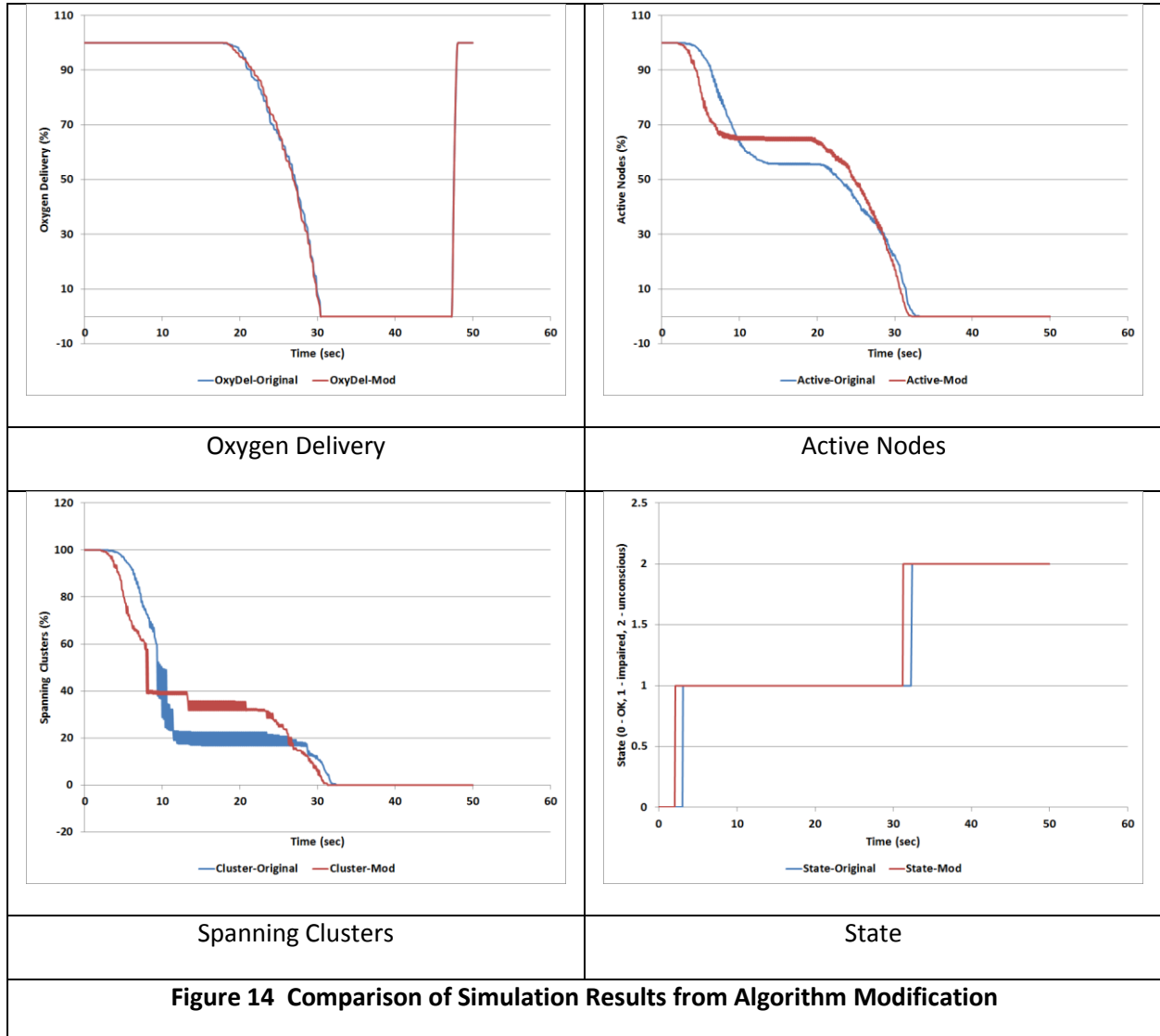
Starting total of 129,888 bytes compared to current total of 33,392 (excluding data buffers)

A single oxygen utilization calculation was used for each node point and a comparison screenshot of results is shown in Figure 13.

Document Title: HAMS Final Report (Technical and Financial)



Comparison model results are shown in Figure 14.



Oxygen delivery should agree closely since no changes are made with that calculation. The percentage of active nodes and spanning clusters differ somewhat by transition timing and level but generically the changes occur at about the same time and to the same levels. The predicted states change at essentially the same times with the modified calculation changing slightly earlier than the original method.

The implementation of the working model must be converted from the Visual Basic for Application version to a further stripped down Basic language version and then translated into at least a C language implementation to be hosted on a small sized microcontroller or embedded system. A larger sized process system such as a tablet or smart phone level approach would still need this conversion under most

implementation scenarios. The most up to date code was stripped of the Excel interface aspects and then converted to C language using BCX, a basic to C translator. The resulting C language code was modified and examined using the IAR embedded workbench set up for the MSP430 processor. The C code could be ported to any other processor with slight modification. Example items that were addressed are unnecessary library references and non-C language array indexing issues.

This processor choice was arbitrary but was influenced by Athena GTX's history of development with this device. The free IAR Workbench is code size limited and once all the errors were worked out one could go no further due to the larger code byte size. Code Composer from Texas Instruments was used to go further which allows for evaluation of various processor families within Texas Instruments product line. The MSP430F67791 was chosen for its large Flash ROM size of 512KB and the code came out to be about 2KB over that size. For the sake of finding a microcontroller that would fit for further debugging and emulation, a TMS470F06607 was used under Code Creator which has 640KB total program flash memory. Under this processor the program easily fit with some lingering errors that can be fixed without issue. Reducing the code size further will be discussed further in Task 4. Now that the real embedded system program storage requirements are understood more clearly we can move on to Task 4 and refine the code to meet the program objectives. The modified USN Consciousness Model code is able to be implemented on a micro-controller platform.

4.3.2 Task 3b – Determine Model Deficiencies for Hypoxia

The HAMS consciousness model works on the basis of rapid cessation of perfusion causing tissue/cell level oxygen reduction without regard for longer time course metabolism having any influence. This approach will not be sufficient for hypoxic hypoxia and a factor that reduces SaO₂ based on metabolism and work rate is needed even when oxygen delivery is fine to fully encompass the scope of anticipated utilization.

The desired relationship has not been found in the literature. At this point, we theorize that a series of runs with HumMod is needed to develop an oxygen utilization rate equation based on long time course hypoxia conditions alone to supplement the current oxygen consumption methodology. Initial work toward this end is discussed later in this section of the report. We will be exploring the validity of this approach as well as the potential for using alternate workload prediction algorithms used in previous Athena GTX projects such as the Hammerhead™ and DogBone™. This is particularly noteworthy for potential end users in ground operations and deploying to the ground in high altitude conditions.

The model mean node “off” threshold setting was varied and the effect examined with the SaO₂ time history from an immediate 40,000 ft. altitude exposure at normal gravity generated using HumMod (Version 1.6.1) and then acceleration response examined with an arbitrary 7G exposure to induce GLOC. An optimum mean “off” threshold of 0.8 was determined based on rapidity of predicting impairment and the altitude and acceleration exposures were combined for a simulation and the results are shown. Table 7 shows the summary prediction times while varying threshold level.

Table 7 Summary Simulation Results

“Off” threshold	Impairment Onset (sec)	Impairment Full Development (sec)	Unconsciousness (sec)
40,000 feet			
0.5	27.4	32.4	-
0.6	16.7	19.5	-
0.7	11.6	13.4	41.1
0.8	4.9	6.9	49.5
7 Gz			
0.5	9	9	10.9
0.6	8.5	8.5	10.3
0.7	8.2	8.2	10.4
0.8	7.7	7.7	10.3

Figure 15 through Figure 18 shows the time history response while varying the mean “off” threshold for both the 40,000 feet and 7Gz exposures.

Document Title: HAMS Final Report (Technical and Financial)

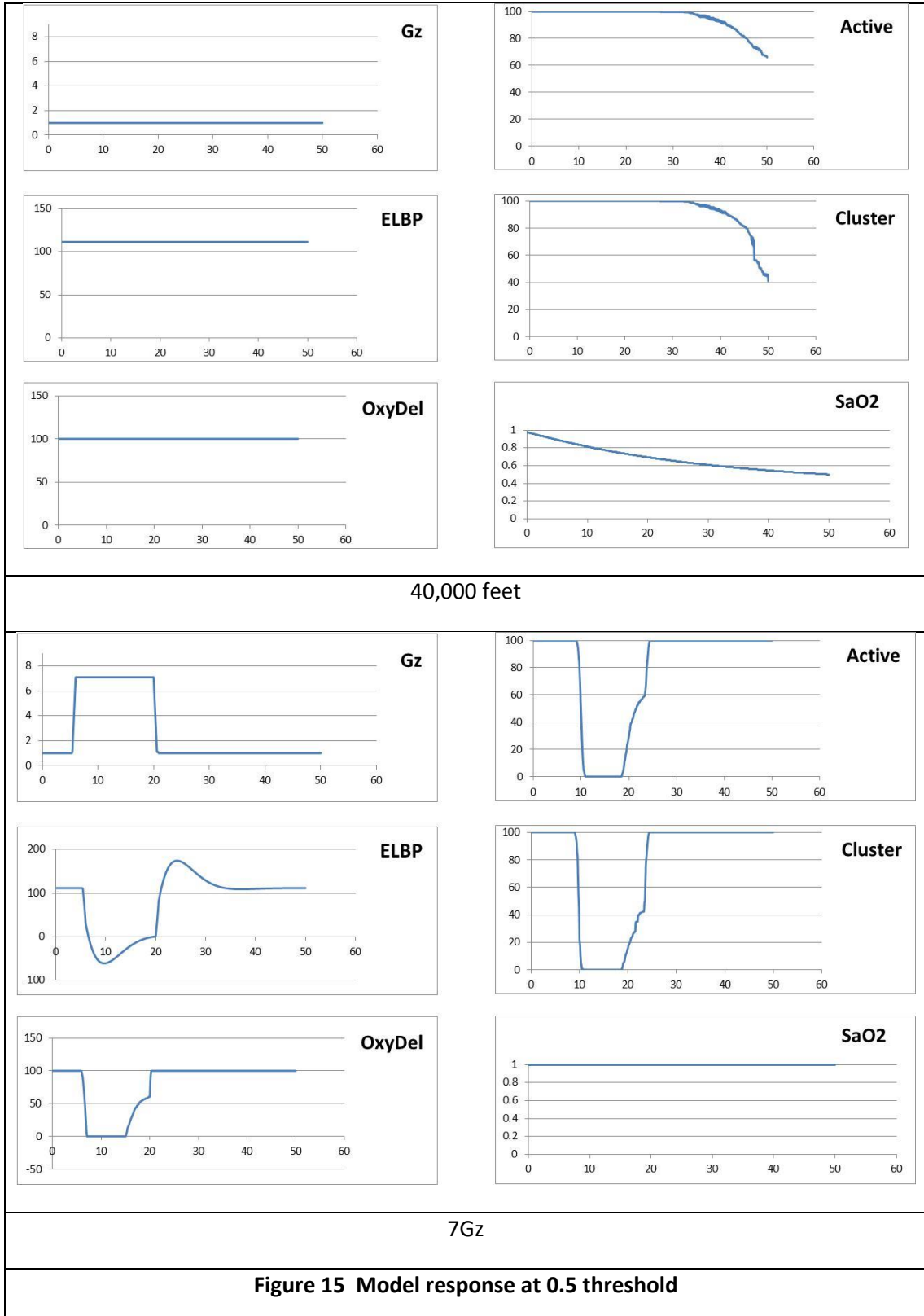


Figure 15 Model response at 0.5 threshold

Document Title: HAMS Final Report (Technical and Financial)

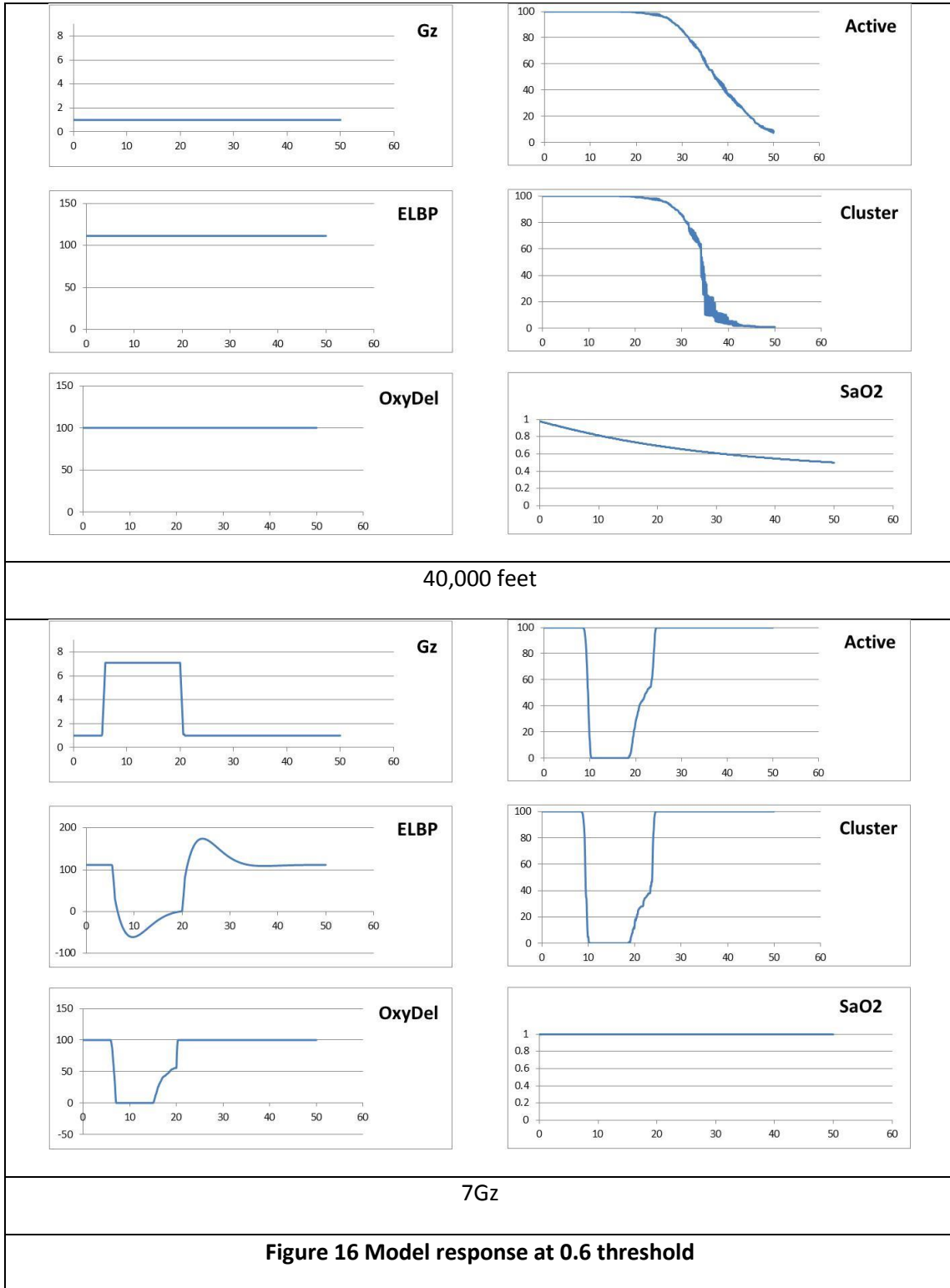


Figure 16 Model response at 0.6 threshold

Document Title: HAMS Final Report (Technical and Financial)

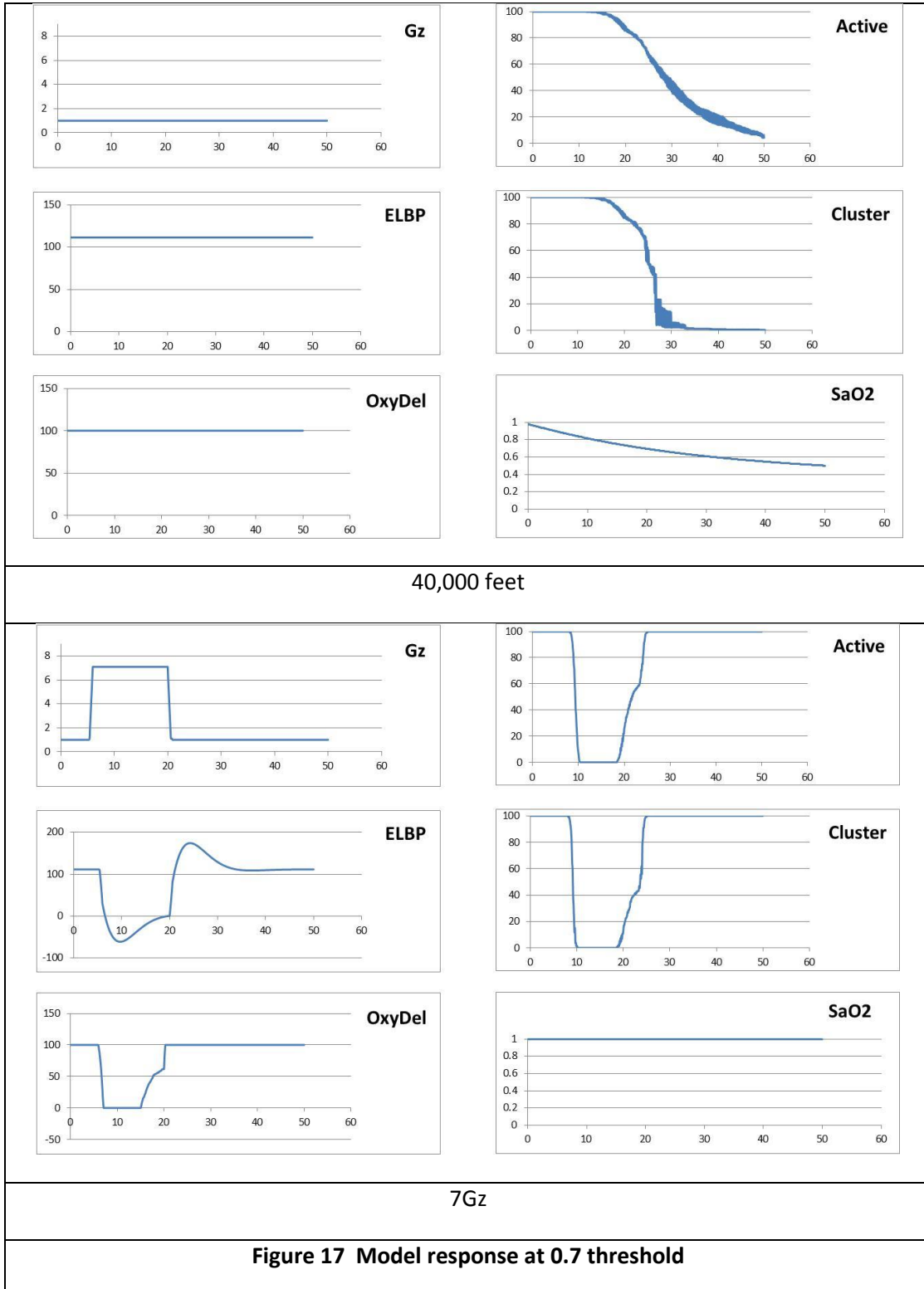
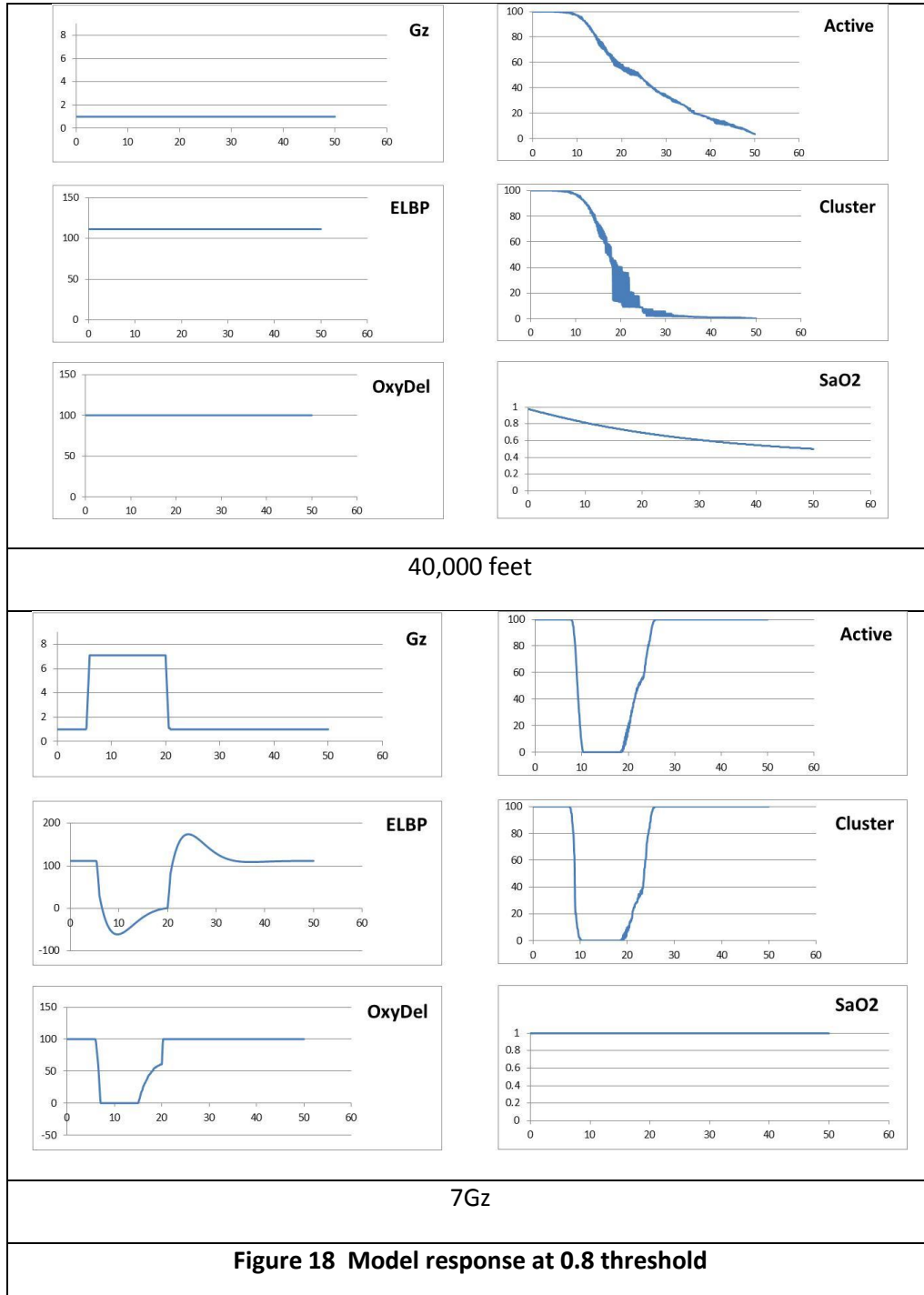


Figure 17 Model response at 0.7 threshold

Document Title: HAMS Final Report (Technical and Financial)



Both test conditions would be considered to induce unconsciousness in rapid fashion in less than or equal to 10 seconds given an initial subject seated, in a non-working condition. Increasing the mean “off” threshold lowers the impairment times for the hypoxia case but unconsciousness prediction is elusive

owing the likelihood that a connection still exists within the matrix. This can be improved unless we determine that the onset of impairment prediction is sufficient for our usage. For the acceleration case, the onset and development of full impairment are the same and times decrease as the threshold is raised. Unconsciousness is predicted and the threshold change shows little effect on the time predictions.

The combination of the 40,000 feet and 7Gz exposures were simulated and shown in Figure 19.

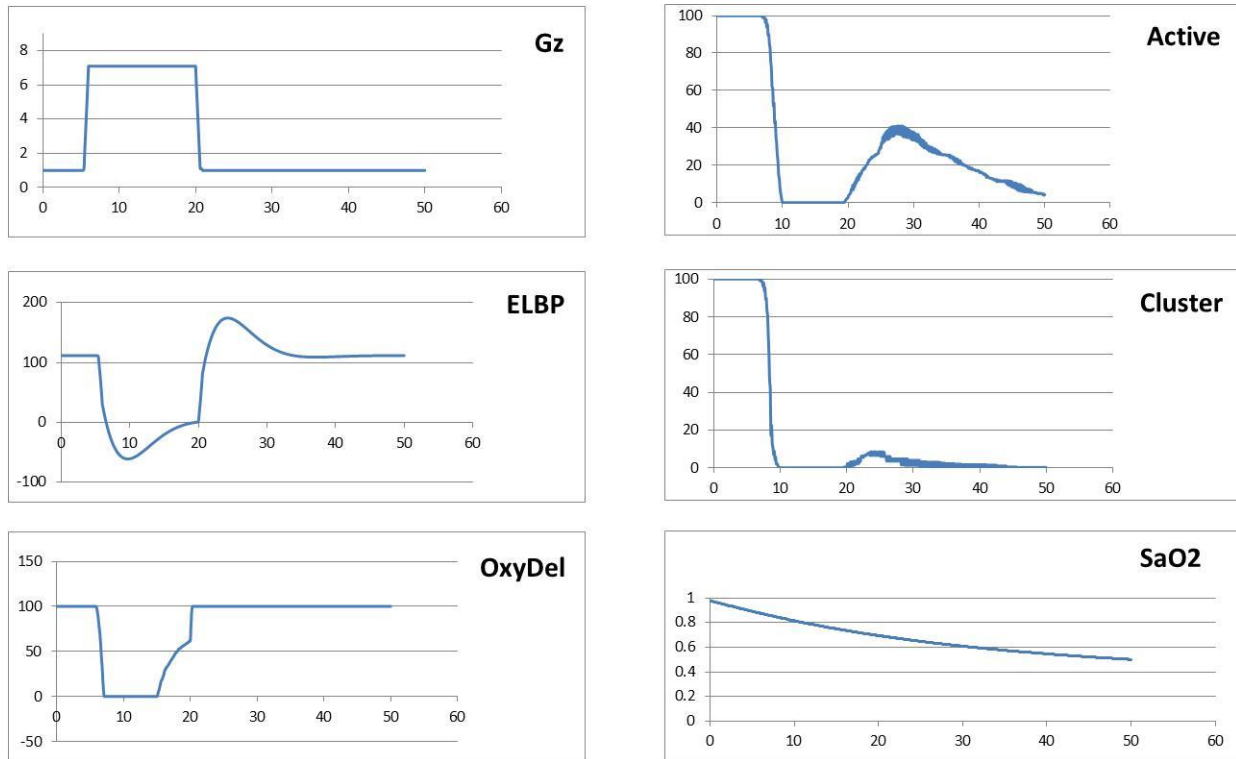


Figure 19 Combination of altitude and acceleration exposures

The onset and full development of impairment was 6.8 seconds and unconsciousness occurred at 10 seconds. After G offset from 7Gz, temporary recovery to impaired state was predicted but oscillated between impaired and unconscious 11 seconds after G offset through to the end of the simulation.

Preliminary HumMod model runs have been conducted to examine whether an SaO₂ based utilization function can be generated for use in conjunction with the unconsciousness model to cover longer, less extreme exposures to altitude while seated and during working activity such as walking and running. Walking or running at high terrestrial altitudes generally results in HumMod indicated muscle fatigue early on, which may indeed be correct. A mission profile needs to be developed that reflect change in altitude, pace and grade to be more realistic.

These results are encouraging for the utilization of the reduced model in the prediction of an abrupt exposure to an unconsciousness inducing exposure.

The HumMod model based on the Guyton work has been used to generate surrogate sensor data such as SaO₂ for model evaluation, to explore the reaction of the human physiology to longer, less severe acute hypoxia exposures, and the ground soldier physiological reaction to altitude operations. To insure we have the most validated simulation results, CAI has obtained the most current version of HumMod from HC Simulation LLC, the authorized agent for the University of Mississippi, for research purposes. CAI cannot distribute this model but other interested parties can obtain it from Dr. Hester at HC Simulation, LLC. This version of the model allows for creation of model time scenarios and specification of result time history timing.

Dr. Shender placed some raw data on the FTP site so that the 60 Hz SaO₂ data could be run through the unconsciousness model. Some code modification was necessary to shift the data interval from 0.1 to 1 sec but this was accomplished and results for Dr. Shender's Subject 7 which also included composite cognitive/psychomotor scores from a prior upload was examined. Promising State prediction results were found for impairment and recovery by looking at this physiological and cognitive data.

Some interesting observations where made:

- A decrement in composite score is difficult to define with a 4 point moving average for the 18K feet data
- After return to ground altitude the model and subjective response indicated an impaired state. Not too sure what this means.
- Interestingly, administration of 100% oxygen and return to ground altitude improved the SaO₂ response but composite score, predicted State and subjective response all indicate continued impairment and hypoxia effects indicating that SaO₂ alone may not be sufficient for neurological state prediction.

More subjects where the raw (60 Hz) SaO₂ data can be combined with the composite score data are needed for validation and tuning of thresholds. The details of the analysis are included below.

Two exposures, one to 18,000 and the other to 25,000 feet, were given. The session started at ground altitude and then progressed to 10,000 feet before the simulated ascension to the test altitude using a reduced oxygen mixture to simulate altitude.

Figure 20 shows Subjects 7's SaO₂ 18,000 feet data and predicted values for active nodes, connected clusters and neurological state at a threshold of 100% loss of spanning clusters and at 80% loss of spanning clusters. Considering "impairment" as State "1", once the SaO₂ dropped below 90% an impaired state was indicated. With the threshold of 100% loss of a spanning cluster no loss of consciousness (LOC) was indicated but when changed to 80% an LOC was indicated as SaO₂ approached 60%.

	<p>Oxygen saturation</p>
	<p>Percentage of Active nodes</p>
	<p>Percentage of Nodes Connected.</p>
	<p>Cluster threshold at 0% for LOC. Impairment predicted but on "LOC" even with low percentage of connectivity. Wide blue areas represent uncertainty in non-impaired and impaired state.</p>
	<p>Cluster threshold at 20% for LOC. "LOC" predicted (none occurred) but span of blue between approximately 1200 and 1600 represent uncertainty in impaired and LOC states.</p>

Figure 20 Subject 7 exposure to 18,000 simulated with the USN Consciousness Model

A closer look is seen in Figure 21 and Figure 22 where the composite score from cognitive and psychomotor testing is also shown along with SaO₂ and State. A decrement in composite score is difficult to ascertain even with a 4 point moving average.

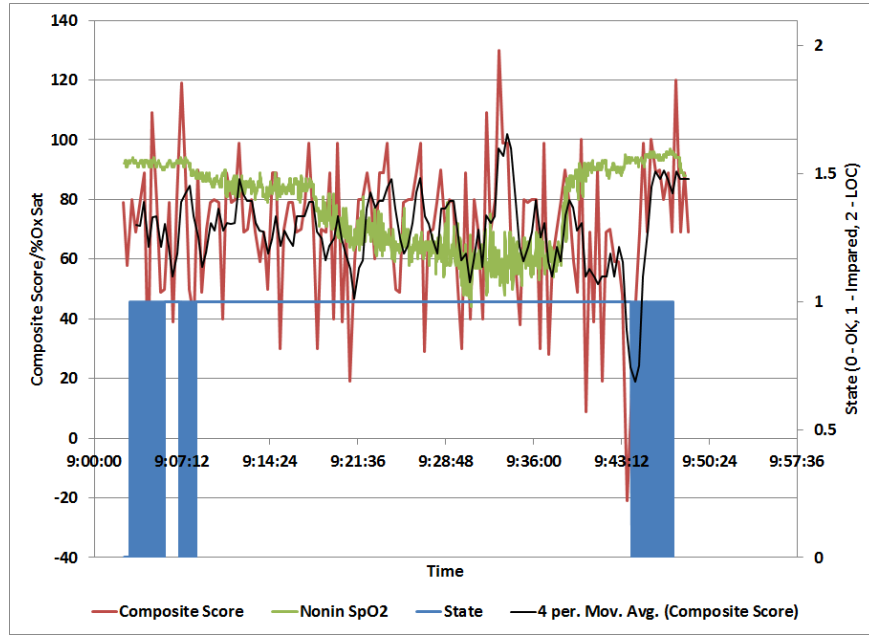


Figure 21 LOC threshold at 0% Connectivity for Subject 7 at 18,000 feet.

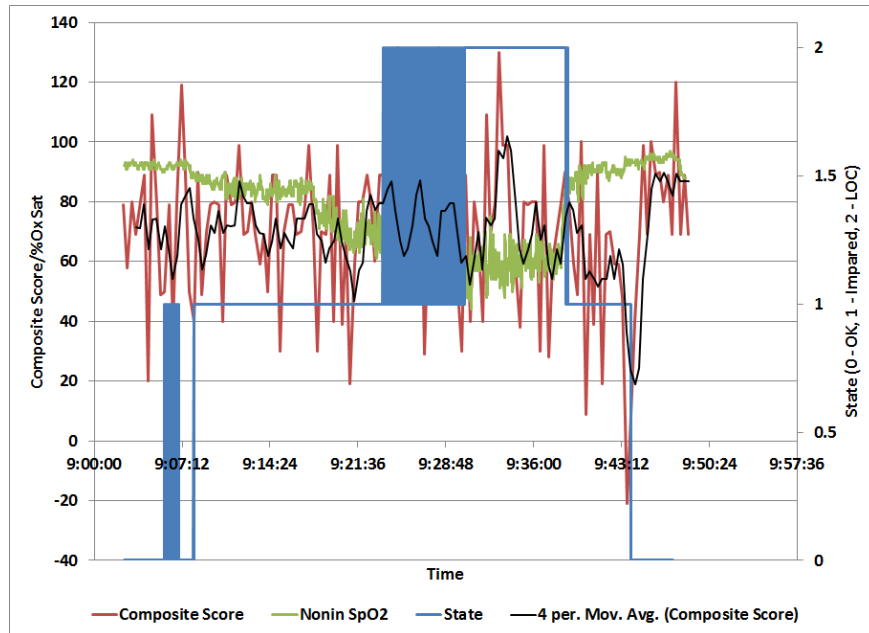


Figure 22 LOC threshold at 20% Connectivity for Subject 7 at 18,000 feet.

Table 8 shows the subjective response for Subject 7 where lightheadedness was indicated at times where significant loss of active nodes and connectivity were predicted.

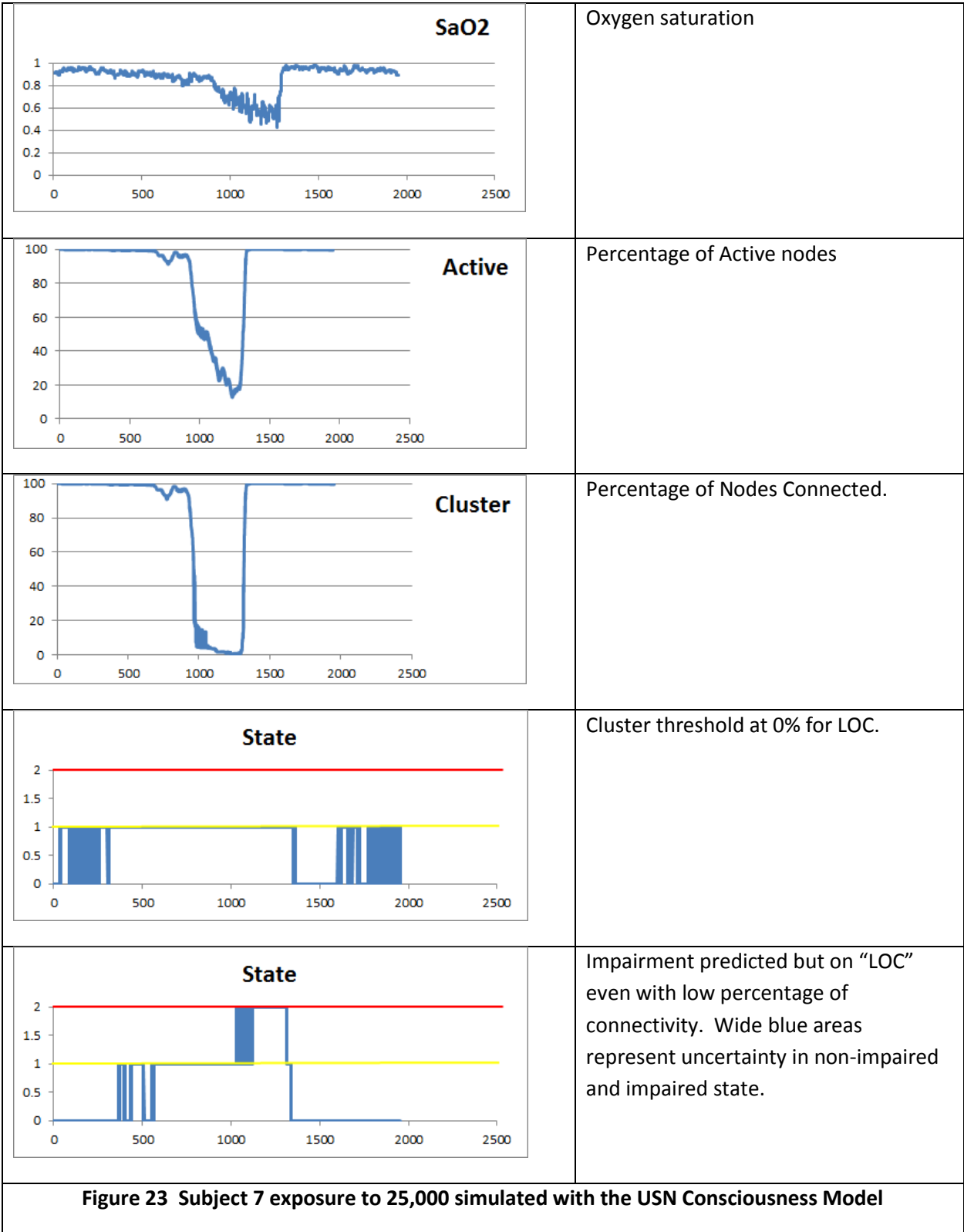
Table 8 Experimental Subjective Response for Subject 7 at 18,000 feet

9:07:49	10,000	
	10,000	
9:17:57	18,000	
9:19:38	18,000	lightheaded
	18,000	
9:28:46	18,000	lightheaded
	18,000	
9:37:54	0	
9:40:16	0	lightheaded

Even after return to ground altitude the model and subjective response indicated an impaired state.

Figure 23 shows Subject 7's SaO₂ 25,000 feet data and predicted values for active nodes, connected clusters and neurological state at a threshold of 100% loss of spanning clusters and at 80% loss of spanning clusters. Considering "impairment" as State "1", once the SaO₂ dropped below 90% an impaired state was again indicated. With the threshold of 100% loss of a spanning cluster no loss of consciousness (LOC) was indicated but when changed to 80% an LOC was indicated as SaO₂ approached 60%. The loss of active nodes and spanning clusters was faster for the 25,000 feet exposure compared to the 18,000 feet exposure due to the more rapid drop in SaO₂.

Looking at Figure 24 and Figure 25 where the composite score from cognitive and psychomotor testing is shown along with SaO₂ and State. A marked drop in composite score is shown that corresponds to the onset of the oscillation between impaired and LOC states. Subject 7 was administered 100% Oxygen and while the SaO₂ rose towards normal, the composite score and predicted State both showed impairment indicating that SaO₂ alone may not be sufficient for neurological state prediction.



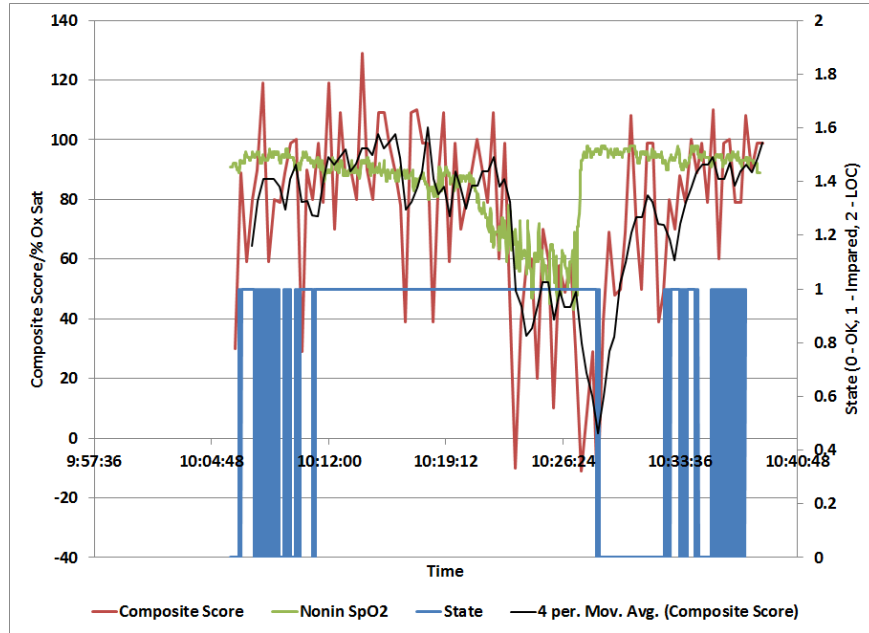


Figure 24 LOC threshold at 0% Connectivity for Subject 7 at 25,000 feet.

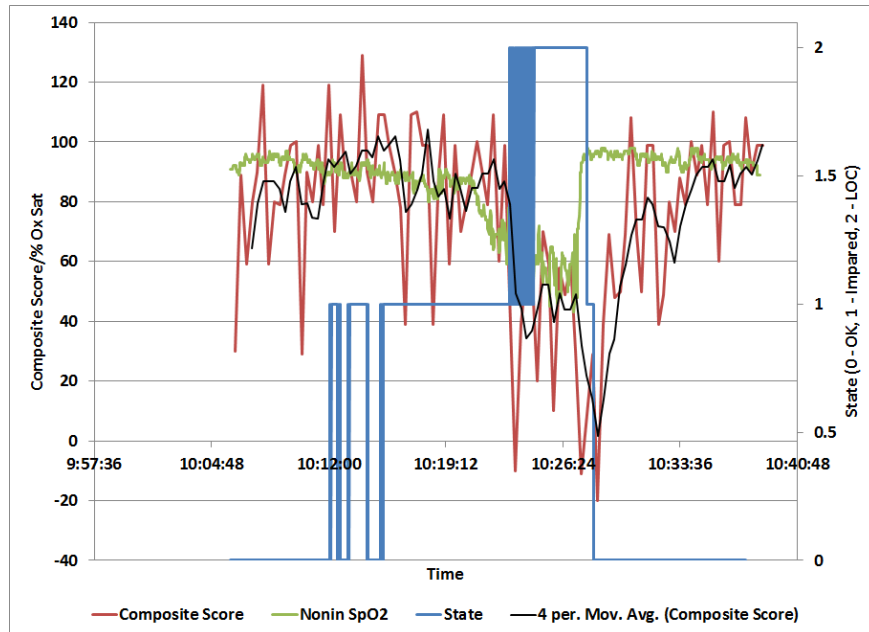


Figure 25 LOC threshold at 20% Connectivity for Subject 7 at 25,000 feet.

Table 9 shows the subjective response and study events for Subject 7 at 25,000 feet. Indications of lightheadedness and tingling fingers occur during predicted impairment and LOC periods.

Table 9 Experimental Subjective Response for Subject 7 at 25,000 feet

10:22:29	25000	lightheaded
10:22:49	25000	
10:23:09	25000	lightheaded
10:23:29	25000	
10:23:50	25000	
10:24:10	25000	tingling fingers
10:24:30	25000	
10:24:50	25000	lightheaded
10:25:11	25000	
10:25:31	25000	
10:25:51	25000	
10:26:11	25000	
10:26:32	25000	lightheaded
10:26:52	25000	
10:27:12	25000	
10:27:33	25000	tingling fingers
10:27:53	100% O2	brightness
10:28:13	100% O2	
10:28:33	0	
10:28:54	0	
10:29:15	0	
10:29:35	0	
10:29:55	0	LH & Tingling

Interestingly administration of 100% oxygen and return to ground altitude improved the SaO₂ response but composite score, predicted State and subjective response all indicate continued impairment and hypoxia effects.

Time differences between data sources may render an exact alignment of SaO₂, predicted State, and composite score difficult, but one can see that the corroboration is good for the one subject at 25,000 feet. Further understanding of the composite score results and even a breakdown of constituent metrics at 18,000 feet are needed before any real indication of impairment can be made.

The above analysis indicated some promising results in terms of prediction of onset and recovery, but there were spans where the model exhibited regions of uncertainty and bounced back and forth between states. This aspect of the prediction was investigated to see if that behavior could be minimized or eliminated. Two factors influence this behavior. One factor is the threshold for a node being turned off within the connected node set and the other factor is the connectivity top to bottom in the node set. If

the connectivity was zero then unconsciousness was declared in the original algorithm for GLOC but the model results displayed some possible computational features that might not drive the value to zero in the hypoxia only state, so altering this relationship could produce more sensitivity. Using the Subject 7 at 18,000 feet, these two factors, threshold and connectivity, were adjusted with positive results. The detailed analysis is included below.

The threshold was adjusted to 0.5, 0.69 (starting), 0.8, 0.85 and 0.9. The connectivity was adjusted between zero and < 20 for each of the threshold factors. The < 20 value was used based on preliminary adjustments where that value made a difference in predicted results.

Figure 26 shows the SaO₂ for this subject during the run. The SaO₂ starts out in the low 0.9 range likely due to the 10,000 ft. ascension at the beginning.

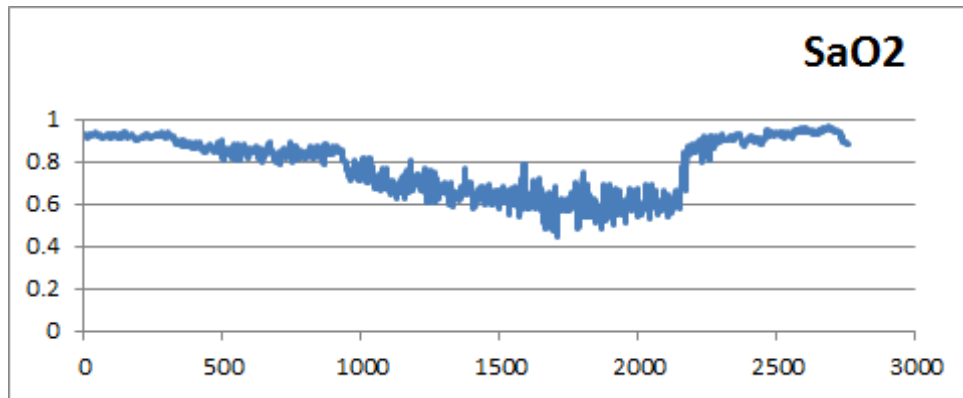
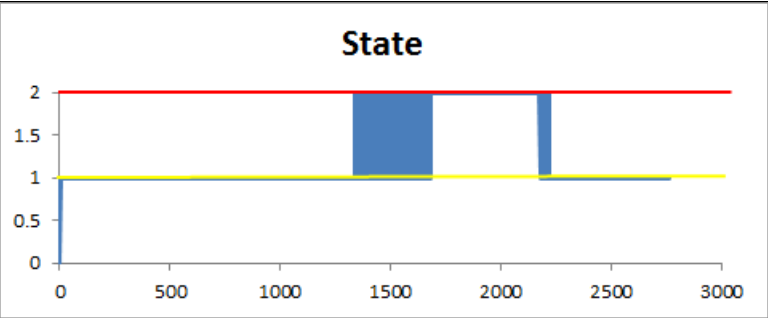
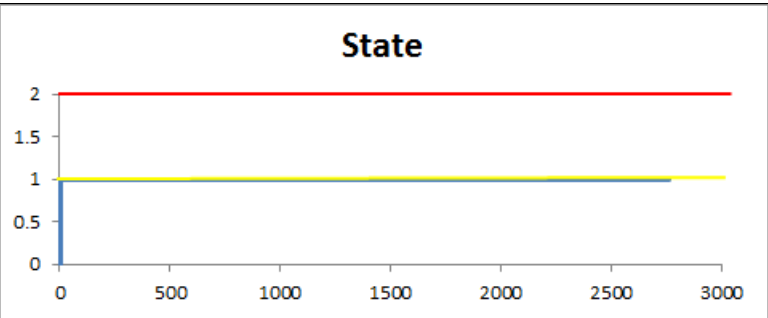
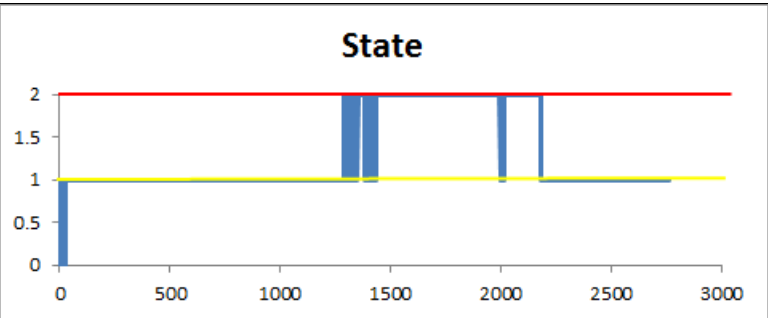
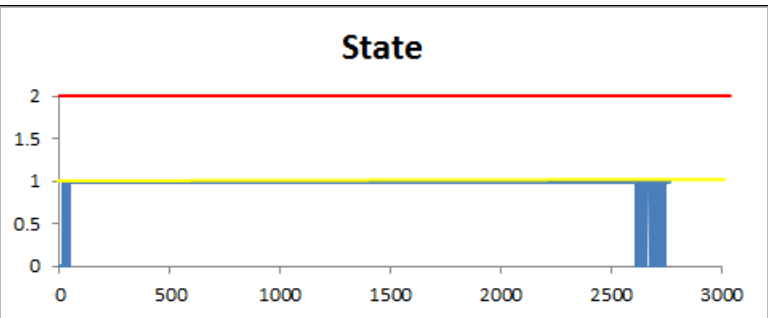


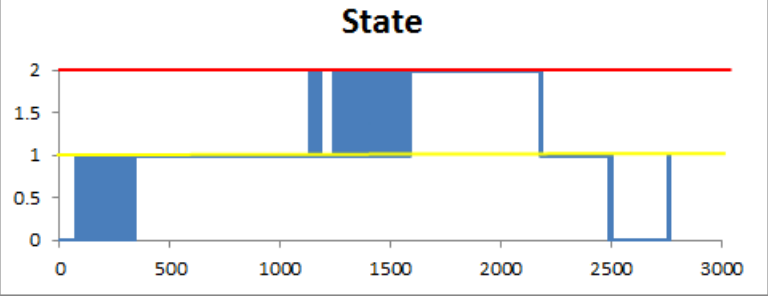
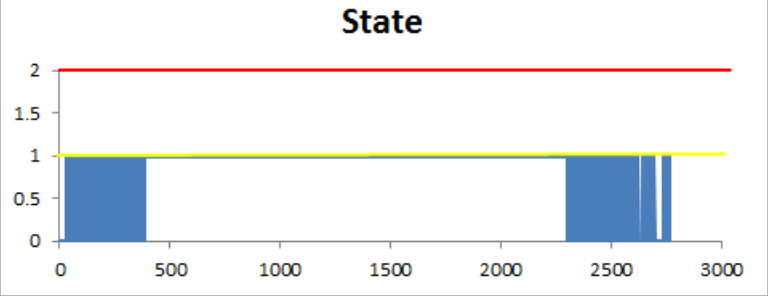
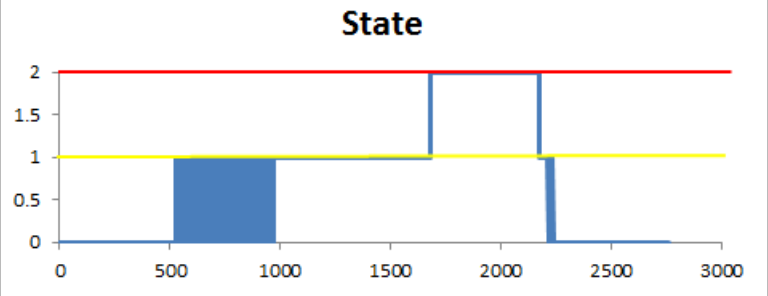
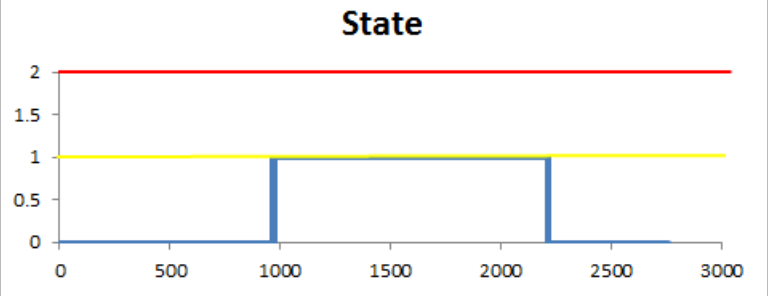
Figure 26 Subject 7 SaO₂ values at 18,000 feet. (Horizontal axis – time (sec))

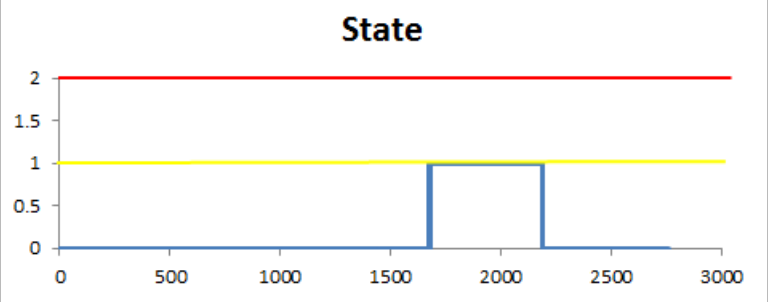
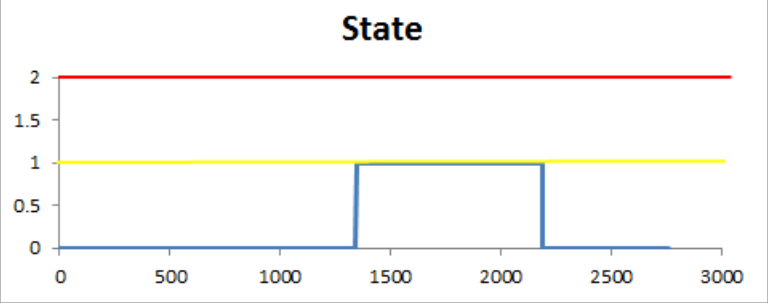
At approximately 500 seconds the SaO₂ value drops to 85% and drops below 80% at 937 seconds. These values are significant based on clinical factors but also that SaO₂ monitors may be less reliable or at least not calibrated below 80%.

Table 10 shows the “State” prediction results from the model where the threshold and connectivity were varied as indicates. A State of zero indicates no impairment, a “1” (yellow line) indicates impairment and a “2” (red line) indicates unconsciousness. As Subject 7 did not experience unconsciousness moving the connectivity parameter to < 20 appears unwarranted since it tended to predict a loss of consciousness. With the threshold value at 0.9 a prediction of impairment was immediately indicated and as the threshold value was lowered, the impairment prediction shifted in time but with the oscillation in impairment prediction as noted before. The one combination of threshold and connectivity that had the least amount of uncertainty was a threshold of 0.69 and a connectivity of zero. While this removed the unwanted behavior, this combination did not predict impairment until SaO₂ crossed below 80% but did show the demonstrated lag in predicting non-impaired state after the SaO₂ had recovered to baseline.

Table 10 Decision value variations for the Neurological State Model

State Prediction	Threshold	Connectivity
	0.9	< 20
	0.9	0
	0.85	< 20
	0.85	0

State Prediction	Threshold	Connectivity
	0.8	< 20
	0.8	0
	0.69	< 20
	0.69	0

State Prediction	Threshold	Connectivity
	0.5	< 20
	0.5	0

Horizontal axis is time in seconds

Figure 27 shows a comparison of SaO₂ with two simulation output parameters, active and cluster mass for the Subject 7, 18,000 ft. run with threshold at 0.69 and connectivity at zero. Active indicates the percentage of nodes active and cluster mass indicated the percentage of nodes connected.

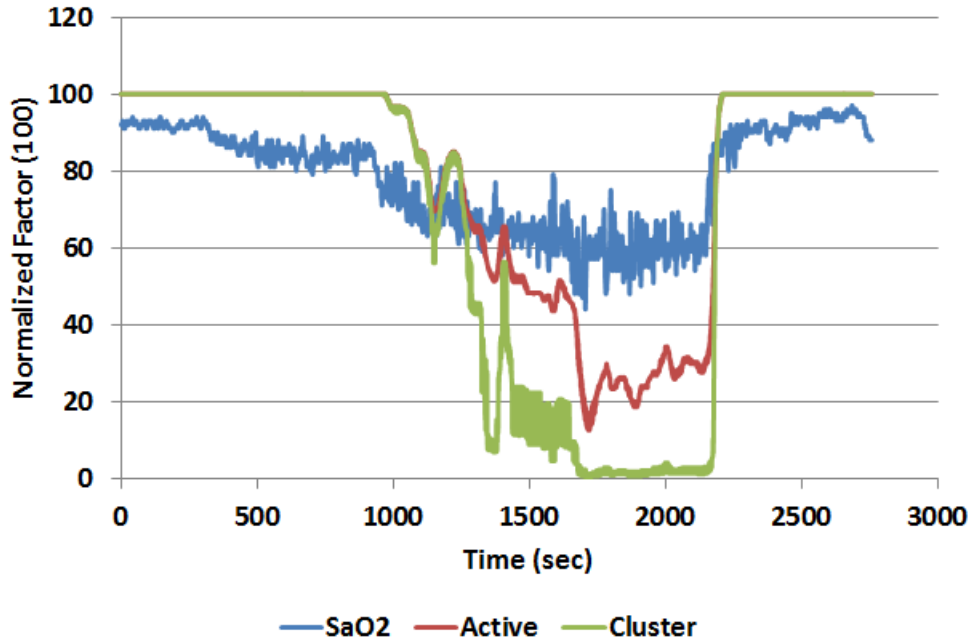


Figure 27 Simulation output values, active and cluster mass, compared to SaO₂

Interestingly the two parameters track each other starting to decrease when SaO₂ goes below 80% but diverge around 1250 seconds. The two parameters track with SaO₂ recovery almost exactly and do not show the demonstrated lag in performance recovery. Using these predicted parameters may not prove useful in neurological state prediction.

More subjects where the raw (60 Hz) SaO₂ data can be combined with the composite score data are needed for validation and turning of thresholds that were analyzed above.

4.3.3 Task 3c – Determine Model Deficiencies - Other

Several existing models and algorithms from recent and on-going programs at Athena (ACCS state assessment, Hammerhead™ and mini-Medic®) have been evaluated for their applicability to this project. The following summarizes the current findings.

Autonomous Combat Casualty Care System (ACCS) – The current algorithm development under the ACCS program includes a comprehensive multi-parameter medical status determination on the casualty from point of injury (POI) to definitive care. This diagnostic algorithm includes near real time non-invasive assessments with closed loop control of therapeutics which includes ventilation, fluid resuscitation and anesthetics/analgesics. The coding underway for the program includes remote care providers interfacing directly with both the diagnostics and therapies via wired on site (Tablet) and wireless off site providers and subject matter experts. As the casualty is transported from the POI transitions to environmental extremes of altitude exacerbate the pressure, vibratory interferences, and temperature of the patient and system. In addition specific diagnosis and therapies for suspected mild to moderate TBI are included. These in turn impact therapies. These codes are directly relevant to the Phase 1 HAMS CASEVAC application.

Hammerhead – When this task was completed Athena was waiting for permission to use the algorithms developed under this project in HAMS. These algorithms are particularly applicable to workload and fatigue at altitude when hypoxia may be apparent. The primary application is ground troop operations. Permission was granted late in the program and further discussion is included in Section 4.4.1 of this report.

Mini-Medic – Mini-Medic is a multi-parameter, FDA cleared monitor that incorporates a summary alarm feature called Murphy Factor. Murphy Factor is a concept for integrating multiple parameters into a single output alarm signal. Although the exact algorithm would need to be modified for HAMS a similar approach is applicable to this project and is applicable to both the ground operations and CASEVAC applications.

4.4 Task 4 – BETA Model Software Development/Definition

The two algorithm approaches developed under this program have both proved to be viable. In their current form each can provide predictions based on only a few input variables and have the potential to be further customized to individual tolerances. There are several options that can be implemented moving forward:

- Each model can act independently with a decision fusion for a final outcome,
- One can focus on prediction of parameters and one can predict state,
- One model can feed the other data during periods of sensor dropouts or
- Combinations of the above depending on the data availability.

Individual model approach adjustments and refinements have continued as we worked towards an integrated model. The top level block diagram for the model is shown below.

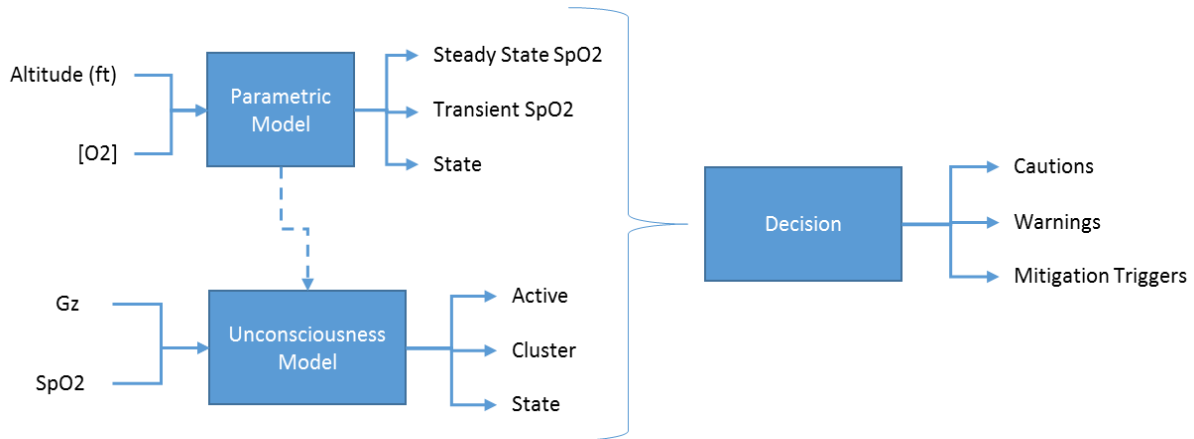


Figure 28. Integrated BETA Model Block Diagram

To fully integrate the models in a meaningful way will require a specific hardware solution to be available. This will be accomplished in HAMS II. Final results will be reported under this task individually for each model (parametric and unconscious model).

4.4.1 Parametric Model

Several options were explored for the altitude dependent exponent time constant (a) for the time dependent function of the form:

$$K_1 + K_2 e^{-at}$$

The following functions were evaluated:

Option for "a" term	Altitude (feet)	Function
Constant	0 to 18K	0.0045
	18K to 40K	0.015
Linear	0 to 18K	0.0045
	18K to 40K	0.0000015*Alt-0.0225
Exponential	0 to 18K	0.0045
	18K to 40K	0.0002*EXP(0.000172*Alt)

Additionally the delay term needs to be removed at 40,000 feet. Example responses using the above options are shown in the graphs below.

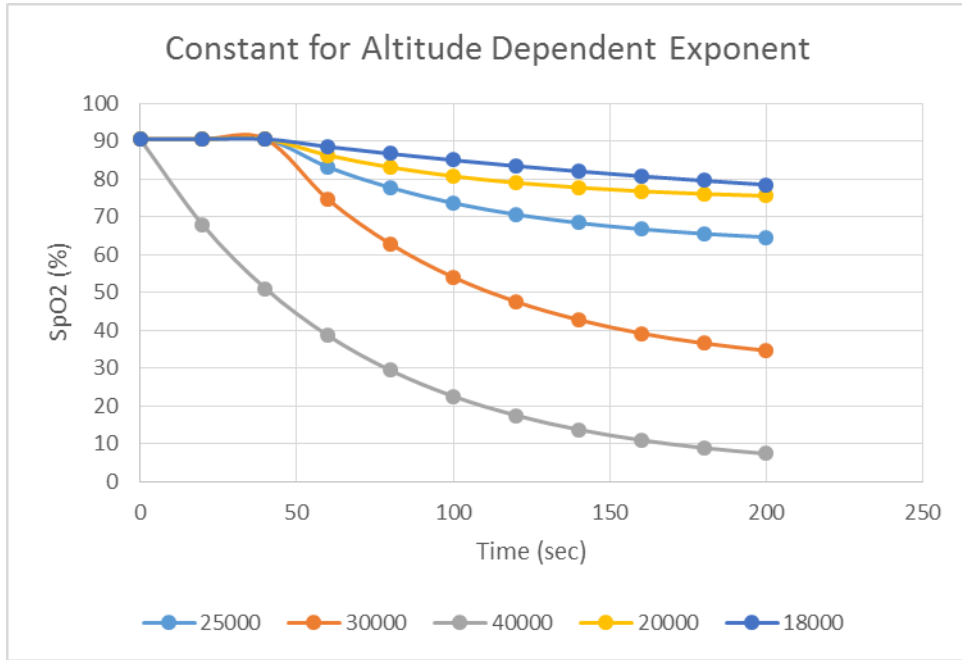


Figure 29. Altitude Dependent Exponent Evaluation - Constant

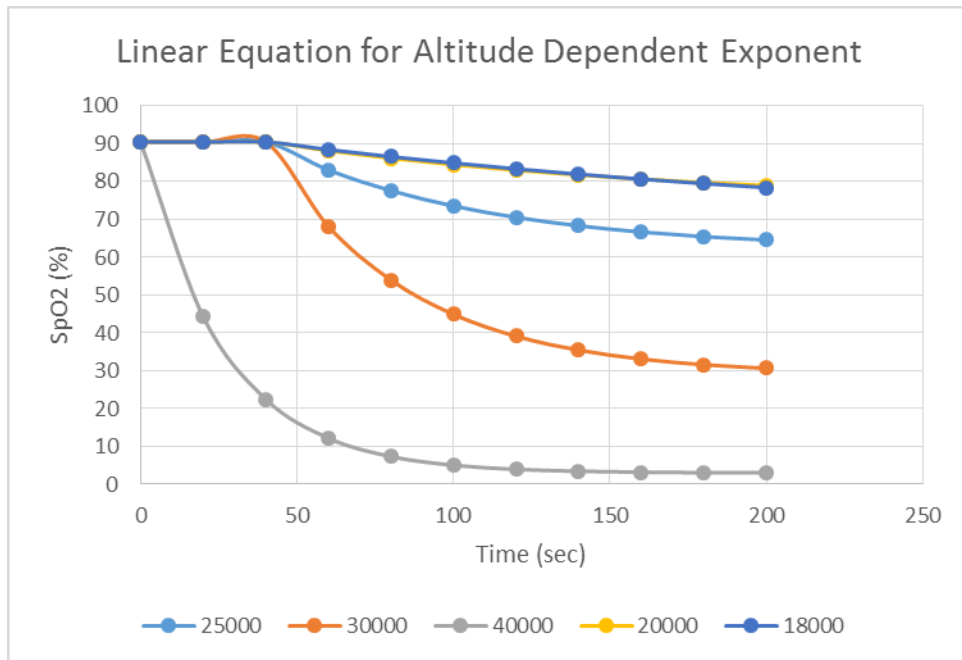


Figure 30. Altitude Dependent Exponent Evaluation – Linear Equation

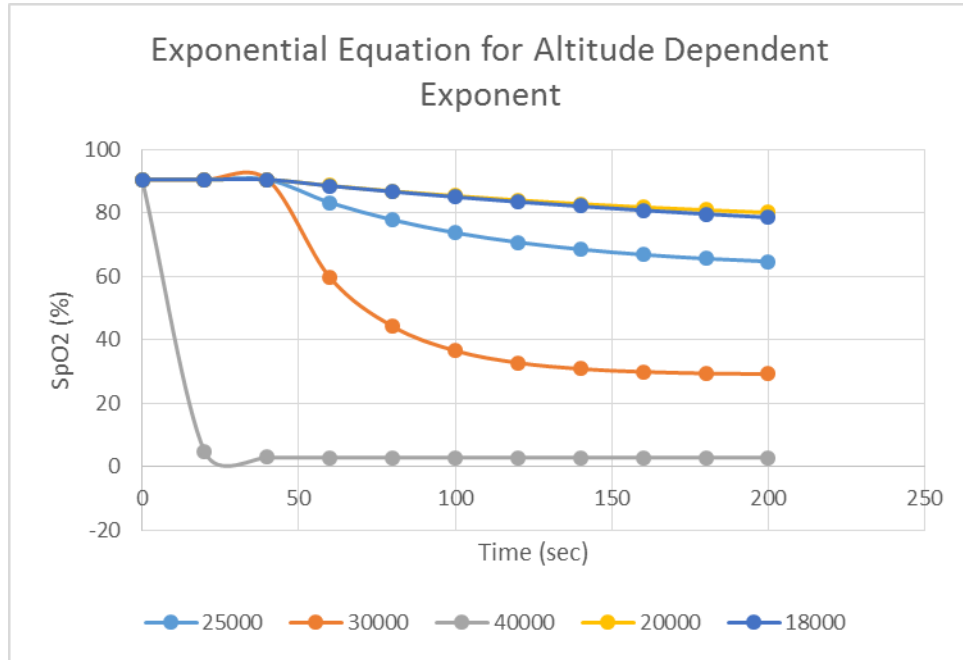


Figure 31. Altitude Dependent Exponent Evaluation - Exponential Equation

The exponential function was chosen and more closely matches the expected results at 40,000 feet based on classic time of useful consciousness values of 15 to 20 seconds as discussed in DeHart Table 5-12.

During the initial stages of model verification, an anomaly at 10,000 feet was discovered in the model output data. The model was predicting SpO2 to be too high (97% vs. expected 90%). The oxygen dissociation curve pH shift correction part of the model was found to be the cause and needed to be corrected. This has been accomplished, but required an alternate approach to account for the pH shift in the oxygen dissociation curve. The algorithm still relies on the Henderson-Hasselbach Equation for estimating the blood pH, however the SpO2 estimation now uses an adaptation of Hill’s equation to estimate the steady state SpO2 values at a given altitude and oxygen breathing concentration. We now feel that this prediction is much improved over the previous method.

$$pH = 6.1 + \log_{10} \left(\frac{HCO_3^-}{0.03 \cdot PCO_2} \right) \quad \text{Henderson-Hasselbach}$$

$$SpO2 = \left(\frac{PO_2}{P_{50}} \right)^n \div \left[1 + \left(\frac{PO_2}{P_{50}} \right)^n \right] \quad \text{Hill's Equation}$$

Where, P_{50} is the PO_2 at which O_2 saturation is 50% at a given blood pH and n is about 2.7 for human blood. The P_{50} values are calculated based on the estimated pH and data from DeHart (pg. 83). The results are shown in the figure below.

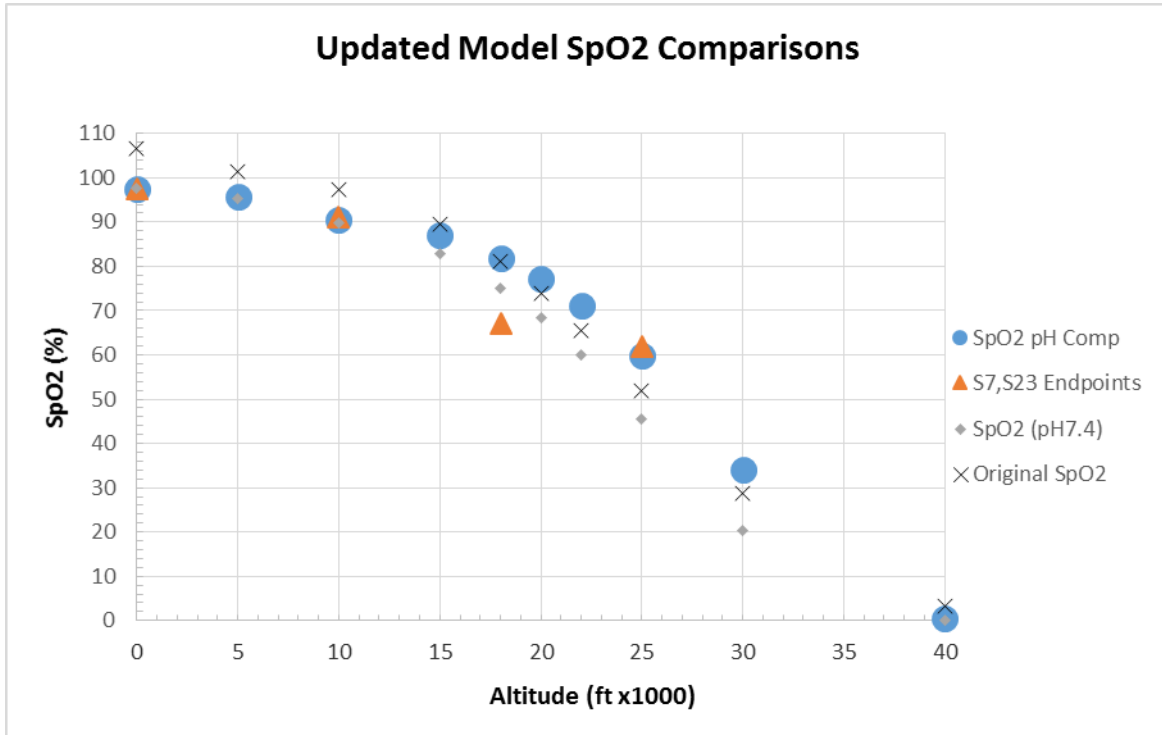


Figure 32. Updated Model for SpO2 Calculations

The original SpO2 calculation (X) overestimates at lower altitudes and underestimates at higher altitudes. Without pH correction (SpO2 (pH7.4), grey diamond) the estimate is better at lower altitudes, but still underestimates at higher altitudes. By adding the pH compensation (blue dots), the estimate appears to be better at all altitudes. This can be seen when compared to the steady state endpoints of S7 and S23 (orange triangles) with the exception of the 18,000 ft. data. At this point we are not sure why this data point is much lower than predicted.

The integration of the time dependent algorithm equations was completed. There are two parts to the time-dependent equations:

- Delay
- Ordinary Differential Equation with an analytical solution in the form

$$K_1 + K_2 e^{-at}$$

This is of the same form as a simple Resistor/Capacitor network. Consequently, the transient analysis (or simulation) can be implemented using numerical integration techniques similar to how the SPICE algorithm performs this analysis using the Backward-Euler method:

$$x_{n+1} = x_n + h \frac{dx_{n+1}}{dt}$$

Where “h” is the time step.

We can derive a transient analysis/simulation equation in terms of the time step “h”, time constant “a”, the current SpO2 value and steady state SpO2 estimate/prediction. The resulting equation is as follows:

$$SpO2rt_{n+1} = \frac{\frac{1}{h} \cdot SpO2rt_n + SpO2 \cdot a}{\frac{1}{h} + a}$$

Where SpO2rt is the output estimate of the algorithm at each time step “h”. The “n” is the current state and “n+1” is the next state of the model output.

To illustrate the implementation of this approach the figure below shows a comparison between how each method would perform if implemented in a “real-time” mode using the ROBD study run of 0K to 10K to 18K to 0K. The actual data from one of the sensors from both S7 and S23 are also included. The Outputs are as follows:

- AS out – This represents the model output over time using the Analytical Solution. Notice that once a sufficient amount of time has elapsed, the decaying exponential becomes negligible and the output immediately goes to the steady state at the transition points which is not representative of the actual response we intend to model.
- AS out (reset) – To demonstrate the “desired” response using the Analytical Solution, we have to artificially reset the time to “zero” at each transition. This is relatively easy for our example below because we know the transition points and they are simple step changes in altitude. “AS out” shows the results of this approach, but is not practical to implement in real-time.
- BE out (Simple) – This represents the Backward-Euler method implementation. The response is as desired and does not require the time to be “reset to zero” at a transition point. The model will respond to an input change at any time.
- S7 and S23 – These plots are the data from S7 and S23 from one of the sensors of each subject as a reference point for the model output.

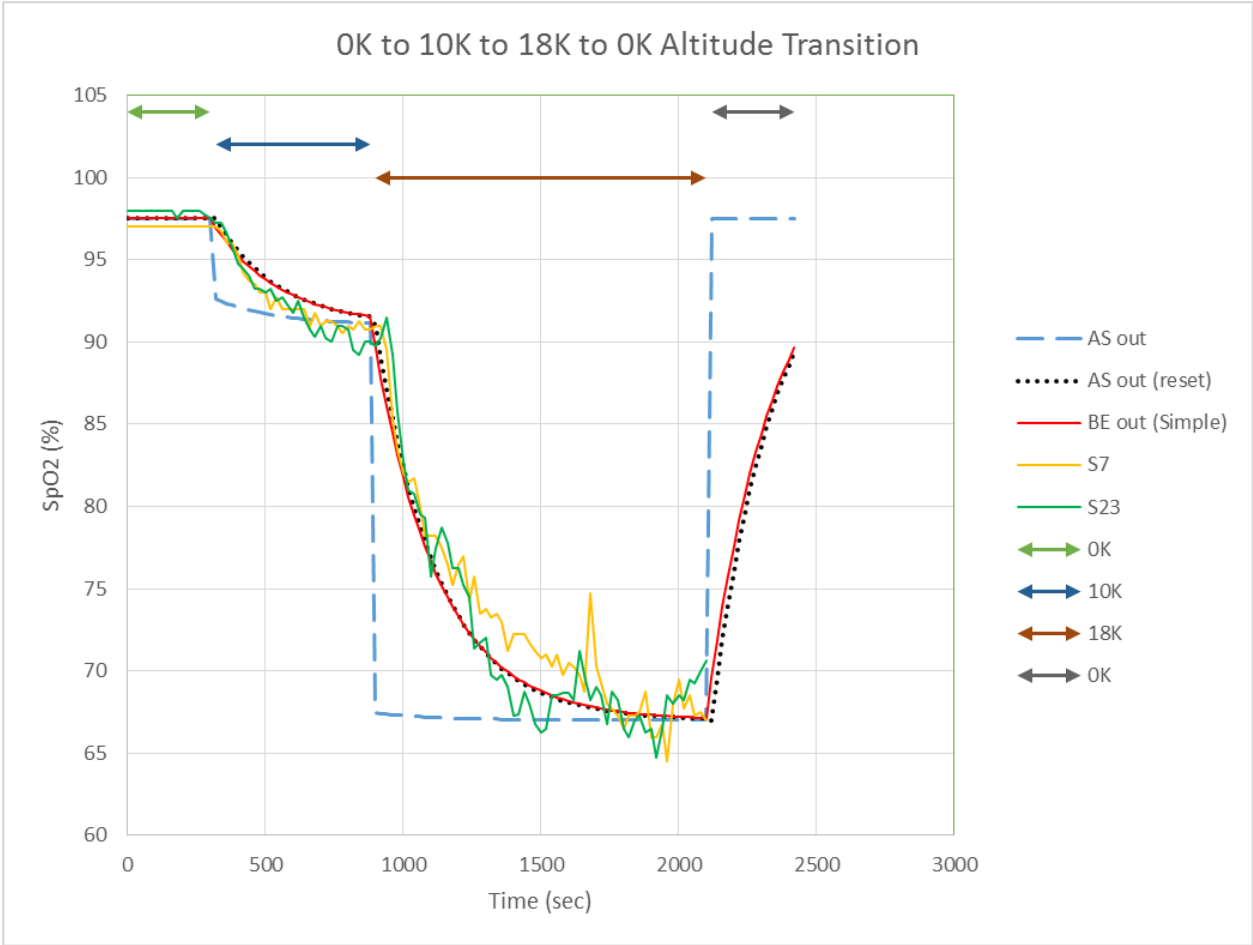


Figure 33. Parametric Transient Time Dependent Output

The above example does not include the delay function, but that is a straightforward sample delay and memory allocation issue that is simple to accommodate and will depend on the “sample rate”. This is left for the hardware implementation stage.

The modifications made to the model were updated in the “C” Code implementation and verified. The following table shows the steady state verification table that includes the inputs (Altitude and [O2]) and corresponding outputs from the Excel and “C” Code implementations. These outputs agree with the exception of some small rounding errors that are insignificant (0.1 %SpO2 – Only whole number SpO2 values are needed).

Table 11 "C" Code Output Verification – Steady State Output

Altitude (feet)	[O2]	Excel Model Output	"C" Code Model Output
0	0.21	97.5	97.5
5000	0.21	95.6	95.6
10000	0.21	92.5	92.5
15000	0.21	87.0	87.0
18000	0.21	81.8	81.8
20000	0.21	77.2	77.1
22000	0.21	71.3	71.3
25000	0.21	59.8	59.8
30000	0.21	34.2	34.1
40000	0.21	0.4	0.5

The time-based function was also verified. The plot below shows an example of this verification using the S23 D1 subject 18,000 feet exposure profile (0K to 10K to 18K to 0K). The outputs of each implementation are exactly overlaid as expected.

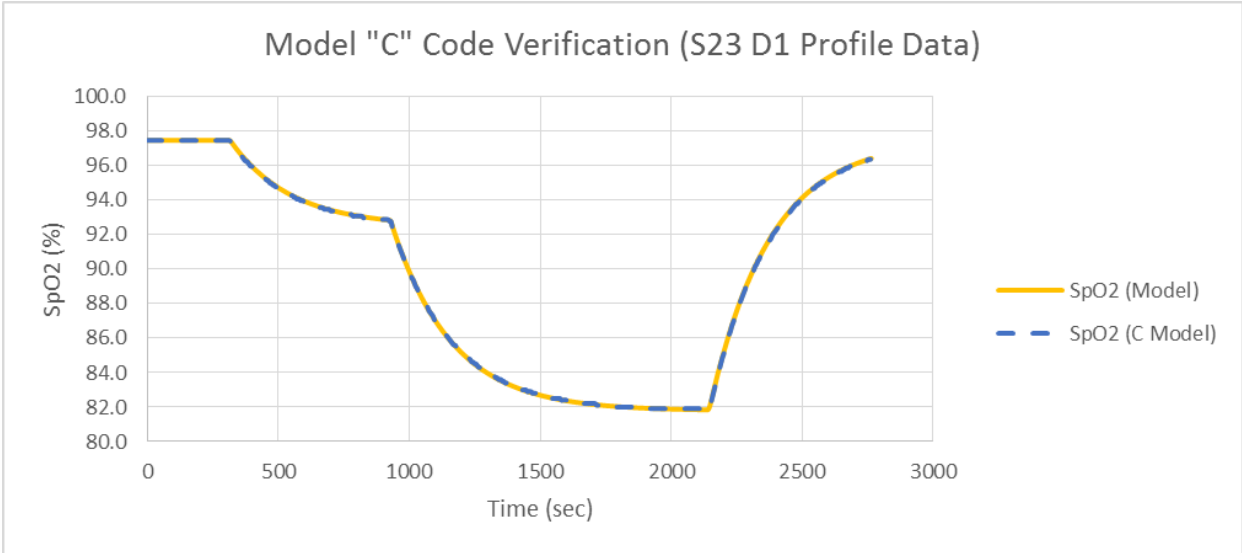


Figure 34. "C" Code Verification - Transient Output

Once the model was responding in the desired manner, attention was diverted to further verification with subject data. Since the data already exists in MS EXCEL, each calculation step of the algorithm was reproduced in EXCEL to facilitate verification tracking and plotting the results. Beginning with data from

S23, the input parameters (time, Altitude) were copied from the subject data files and [O₂] was fixed at 0.21. The model was allowed to run and the Steady State as well as “real time” prediction of SpO₂ were generated. The results are shown in the figures below as the Red line (SpO₂ (Model)). The figures show subjects that were exposed to the same test profile of 0K, 10K, 18K and 0K feet simulated altitude using a ROBD. Several observations were made:

1. The model output (red line) is significantly higher than the subject data (Blue line – SpO₂ (S23)).
2. The model decay profile is of the desired shape.
3. The Steady State predictions are above what the subject data indicates.
4. The recovery profile is much faster than the model predicts.

Since the subject data was taken under normobaric conditions using the ROBD, we suspected that this could have an effect on the results. The steady state model is based on hypobaric conditions. One potential consequence of normobaric testing is that the pH shift is affected due to higher than expected CO₂ in the blood. This would result in a lower pH and a similar lower steady state SpO₂ prediction. If we run the model keeping the pH at 7.4 (See below figures) this significantly reduces the model prediction (Grey line – SpO₂ (Model pH7.4)). However it is still significantly higher than the subject data. Looking at the subject data more closely, the simulated altitude was assumed to be 0, 10K and 18K exactly (the intended target altitudes), but in reality it was not perfectly set to these altitudes. The ROBD simulates the altitude by adjusting the % O₂ in the breathing gas. This %O₂ concentration is recorded in the data sets. When this information is used to adjust the “actual” altitude in place of the target test altitude the results were again significantly affected. The Yellow line (SpO₂ (Model pH7.4) TAC) represents the model prediction that accounts for potential effects of normobaric tests as well as correcting for the test altitude and shows a much closer representation of the subject data. Individual test days (S23 D1 vs. S23 D2) as well as individual subject response (S23 vs. S5) are still evident. The S5 SpO₂ (Model pH7.4) TAC yellow line output also includes an initial concept for differentiating the decay vs. recovery transient response of the model prediction. The recovery portion of the model still requires additional development.

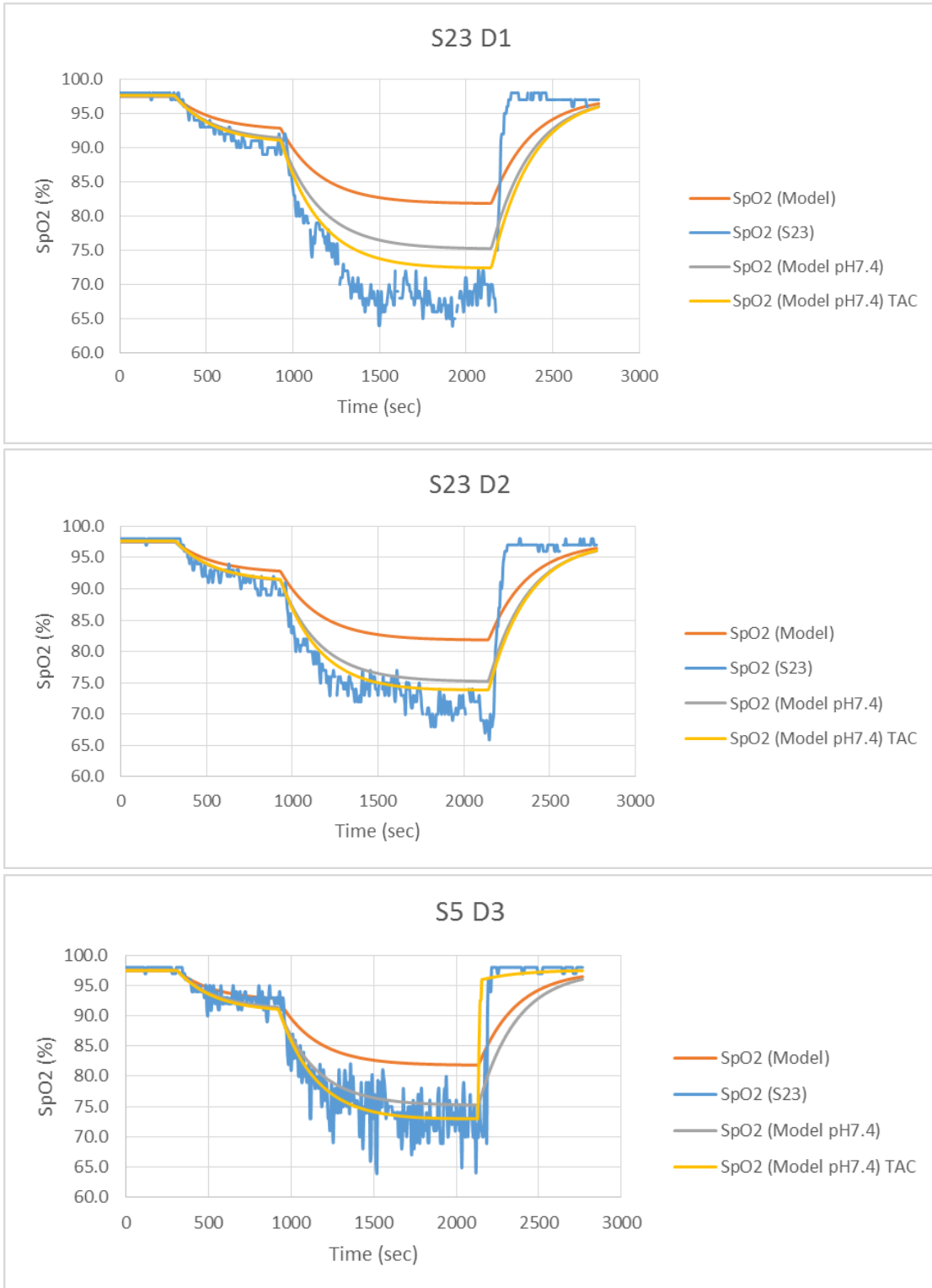


Figure 35. Parametric Model Initial Verification Analysis

A more comprehensive verification using additional data sets from the ONR data file “RawAmbientTempHypoxiaPhysiologicDatawithNIRSandO2” was completed. Figure 36 shows an example of the data plots generated for the parametric model. It summarizes the comparison between the subject data provided by ONR and the model results against the same input conditions. There is good correlation to the data in most cases. The plots are provided to document the work completed and to give a representation of the results. There are also a number of cases where the data is miss-aligned, noisy or drop-outs occur indicating the types of challenges with developing an algorithm for this type of application.

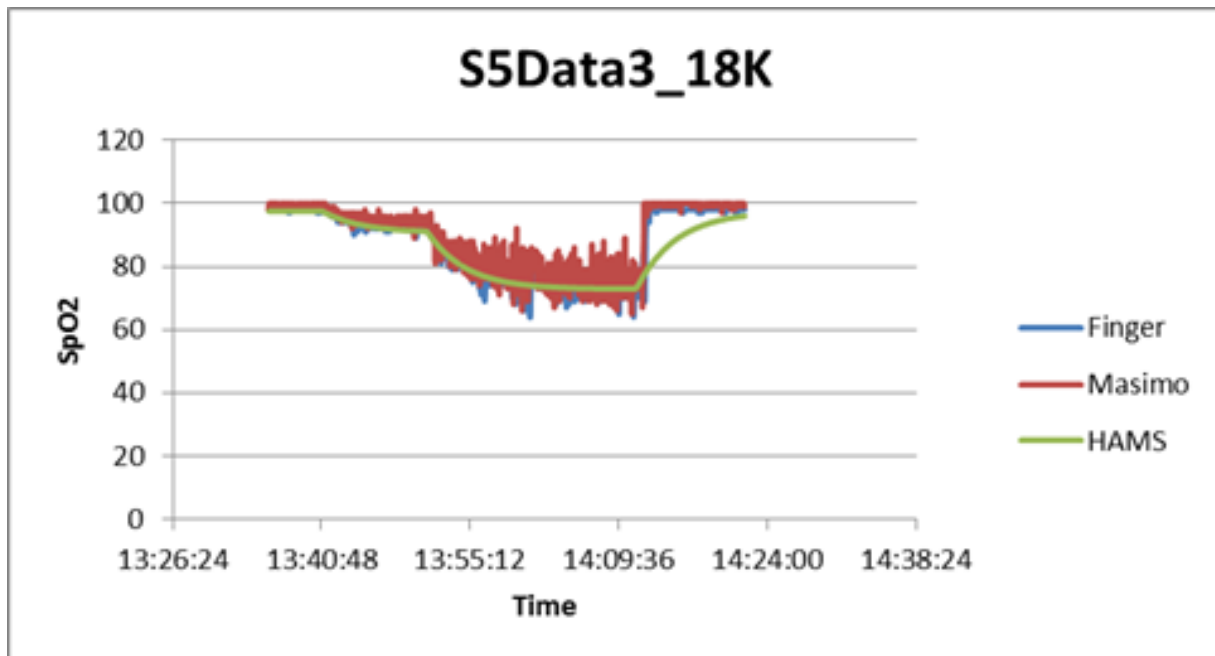


Figure 36. Example of Parametric Model Verification Data Plot

A summary of the overall observations and general correlations is included below:

- The model exhibits the desired general shape of the subject data during ascent to altitude
- The data indicates that recovery (or re-saturation) occurs much faster than ascent (or de-saturation). This appears to be independent of adding 100% oxygen to the recovery phase of the protocol. The model does not currently account for this as can be seen from Figure 36. This will need further development.
- General Correlations (R^2 value) between the model and the Finger SpO2 data by test region
 - Sea-Level Baseline: 0.9 to 0.95
 - Ascent to 10K feet: 0.52 to 0.97 (Ave = 0.89)
 - Ascent from 10K to 18K feet: 0.11 to 0.97 (Ave = 0.77)
 - Ascent from 10K to 20K feet: 0.63 to 0.97 (Ave = 0.89)

- Model usually reports higher levels of SpO2 than the subject data with the exception of 5 cases (S14Data4_25K, S27Data1_25K, S28Data1, S30Data1_18K, S32Data1_25K)
- SpO2 Sensors and sensor sites often do not agree with each other.

Late in the program, approval was received to incorporate the Hammerhead energy expenditure algorithms. These provide a means for initiating individual customization of the algorithm. The inputs and their corresponding outputs can be seen in Table 12. The algorithm uses the subject’s weight, five kilometer run time (measure of fitness), Height and Age to determine their maximum heart rate. Then as the subject is being monitored a one minute average heart rate is compared to the maximum heart rate to calculate a fatigue state.

Table 12 Inputs and Outputs of the Customizable Energy Expenditure

Inputs	Outputs
Weight	Heart Rate Max
5K Time	
Height	
Age	
Average Heart Rate	Fatigue State
Heart Rate Max	

Additional work will be needed to formulate interaction between the hammerhead code and the hypoxia prediction algorithms. For now the fatigue predictions and energy expenditure can be used in the decision matrix to modify warnings and mitigations as these indicate a high workload or fatigued individual.

4.4.2 Unconsciousness Model

Locating a microcontroller platform to accommodate the C Code seems to be a solvable problem but further development with an unrestricted IDE is likely necessary. The C language work in Code Composer Studio from Texas Instruments has suffered from issues in compiler linkage of the project but not of the c-code of the model. The issue may be that the code limitations of the “free” version may extend to the code-unlimited GNU compiler being used. The MSP430F67791 had been chosen for its large Flash ROM size of 512KB and the code compiled and came out to be about 2KB over that size. For the sake of finding a microcontroller that would fit for further debugging and emulation, a TMS470F06607 was used under Code Creator which has 640KB total program flash memory. In that change over these compiler issues have arisen. Athena GTX has shared the Freescale processors group that they use and it is probably best to move over to that processor. We will continue discussions and development toward this goal. Tasking in the effort may be moving away from further work along these lines but it appears to be a minor issue to be resolved.

Based on the review held on 20 February, three items emerged.

- [1] A version of the consciousness model was modified to run as if it were getting time history data in a real application to understand model response. This modified model is under examination to insure that it is performing as required. Most of the questions have to do with accessing the data and displaying the results based on sliding down the Excel data column. This exercise has generated thought about the continuous running of the model and how to initialize and continue running without losing the end of data segment results as initial conditions for the next data segment.
- [2] More of Dr. Shender's data were run through the original version of the Excel model. The datasets (1 and 2) for the LifeShirt data runs with the Nonin SaO₂ data at a 60 Hz rate were used. Thirteen subjects at 18K and 25K feet were run through the model with the screenshots of the simulation results reproduced in Section 10.2.2. The problem of data drop outs was addressed by manually setting the data values to the last known data point which in most cases was for a short period of time and was contiguous with the next valid data point (the same data value). The general theme that below 80% SaO₂ the model indicated impairment and below 70% the Active and Cluster values went to zero which triggered a loss of conscious indication by the model. In most cases by the experimental protocol 100% Oxygen was administered at this point which probably prevented any loss of consciousness to occur, in which none did occur. The individual subject response was in no way homogeneous. Some subjects' SaO₂ dropped significantly at 18K feet while some did not. Most subjects responded with significant loss of SaO₂ at 25K feet. Using a calculation of altitude, pressure and SaO₂ may miss some impairment cases unless we can find a way to personalize the model calculation. The model demonstrated a lag in state change from impaired to baseline after restoration of greater than 90% SaO₂. While these statements are generalized, more specific statements of timing and SaO₂ levels can be generated for the possible development of some parameter relationships if it is felt it would be beneficial.
- [3] More realistic acceleration-decompression scenarios for the model need to be generated and this will be done.

By modifying data types defined in the original code the C code Model version has been reduced to the smallest code size to date. The C language code has been compiled and is being debugged under a standard C99 compiler running under the Eclipse IDE. One large data array within the program held values from 0 to 2 and the data type for this array was changed to byte/char under both the Excel VBA and C implementation without problems. The Excel VBA code ran as before the data type change. Other miscellaneous over-specified data type declarations were changed which including the above array redefinition have resulted in an executable file of 118,344 bytes. After continued elimination of miscellaneous over-specified data type declarations and unused declarations were changed or eliminated the executable file size was 116,854 bytes. The data arrays for acceleration and oxygen saturation are still specified in the code which would be in RAM on board the embedded system and not count against the program size. The code was ported to an embedded system IDE where it compiled

successfully but could not be debugged on the target embedded system since there was no processor emulator.

Exploration of the limitations of the neurological model using experimental data continues. The most recent analysis is discussed below. The data from the Wolf 2014 paper (reported last month) which cited the Hoffman et al 1946 paper was run in the Excel VBA model operating at 1 second intervals. The plot below is from the Wolf paper which the Hoffman data points were digitized and then fit with a model to give 1 second time points for the Excel VBA model.

Wolf M. Physiological consequences of rapid or prolonged aircraft decompression: evaluation using a human respiratory model. *Aviat Space Environ Med* 2014; 85: 466 – 72 .

Hoffman CE, Clark RT, Jr., Brown EB, Jr. Blood oxygen saturation and duration of consciousness in anoxia at high altitude. *Am J Physiol* 1946 ; 145 : 685 – 92 .

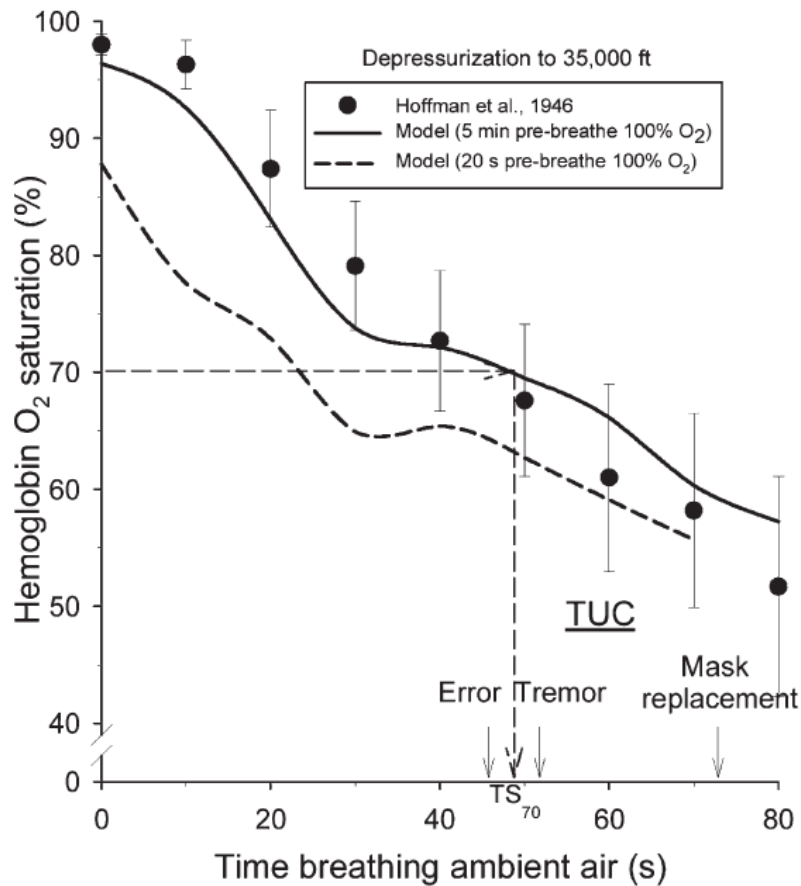


Figure 37 Wolf Paper Figure

To examine the model’s recovery response an arbitrary period of recovery was inserted after the above mask placement time point as seen in Figure 37. Table 13 shows the neurological states reported by Hoffman and the predicted impairment points in the model.

Table 13 Result summary compared to Hoffman

Hoffman results	Time (sec)	Neurological Model	Time (sec)
First Error	46		
Tremor	51	First Impairment Time Point	57
		Impaired State	65-127
Imminent Unconsciousness	72		

No unconsciousness event occurred in the experiment and none was predicted by the model but in Figure 38, the time history simulation data, the “Cluster Mass” dropped near zero which is indicative of impending unconsciousness. The “red” line in Figure 38 shows the described imminent unconsciousness point from Hoffman which is a somewhat ambiguous non-quantitative descriptor. The model seems to lag the verbal description by 20 seconds. The Hoffman arterial oxygen saturation sample values are far below what would be trusted on a pulse oximeter. No indication was given after oxygen mask placement on subjective neurological factors but as the neurological model has predicted in the past about 20 seconds of impairment are predicted after the oxygen saturation returns to 100% in the arbitrary recovery period.

An executable of the Wolff model that ran under the VisSim Viewer was obtained from the author to provide an alternative prediction of the Shender data. Unfortunately the model outputs were not amenable to obtaining the entire time history as a file for further processing. This model will be held for further examination in the future.

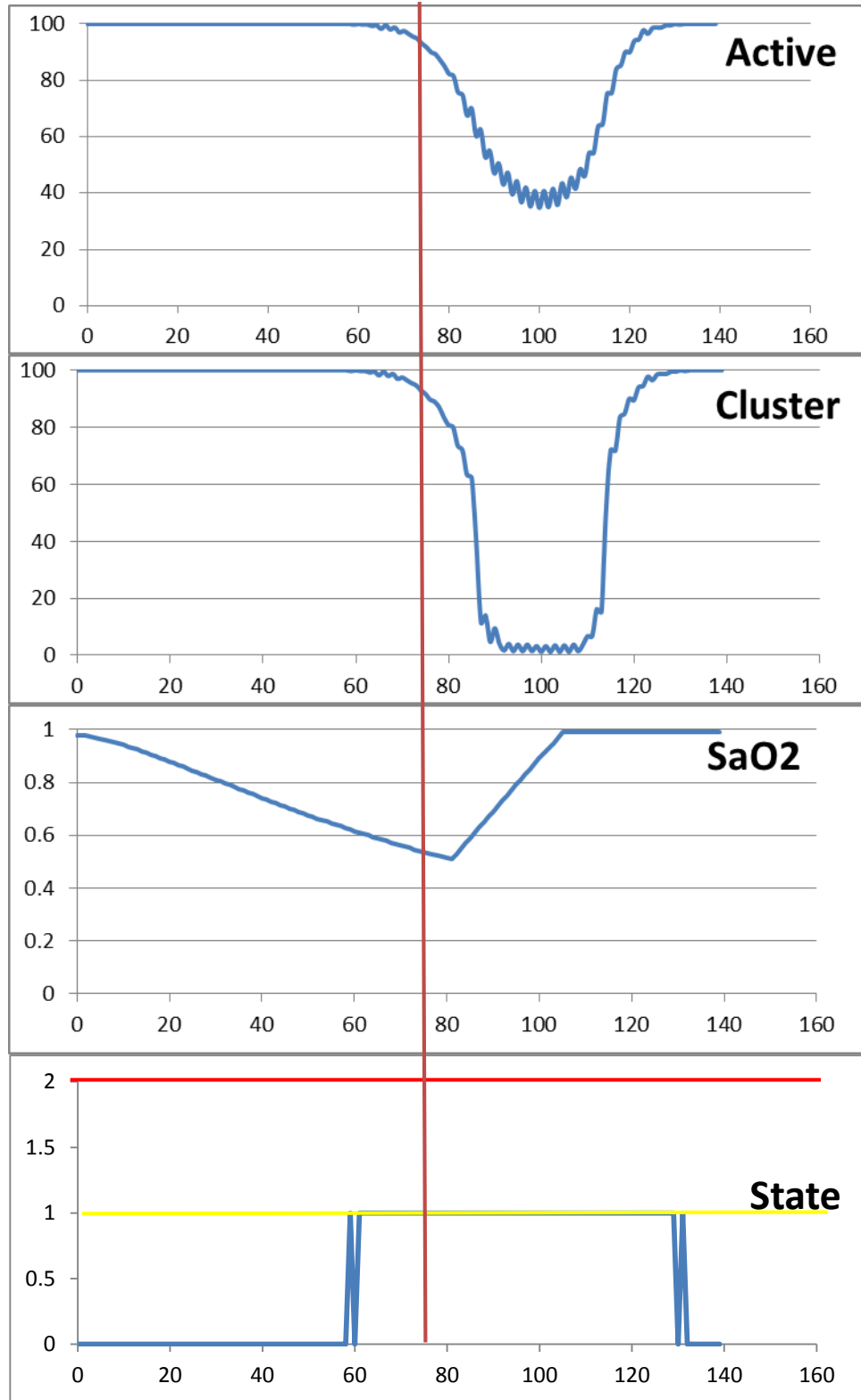


Figure 38 Simulation of the Hoffman Altitude Exposure with arbitrary recovery period

An important change was made to the oxygen utilization equation. The original oxygen utilization S-domain transfer function was converted to the Z-domain (difference equation) in the original work. In confirming this conversion CAI used the Bilinear Transformation which did confirm the coefficients. However the original work was for a sample interval of 0.1 second for the Gz data alone. With the incorporation of SaO₂, the fastest data rate available was a 1 second interval. The Bilinear Transformation had to be re-performed at a 1 second sampling interval which changed the coefficients significantly and are reflected in the final C code.

After the adjustment of the oxygen utilization equation for the change in sampling interval, the data from the Wolf 2014 paper which cited the Hoffman et al 1946 paper was re-run in the updated Excel VBA model operating at 1 second intervals. The plot below is from the Wolf paper which the Hoffman data points were digitized and then fit with a model to give 1 second time points for the Excel VBA model with an arbitrary recovery period.

To examine the model's recovery response an arbitrary period of recovery was inserted after the above mask placement time point as seen in Figure 37. Table 14 shows the neurological states reported by Hoffman and the predicted impairment points in the model.

Table 14 Result summary compared to Hoffman

Hoffman results		Prior Neurological Model		Revised Neurological Model	
Event	Time (sec)	Event	Time (sec)	Event	Time (sec)
First Error	46				
Tremor	51	First Impairment Time Point	57	First Impairment Time Point	27
		Impaired State	65-127	Impaired State	33-63
Imminent Unconsciousness	72			Unconscious	64-91

With the modification in the oxygen utilization equation, an unconsciousness event was predicted at approximately 8 seconds before the paper reported imminent unconsciousness. The first and consistent impairment prediction points were earlier than the demonstrated first error but in the time range of the

tremor observation. No recovery data were reported in the paper so it is not possible to comment on the model predictions during the arbitrary SaO₂ recovery period. The adjustment to the oxygen utilization has brought about an improvement in the predictive capability of the model for hypoxic hypoxia.

4.5 Task 5 – (Option) – Concept System Refinement

This option has been exercised and will be submitted under separate documentation, CDRL A004.

4.6 Task 6 - Deliverables

See Section 6.2 below.

5.0 Financial Results

The total base budget for the HAMS program is \$385K plus an option of \$71K. The contractually obligated amount in FY2013 towards the total budget was \$170K. The contractually obligated amount in FY2014 towards the total budget was \$286K (this includes the Option).

- Cost incurred for the FY2013 budget was \$170K or 100%.
- Costs incurred through May 2014 for the FY2014 budget was \$210K or approximately 73%.
- Costs incurred for the total baseline budget through May 2014 was \$380K or approximately 99%.

The tables below summarize the costs incurred to date against the FY 2013 and FY 2014 obligated funding to date (\$170K and \$286K, respectively). A more detailed spread sheet has been included in the Appendix, Section 10.3.

5.1 FY2013 Funding (\$170K)

Month	HAMS Projected (%)	ONR Benchmarks FY13 Funding (%)	HAMS Actual (%)	Benchmark Delta (%)	Comments
AUG	41	49	58	+9	Additional funding will be needed in NOV to fulfill SOW expectations.
SEP	85	56	81	+25	Additional funding will be needed in NOV to fulfill SOW expectations.
OCT	100	57	93	+35	Additional funding will be needed in NOV to fulfill SOW expectations.
NOV	100	63	100	+36	FY 2013 funds have been exhausted.

5.2 Benchmarks for FY2014 Funding (\$286K)

Month	HAMS Projected (%)	ONR Benchmarks FY14 Funding (%)	HAMS Actual (%)	Benchmark Delta (%)	Comments
OCT	0	0	0		
NOV	0	1	0		
DEC	15	3	10	+7	FY2014 Funds Received (\$160K)
JAN	34	6	21	+15	
FEB	46	12	35	+23	
MAR	57	20	49	+29	Full FY2014 Funds Received and Option Exercised
APR	65	23	63	+40	
MAY	75	29	73	+44	Baseline Ends
JUN	88	35			Option
JUL	100	42			Option

6.0 Schedule and Deliverables

6.1 Schedule

Tasks	CY 2013						CY 2014						
	J u l	A u g	S e p	O c t	N o v	D e c	J a n	F e b	M a r	A p r	M a y	J u n	J u l
1. Preliminary Research and Documentation	█	█	█	█									
2. Develop Parametric Predictive Models	█	█	█	█									
3. Algorithm Development and Refinement	█	█	█	█	█	█	█	█					
4. BETA Model Software Development/Definition							█	█	█	█	█	█	
5. Concept System Refinement (Option)													█
6. Deliverables													
Monthly Updates		█	█		█	█	█	█	█	█	█		█
Quarterly Reports					█			█					
Final Report											█		
Beta Software											█		
Trade-off & Preliminary Specification (Option)													█

 Progress/Completed
 Planned

6.2 Deliverables

6.2.1 Monthly Updates

Nine Monthly updates have been submitted to ONR for the baseline period of performance, July 2013 through April 2014.

6.2.2 Quarterly Reports

The following quarterly reports have been submitted to ONR:

- A001-1, Report for the period July 24, 2013 to October 31, 2013 and
- A001-2, Report for the period November 01, 2013 to January 31, 2014.

6.2.3 Final Report

The A002 Final Report for the period July 24, 2013 to May 31, 2014 has been submitted to ONR.

6.2.4 BETA Software

The A003 BETA Software has been submitted to ONR.

6.2.5 Option – Trade-off Analysis and Preliminary Specification

This option has been exercised and will be submitted under a separate documentation, CDRL A004.

7.0 Conclusion

The Hypoxia Monitoring, Alert and Mitigation System (HAMS) program has progressed as expected and the baseline program has been completed. The optional Task 5 has been exercised and will be documented in a separate deliverable.

The concentrated effort on the literature search activity (Task 1) has been completed. A File Transfer Protocol (FTP) site has been created to share references and data among the team members and Office of Naval Research (ONR).

The baseline parametric hypoxia modeling effort (Task 2) has been completed. A model to predict %O₂ saturation, aircrew state, alveolar pressure of oxygen (PaO₂) and alveolar pressure of carbon dioxide (PaCO₂) has been converted over to the C programming language. This allows the algorithm to eventually run on a micro-controller. Additionally the time based algorithms have been adjusted to better represent the physiological response of the human to high altitude hypoxic events.

The conversion of the United States Navy (USN) Consciousness Model (Task 3) has been completed. Initial verification and sensitivity analysis has shown positive results and the code has been reduced to a size and complexity that will run on a modest microcontroller. The addition of a hypoxia component to the acceleration component of the model has demonstrated good results.

The final baseline task (BETA Model Software Development/Definition – Task 4) has been completed. Software algorithms have been further developed through sequential iterations that progressively refined a prediction for hypoxia and near-hypoxia conditions. The focus on implementation in a memory-limited, bit-constrained microcontroller has remained a top priority. For each iteration the algorithms and software have been evaluated using existing data provide by ONR.

The baseline parametric algorithm to predict %O₂ saturation and aircrew state and the modification of the USN Consciousness Model to predict LOC due to altitude induced hypoxia remain as viable approaches moving into the next phase of development.

8.0 Recommendations

We recommend that the program continue with the planned HAMS Phase II project as proposed under the Long Range Broad Agency Announcement (BAA) for Navy and Marine Corps Science and Technology: ONR BAA 14-001, Special Notice 14-SN-0002 entitled “Hypoxia Monitoring, Alert and Mitigation System” (HAMS).

9.0 References

Not Applicable. See Section 4.1 for additional literature review results relevant to HAMS.

10.0 Appendix

10.1 Task 1: Preliminary Research and Documentation

10.1.1 Additional Literature Search Results – Abstracts Only

The following additional literature review results are included for completeness.

Andersson, J., Linér, M., Rünow, E., Schagatay, E. (2002). Diving response and arterial oxygen saturation during apnea and exercise in breath-hold divers. *Journal of Applied Physiology*. 93:882-886.

This study addressed the effects of apnea in air and apnea with face immersion in cold water (10°C) on the diving response and arterial oxygen saturation during dynamic exercise. Eight trained breath-hold divers performed steady state exercise on a cycle ergometer at 100 W. During exercise, each subject performed 30-s apneas in air and 30-s apneas with face immersion. The heart rate and arterial oxygen saturation decreased and blood pressure increased during the apneas. Compared with apneas in air, apneas with face immersion augmented the heart rate reduction from 21 to 33% ($P < 0.001$) and the blood pressure increase from 34 to 42% ($P < 0.05$). The reduction in arterial oxygen saturation from eupneic control was 6.8% during apneas in air and 5.2% during apneas with face immersion ($P < 0.05$). The results indicate that augmentation of the diving response slows down the depletion of the lung oxygen store, possibly associated with a larger reduction in peripheral venous oxygen stores and increased anaerobiosis. This mechanism delays the fall in alveolar and arterial PO₂ and, thereby, the development of hypoxia in vital organs. Accordingly, we conclude that the human diving response has an oxygen-conserving effect during exercise.

Bailey, D., Bartsch, P., Knauth, M., Baumgartner, R. (2009). Emerging concepts in acute mountain sickness and high-altitude cerebral edema: from the molecular to the morphological. *Cellular and Molecular Life Sciences*.

Acute mountain sickness (AMS) is a neurological disorder that typically affects mountaineers who ascend to high altitude. The symptoms have traditionally been ascribed to intracranial hypertension caused by extracellular vasogenic edematous brain swelling subsequent to mechanical disruption of the blood–brain barrier in hypoxia. However, recent diffusion-weighted magnetic resonance imaging studies have identified mild astrocytic swelling caused by a net redistribution of fluid from the “hypoxia-primed” extracellular space to the intracellular space without any evidence for further barrier disruption or additional increment in brain edema, swelling or pressure. These findings and the observation of minor vasogenic edema present in individuals with and without AMS suggest that the symptoms are not explained by cerebral edema. This has led to a re-evaluation of the relevant pathogenic events with a

specific focus on free radicals and their interaction with the trigeminovascular system. (Part of a multi-author review.)

Brown, J., Grocott, M. (2013) Humans at Altitude: Physiology and Pathophysiology. *Continuing Education in Anesthesia, Critical Care & Pain j.* Volume 13 Number 1.

This article describes the physiological challenge associated with exposure to environmental hypoxia at high altitude along with adaptive (acclimatization) and pathological (acute high altitude illness) responses to this challenge.

Gallagher, S., Hackett, P. (2004). High-Altitude Illness. *Emergency Medical Clinics of North America.* (2):329-55, viii.

Travel to a high altitude requires that the human body acclimatize to hypobaric hypoxia. Failure to acclimatize results in three common but preventable maladies known collectively as high-altitude illness: acute mountain sickness (AMS), high-altitude cerebral edema (HACE), and high-altitude pulmonary edema (HAPE). Capillary leakage in the brain (AMS/HACE) or lungs (HAPE) accounts for these syndromes. The morbidity and mortality associated with high-altitude illness are significant and unfortunate, given they are preventable. Practitioners working in or advising those traveling to a high altitude must be familiar with the early recognition of symptoms, prompt and appropriate therapy, and proper preventative measures for high-altitude illness.

GAO, M., WANG, R., JIAYONG3, Z., LIU, Y., SUN, G. (2013). NT-ProBNP levels are moderately increased in acute high-altitude pulmonary edema. *EXPERIMENTAL AND THERAPEUTIC MEDICINE.* 5: 1434-1438.

The aim of the present study was to investigate the effect of B-type natriuretic peptides (BNPs) in acute high-altitude pulmonary edema (HAPE). The study enrolled 46 subjects from lowland Han, including 33 individuals who had acutely ascended to a high altitude (21 individuals with HAPE as the case group and 12 individuals without HAPE as the high-altitude control group) and 13 healthy normal residents as the plain control group. The serum concentrations of N-terminal probrain natriuretic peptide (NT-proBNP), erythropoietin (EPO), vascular endothelial growth factor (VEGF) and nitric oxide (NO) were measured. There were significant differences in the serum concentrations of NT-ProBNP, NO, VEGF and EPO among the three groups. The serum concentrations of NT-ProBNP, EPO and VEGF were significantly higher in the HAPE patients and high-altitude control individuals than those of the plain group. No significant differences were identified between the HAPE patients and the high-altitude control group. In contrast to these three parameters, the serum concentrations of NO in the high-altitude control group were significantly higher than those of the HAPE patients and the plain group, while there were no significant

differences in the serum concentrations of NO between the HAPE patients and the plain group. Furthermore, serum concentrations of NT-ProBNP and EPO were significantly reduced following treatment in the HAPE patients, however, no significant changes were identified in VEGF or NO concentrations. BNP's are increased in HAPE with severe hypoxia and right ventricular overload, but are decreased subsequent to treatment. BNP's may therefore be a potential biomarker for the diagnosis and prognosis of HAPE.

Golja, P., Kacin, A., Tipton, M., Eiken, O., Mekjavic, I.(2004). Hypoxia increases the cutaneous threshold for the sensation of cold. *European Journal of Applied Physiology*. 92(1-2):62-8.

Cutaneous temperature sensitivity was tested in 13 male subjects prior to, during and after they breathed either a hypocapnic hypoxic (HH), or a normocapnic hypoxic (NH) breathing mixture containing 10% oxygen in nitrogen. Normocapnia was maintained by adding carbon dioxide to the inspired gas mixture. Cutaneous thresholds for thermal sensation were determined by a thermo sensitivity testing device positioned on the plantar side of the first two toes on one leg. Heart rate, haemoglobin saturation, skin temperature at four sites (arm, chest, thigh, calf) and adapting temperature of the skin (T(ad); degrees centigrade), i.e. the temperature of the toe skin preceding a thermo sensitivity test, were measured at minute intervals. Tympanic temperature (T(ty); degrees centigrade) was measured prior to the initial normoxic thermo sensitivity test, during the hypoxic exposure and after the completion of the final normoxic thermo sensitivity test. End-tidal carbon dioxide fraction and minute inspiratory volume were measured continuously during the hypoxic exposure. Ambient temperature, T(ty), T(ad) and mean skin temperature remained similar in both experimental conditions. Cutaneous sensitivity to cold decreased during both HH (P<0.001) and NH conditions (P<0.001) as compared with the tests undertaken pre- and post-hypoxia. No similar effect was observed for cutaneous sensitivity to warmth. The results of the present study suggest that sensitivity to cold decreases during the hypoxic exposure due to the effects associated with hypoxia rather than hypocapnia. Such alteration in thermal perception may affect the individual's perception of thermal comfort and consequently attenuate thermoregulatory behaviour during cold exposure at altitude.

Heiner, M., Sriram, K. (2010). Structural analysis to determine the core of hypoxia response network. *PLoS One*. 5(1).

The advent of sophisticated molecular biology techniques allows to deduce the structure of complex biological networks. However, networks tend to be huge and impose computational challenges on traditional mathematical analysis due to their high dimension and lack of reliable kinetic data. To overcome this problem, complex biological networks are decomposed into modules that are assumed to capture essential aspects of the full network's dynamics. The question that begs for an answer is how to identify the core that is representative of a network's dynamics, its function and robustness. One of the

powerful methods to probe into the structure of a network is Petri net analysis. Petri nets support network visualization and execution. They are also equipped with sound mathematical and formal reasoning based on which a network can be decomposed into modules. The structural analysis provides insight into the robustness and facilitates the identification of fragile nodes. The application of these techniques to a previously proposed hypoxia control network reveals three functional modules responsible for degrading the hypoxia-inducible factor (HIF). Interestingly, the structural analysis identifies superfluous network parts and suggests that the reversibility of the reactions are not important for the essential functionality. The core network is determined to be the union of the three reduced individual modules. The structural analysis results are confirmed by numerical integration of the differential equations induced by the individual modules as well as their composition. The structural analysis leads also to a coarse network structure highlighting the structural principles inherent in the three functional modules. Importantly, our analysis identifies the fragile node in this robust network without which the switch-like behavior is shown to be completely absent.

Jensen, L., Onyskiw, J., Prasad, N. (1998). Meta-Analysis of Arterial Oxygen Saturation Monitoring by Pulse Oximetry in Adults. *Heart & Lung*. 27: 387-408.

The purposes of the study were to: (1) describe the aggregate strength of the relationship of arterial oxygen saturation as measured by pulse oximetry with the standard of arterial blood gas analysis as measured by co-oximetry, (2) examine how various factors affect this relationship, and (3) describe an aggregate estimate of the bias and precision between oxygen saturation as measured by pulse oximetry and the standard in vitro measures.

Karinen, H., Peltonen, J., Kahonen, M., Tikkanen, H. (2010). Prediction of Acute Mountain Sickness by Monitoring Arterial Oxygen Saturation During Ascent. *High Altitude Medicine & Biology*. 11:325-332.

Acute mountain sickness (AMS) is a common problem while ascending at high altitude. AMS may progress rapidly to fatal results if the acclimatization process fails or symptoms are neglected and the ascent continues. Extensively reduced arterial oxygen saturation at rest (R-Spo₂) has been proposed as an indicator of inadequate acclimatization and impending AMS. We hypothesized that climbers less likely to develop AMS on further ascent would have higher Spo₂ immediately after exercise (Ex-Spo₂) at high altitudes than their counterparts and that these post exercise measurements would provide additional value for resting measurements to plan safe ascent. The study was conducted during eight expeditions with 83 ascents. We measured R-Spo₂ and Ex-Spo₂ after moderate daily exercise [50m walking, target heart rate (HR) 150 bpm] at altitudes of 2400 to 5300m during ascent. The Lake Louise Questionnaire was used in the diagnosis of AMS. Ex-Spo₂ was lower at all altitudes among those climbers suffering from AMS during the expeditions than among those climbers who did not get AMS at any altitude during the expeditions. Reduced R-Spo₂ and Ex-Spo₂ measured at altitudes of 3500 and 4300m seem to predict

impending AMS at altitudes of 4300m ($p < 0.05$ and $p < 0.01$) and 5300m (both $p < 0.01$). Elevated resting HR did not predict impending AMS at these altitudes. Better aerobic capacity, younger age, and higher body mass index (BMI) were also associated with AMS (all $p < 0.01$). In conclusion, those climbers who successfully maintain their oxygen saturation at rest, especially during exercise, most likely do not develop AMS. The results suggest that daily evaluation of SpO₂ during ascent both at rest and during exercise can help to identify a population that does well at altitude.

Katayama, K., Fujita, O., Lemitsu, M., Kawana, H., Iwamoto, E., Saito, M., Ishida, K. (2013). The effect of acute exercise in hypoxia on flow-mediated vasodilation. *Eur J Appl Physiol.* 113:349–357.

The purpose of this study was to clarify the effect of acute exercise in hypoxia on flow-mediated vasodilation (FMD). Eight males participated in this study. Two maximal exercise tests were performed using arm cycle ergometry to estimate peak oxygen uptake $\dot{V}O_{2peak}$ while breathing normoxic [inspired O₂ fraction (FIO₂) = 0.21] or hypoxic (FIO₂ = 0.12) gas mixtures. Next, subjects performed submaximal exercise at the same relative exercise intensity 30% $\dot{V}O_{2peak}$ in normoxia or hypoxia for 30 min. Before (Pre) and after exercise (Post 5, 30, and 60 min), brachial artery FMD was measured during reactive hyperemia by ultrasound under normoxic conditions. FMD was estimated as the percent (%) rise in the peak diameter from the baseline value at prior occlusion at each FMD measurement (%FMD). The area under the curve for the shear rate stimulus (SRAUC) was calculated in each measurement, and each %FMD value was normalized to SRAUC (normalized FMD). %FMD and normalized FMD decreased significantly ($P < 0.05$) immediately after exercise in both condition (mean \pm SE, FMD, normoxic trial, Pre: 8.85 ± 0.58 %, Post 5: -0.01 ± 1.30 %, hypoxic trial, Pre: 8.84 ± 0.63 %, Post 5: 2.56 ± 0.83 %). At Post 30 and 60, %FMD and normalized FMD returned gradually to pre-exercise levels in both trials (FMD, normoxic trial, Post 30: 1.51 ± 0.68 %, Post 60: 2.99 ± 0.79 %; hypoxic trial, Post 30: 4.57 ± 0.78 %, Post 60: 6.15 ± 1.20 %). %FMD and normalized FMD following hypoxic exercise (at Post 5, 30, and 60) were significantly ($P < 0.05$) higher than after normoxic exercise. These results suggest that aerobic exercise in hypoxia has a significant impact on endothelial-mediated vasodilation.

Levett, D., Fernandez, B., Riley, H., Martin, D., Mitchell, K., Leckstrom, C., Ince, C., Whipp, B., Mythen, M., Montgomery, H., Grocott, M., Feelisch, M. (2011). The role of nitrogen oxides in human adaptation to hypoxia. *SCIENTIFIC REPORTS.* 1: 109.

Lowland residents adapt to the reduced oxygen availability at high altitude through a process known as acclimatization, but the molecular changes underpinning these functional alterations are not well-understood. Using an integrated biochemical/whole-body physiology approach we here show that plasma biomarkers of NO production (nitrite, nitrate) and activity (cGMP) are elevated on acclimatization to high altitude while S-nitrosothiols are initially consumed, suggesting multiple nitrogen oxides contribute to improve hypoxia tolerance by enhancing NO availability. Unexpectedly, oxygen cost of exercise and mechanical efficiency remain unchanged with ascent while microvascular blood flow correlates inversely

with nitrite. Our results suggest that NO is an integral part of the human physiological response to hypoxia. These findings may be of relevance not only to healthy subjects exposed to high altitude but also to patients in whom oxygen availability is limited through disease affecting the heart, lung or vasculature, and to the field of developmental biology.

Netzer, N., Strohl, K., Faulhaber, M., Gatterer, H., Burtscher, M. (2013). Hypoxia-Related Altitude Illnesses. *Journal of Travel Medicine*. Volume 20 (Issue 4): 247–255.

Acute mountain sickness (AMS) represents the most common and usually benign illness, which however can rapidly progress to the more severe and potentially fatal forms of high-altitude cerebral edema (HACE) and high-altitude pulmonary edema (HAPE) 2, 3, 6, 7. As altitude medicine specialists are rare, the primary care practitioner has to provide advice to the novice traveler. High altitudes may be associated with many conditions not related to hypoxia per se, e.g., cold, UV radiation, physical exertion, infections, and trauma, which are not covered in this article. For respective information, the interested reader is referred to the article by Boggild and colleagues 8. The purpose of this review is to introduce the travel health provider to basic concepts of hypoxia-related high-altitude conditions and to provide state-of-the art recommendations for prevention and therapy of high-altitude illnesses.

Parell, J., Becker, G. (1993). Inner ear barotrauma in scuba divers. A long-term follow-up after continued diving. *Arch Otolaryngol Head Neck Surg*. 119(4):455-7.

Divers who suffer inner ear barotrauma are usually counseled to permanently avoid diving, reasoning that the injured inner ear is at increased risk of further damage. Twenty patients who suffered inner ear barotrauma while diving, but continued to dive against medical advice, were assessed on an interim basis for 1 to 12 years. As difficulty equalizing the ears during the barotraumatic event was a universal finding, prior to resuming diving, all patients were reinstructed on methods of maximizing eustachian tube function. No further deterioration of cochleo-vestibular function was noted. Based on these preliminary results, we conclude that recommending no further diving after inner ear barotrauma may be unnecessarily restrictive.

Penneys, R. Thomas, C. (1950). The Relationship between the Arterial Oxygen Saturation and the Cardiovascular Response to Induced Anoxemia in Normal Young Adults. *American Heart Association: Circulation*. 1:415-425.

At the present time the most widely used method of studying the effect of induced anoxemia on the cardiovascular system consists of giving the subjects low oxygen gas (usually 10 per cent) inhalation for approximately twenty minutes and making observations during this period. In previous communications the variability of the degree of anoxemia, as measured by the blood arterial oxygen saturation, during inhalation of a gas of fixed low oxygen concentration was pointed out. The physiologic importance of

standardizing the induced anoxemia test of cardiovascular function according to the level of the arterial oxygen saturation was discussed and a method of inducing and maintaining a constant degree of anoxemia by administering a gas of variable oxygen concentration was described. In one of these reports' the nature of the cardiovascular response of a small group of young men at levels of 85, 80, and 75 per cent arterial oxygen saturation was presented. It is the purpose of this report to give a detailed description and analysis of the effect of anoxemia upon the heart rate, blood pressure, and electrocardiogram at levels of 80, 75, and 70 per cent arterial saturation in a substantial number of normal young adults.

Ren, Y., Cui, F. Lei, Y., Fu, Z., Wu, Z., Cui, B. (2012). High-Altitude Pulmonary Edema Is Associated With Coagulation and Fibrinolytic Abnormalities. *The American Journal of the Medical Sciences*.

High-altitude pulmonary edema (HAPE) can develop in unacclimatized persons after acute ascent to high altitude and is associated with fibrinolytic and coagulation abnormalities. The authors investigated whether fibrinolytic and coagulation abnormalities were associated with the severity of HAPE. Methods: Sixty-one patients who developed HAPE after acute ascent to altitudes above 3600 m were recruited. Twenty unacclimatized controls who acutely ascended to the same altitude and 20 acclimatized inhabitants served as controls. Tissue plasminogen activator (t-PA) and plasminogen activator inhibitor-1 (PAI-1) levels were measured using chromogenic substrate assays. Plasma fibrinogen concentration was determined by the sodium sulphite fractionation method. The concentrations of fibrin/fibrinogen degradation products (FDP) and D-dimer were measured by enzyme linked immunosorbent assay. Results: The plasma concentrations of D-dimer, fibrinogen, FDP and t-PA and PAI-1 were significantly higher in patients with HAPE than controls. In addition, these abnormalities were correlated with the severity of HAPE. The plasma concentrations of D-dimer and fibrinogen recovered to normal upon recovery from HAPE while t-PA, PAI-1 and FDP levels in HAPE patients still remained significantly increased over those of unacclimatized controls. Conclusion: The development of HAPE is associated with abnormalities in the fibrinolysis and coagulation system, and these abnormalities correlate with the severity of HAPE.

Romer, L., Haverkamp, H., Amann, M., Lovering, A., Pegelow, D., Dempsey, J. (2007). Effect of Acute Severe Hypoxia on Peripheral Fatigue and Endurance Capacity in Healthy Humans. *American Journal of Physiology. Regulatory, Integrative, Comparative Physiology*. 292(1):R598-606.

We hypothesized that severe hypoxia limits exercise performance via decreased contractility of limb locomotor muscles. Nine male subjects [mean +/- SE maximum O(2) uptake (Vo(2 max)) = 56.5 +/- 2.7 ml x kg(-1) x min(-1)] cycled at > or =90% Vo(2 max) to exhaustion in normoxia [NORM-EXH; inspired O(2) fraction (Fi(O(2))) = 0.21, arterial O(2) saturation (Sp(O(2))) = 93 +/- 1%] and hypoxia (HYPOX-EXH; Fi(O(2)) = 0.13, Sp(O(2)) = 76 +/- 1%). The subjects also exercised in normoxia for a time equal to that achieved in hypoxia (NORM-CTRL; Sp(O(2)) = 96 +/- 1%). Quadriceps twitch force, in response to supramaximal single (non-potentiated and potentiated 1 Hz) and paired magnetic stimuli of the femoral nerve (10-100

Hz), was assessed pre- and at 2.5, 35, and 70 min post exercise. Hypoxia exacerbated exercise-induced peripheral fatigue, as evidenced by a greater decrease in potentiated twitch force in HYPOX-EXH vs. NORM-CTRL (-39 +/- 4 vs. -24 +/- 3%, $P < 0.01$). Time to exhaustion was reduced by more than two-thirds in HYPOX-EXH vs. NORM-EXH (4.2 +/- 0.5 vs. 13.4 +/- 0.8 min, $P < 0.01$); however, peripheral fatigue was not different in HYPOX-EXH vs. NORM-EXH (-34 +/- 4 vs. -39 +/- 4%, $P > 0.05$). Blood lactate concentration and perceptions of limb discomfort were higher throughout HYPOX-EXH vs. NORM-CTRL but were not different at end-exercise in HYPOX-EXH vs. NORM-EXH. We conclude that severe hypoxia exacerbates peripheral fatigue of limb locomotor muscles and that this effect may contribute, in part, to the early termination of exercise.

Smith, A. (2008). Hypoxia symptoms in military aircrew: long-term recall vs. acute experience in training. *Aviation Space Environmental Medicine*. 79:54 – 7.

It has been reported that many aircrew who experience hypoxia-related incidents are able to recognize hypoxia because of similarity to symptoms they experienced during hypoxia awareness training. This study aimed to explore the degree of similarity between symptoms reported after acute hypoxia and those remembered from previous hypoxia awareness training.

Stein, J., Ellsworth, M. (1993). Capillary oxygen transport during severe hypoxia: role of hemoglobin oxygen affinity. *Journal of Applied Physiology*. 75(4):1601-7.

The efficacy of an increased hemoglobin oxygen affinity [decreased oxygen half-saturation pressure of hemoglobin (P50)] on capillary oxygen transport was evaluated in the hamster retractor muscle under conditions of a severely limited oxygen supply resulting from the combined effects of a 40% reduction in systemic hematocrit and hypoxic ventilation (inspired oxygen fraction 0.1). Two groups of hamsters were utilized: one with a normal oxygen affinity (untreated; P50 = 26.1 +/- 2.4 Torr) and one with an increased oxygen affinity (treated; P50 = 15.7 +/- 1.4 Torr) induced by the chronic short-term administration of sodium cyanate. Using in vivo video microscopy and image analysis techniques, we determined oxygen saturation and associated hemodynamics at both ends of the capillary network. During hypoxic ventilation, the decrease in oxygen saturation across the network was 3.6% for untreated animals compared with 9.9% for treated animals. During hypoxia, estimated end-capillary PO₂ was significantly higher in the untreated animals. These data indicate that, at the capillary level, a decreased P50 is advantageous for tissue oxygenation when oxygen supply is severely compromised, because normal oxygen losses in capillaries are maintained in treated but not in untreated animals. The data are consistent with the presence of a diffusion limitation for oxygen during severe hypoxia in animals with a normal hemoglobin oxygen affinity.

Still, D., Temme, L. (2012). An independent, objective calibration check for the reduced oxygen breathing device. *Aviation, Space Environmental Medicine*. 83(9):902-8.

Normobaric hypoxia, which does not entail an altitude chamber, but reduces the fraction of inspired oxygen (O₂) by diluting air with nitrogen, is finding increased use. The reduced oxygen breathing device (ROBD-2) is one of several commercial devices for generating such normobaric hypoxia. Reported here are results of a procedure to check the calibration of the ROBD-2 using methods that may be readily available in physiology and psychophysiology facilities.

Tannheimer, M., Hornung, K., Gasche, M., Kuehlmuess, B., Mueller, M., Welsch, H., Landgraf, K., Guger, K., Schmidt, R., Steinacker, J. (2012). Decrease of Asymmetric Dimethylarginine Predicts Acute Mountain Sickness. *Journal of Travel Medicine* 2012; Volume 19 (Issue 6): 338–343.

Each year, 40 million tourists worldwide are at risk of getting acute mountain sickness (AMS), because they travel to altitudes of over 2500 m. As asymmetric dimethylarginine (ADMA) is a nitric oxide synthase (NOS) inhibitor, it should increase pulmonary artery pressure (PAP) and raise the risk of acute mountain sickness and high-altitude pulmonary edema (HAPE). With this in mind, we investigated whether changes in ADMA levels (ADMA) at an altitude of 4000m can predict an individual's susceptibility to AMS or HAPE.

Tyler, I., Tantisira, B., Winter, P., Motoyama, E. (1985). Continuous Monitoring of Arterial Oxygen Saturation With Pulse Oximetry during Transfer to the Recovery Room. *Anesth Analg*. 64:1108-12.

The incidence of hypoxemia in the immediate postoperative period was determined using a pulse oximeter for continuous monitoring of arterial oxygen saturation (SaO₂) in 95 ASA class I or II adult patients breathing room air during their transfer from the operating room to the recovery room. Hypoxemia was defined as 90% SaO₂ (arterial oxygen partial pressure (PaO₂) approximately equal to 58 mm Hg). Severe hypoxemia was defined as 85% SaO₂ (PaO₂ approximately equal to 50 mm Hg). Hypoxemia occurred in 33 (35%) patients; severe hypoxemia occurred in 11 (12%). Postoperative hypoxemia did not correlate significantly with anesthetic agent, age, duration of anesthesia, or level of consciousness. There was a statistically significant correlation (P less than 0.05) between hypoxemia and obesity. All three patients with a history of mild asthma became severely hypoxemic even though none had perioperative evidence of obstructive disease, also a statistically significant (P less than 0.003) finding.

Wagner, D., Knott, J., Fry, J. (2012). Oximetry Fails to Predict Acute Mountain Sickness or Summit Success During a Rapid Ascent to 5640 Meters. *Wilderness & Environmental Medicine*.

The purpose of this study was to determine whether arterial oxygen saturation (SpO₂) and heart rate (HR), as measured by a finger pulse oximeter on rapid arrival to 4260 m, could be predictive of acute mountain sickness (AMS) or summit success on a climb to 5640 m.

Weathersby, P., Survanshi, S., Homer, L., Parker, E., Thalmann, E. (1992). Predicting The Time of Occurrence of Decompression Sickness. *Journal of Applied Physiology*. 72: 1541 - 1548.

Probabilistic models and maximum likelihood estimation have been used to predict the occurrence of decompression sickness (DCS). We indicate a means of extending the maximum likelihood parameter estimation procedure to make use of knowledge of the time at which DCS occurs. Two models were compared in fitting a data set of nearly 1,000 exposures, in which MO cases of DCS have known times of symptom onset. The additional information provided by the time at which DCS occurred gave us better estimates of model parameters. It was also possible to discriminate between good models, which predict both the occurrence of DCS and the time at which symptoms occur, and poorer models, which may predict only the overall occurrence. The refined models may be useful in new applications for customizing decompression strategies during complex dives involving various times at several different depths. Conditional probabilities of DCS for such dives may be reckoned as the dive is taking place and the decompression strategy adjusted to circumstance. Some of the mechanistic implications and the assumptions needed for safe application of decompression strategies on the basis of conditional probabilities are discussed.

Westerman, R. (2004). Hypoxia familiarization training by the reduced oxygen breathing method. *Aviation Medicine*. 5: 11-15.

Hypoxia familiarization training demonstrates and measures (1) cardiorespiratory adjustments in healthy volunteers to a simulated altitude of 25000 ft. (7620 m); (2) the spectrum of signs and symptoms accompanying hypoxia; (3) individual variability in susceptibility to hypoxia and oxygen paradox; and (4) time of useful consciousness. Trainees experience the insidious onset and obvious performance decrements resulting from hypoxia. Hypobaric chambers are traditionally used for this purpose, but carry a risk of inducing decompression sickness in trainees. An alternative is the use of low oxygen gas mixtures to simulate breathing conditions at high altitude.

West, J. (2004). The Physiologic Basis of High-Altitude Diseases. *Ann Intern Med.* 2004; 141:789-800.

Many physicians are surprised to learn how many people live, work, and play at high altitude. Some 140 million persons reside at altitudes over 2500 m, mainly in North, Central, and South America; Asia; and eastern Africa (1). Increasingly, people are moving to work at high altitude. For example, there are telescopes at altitudes over 5000 m (2) and mines at over 4500 m (3), and the Golmud–Lhasa railroad being constructed in Tibet will have 30 000 to 50 000 workers at high altitudes, including many who work at more than 4000 m. Skiers, mountaineers, and trekkers go to altitudes of 3000 m to more than 8000 m for recreation, and sudden ascents to high altitude without the benefits of acclimatization are common. All of these groups are prone to high-altitude diseases that sometimes have fatal consequences. In addition, the physiology of hypoxia, which is at the basis of high-altitude medicine, plays an important role in many lung and heart diseases.

Zhou, Qiquan. (2011). Standardization of Methods for Early Diagnosis and On-Site Treatment of High-Altitude Pulmonary Edema. *Hindawi Publishing Corporation, Pulmonary Medicine.*

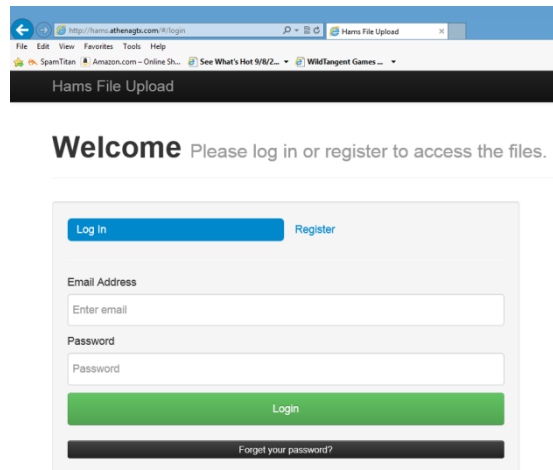
High-altitude pulmonary edema (HAPE) is a life-threatening disease of high altitude that often affects nonacclimatized apparently healthy individuals who rapidly ascend to high altitude. Early detection, early diagnosis, and early treatment are essential to maintain the safety of people who ascend to high altitude, such as construction workers and tourists. In this paper, I discuss various methods and criteria that can be used for the early diagnosis and prediction of HAPE. I also discuss the preventive strategies and options for on-site treatment. My objective is to improve the understanding of HAPE and to highlight the need for prevention, early diagnosis, and early treatment of HAPE to improve the safety of individuals ascending to high altitude.

10.1.2 Hams File Sharing Management System

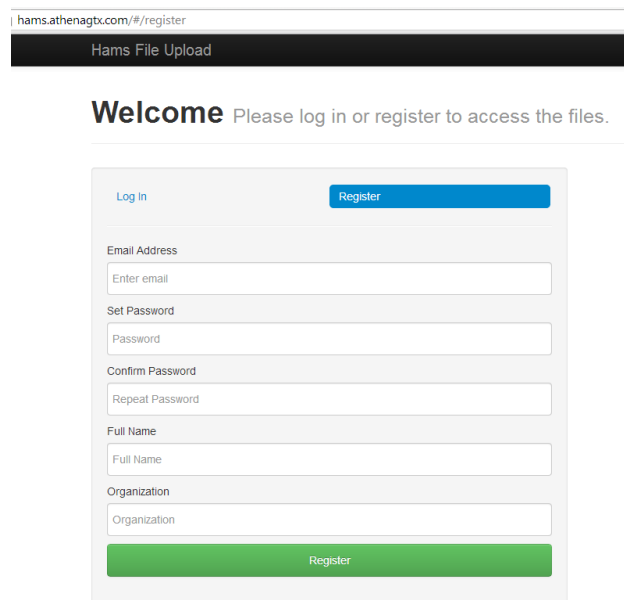
To upload files using the Hams File system, you must first register with the system from the home page. After you have registered an approval email will be sent to your account.

The HAMS File Share home page is accessed by entering the following URL in your browser:

<http://hams.athenagtx.com>

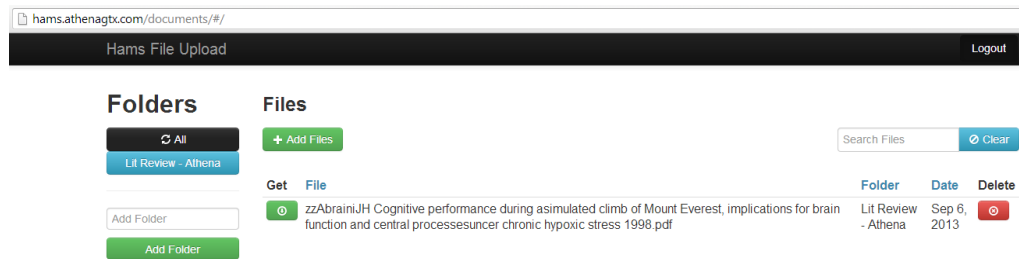


Clicking on **Register** brings you to the registration input screen. Fill in the required information and click the green **“Register”** button. An approval email will be sent to your account.



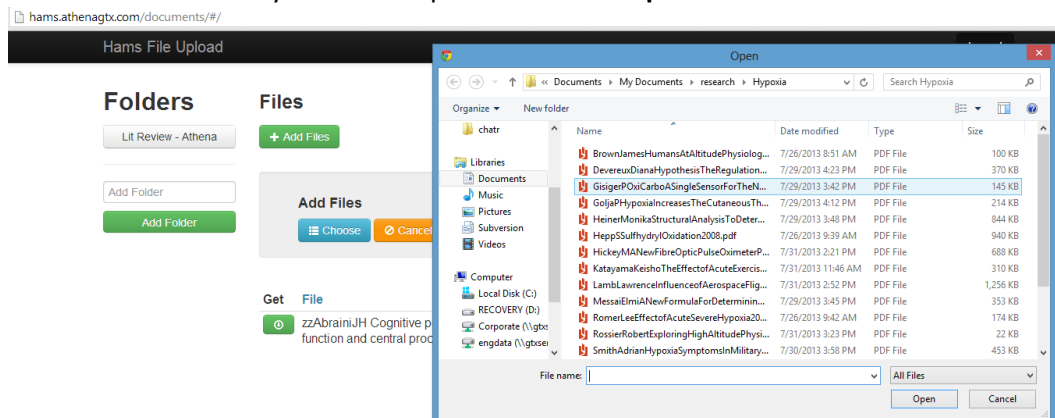
Once you have been approved, you will be able to log into the system through the home page. Logging into the system will take you to the documents page. Here you will be able to download, delete, upload and search documents and folders.

- To download a document, click the green **(Get)** button to the left of the file name. It will then begin to download in your browser.
- To delete a file from the system, click on the red **(Delete)** button to the right of the file.
- All folders are listed in the upper left hand corner of the screen. By clicking on a folder, you may see the documents that are in that folder. Click the black **“All”** button above the folders or the clear button in the upper right corner to see all of the documents.
- To create a folder in which to store documents, type the folder name in the input box that reads **“Add Folder”** and click the green **“Add Folder”** button. You may then add documents to that folder by using file upload.



Upload Files:

- Selecting the green **“+ Add files”** button allows documents or data files to be uploaded.
- Select a folder (optional)
- Next, click the light blue **“Choose”** button and a window will pop up. From here, browse and select the documents you wish to upload and click **“Open”**.



- Then you may change the name of the document you are uploading and select or change the folder. (optional)
- To remove the document(s) select the orange **(Remove)** button to the left of the file.

- Once the files are named and folders are selected click the dark blue **“Upload All”** button.

The screenshot shows the HAMS File Upload interface. At the top, there is a navigation bar with the URL 'hams.athenagtx.com/documents/#/' and a 'Logout' button. Below this, the main interface is divided into 'Folders' and 'Files' sections. The 'Folders' section on the left shows a list of folders, including 'Lit Review - Athena', and an 'Add Folder' button. The 'Files' section on the right features an 'Add Files' area with 'Choose', 'Upload All', and 'Cancel' buttons. Below this, a table lists files with columns for 'File Name (type to change)', 'Folder', and 'Remove'. The files listed are:

File Name (type to change)	Folder	Remove
DevereuxDianaHypothesisTheRegulationofthePartialPressureofOxygenbytheSeroto	Lit Review - Athena	[Remove]
HeinerMonikaStructuralAnalysisToDeterminingtheCoreofHypoxiaResponseNetwork20	Lit Review - Athena	[Remove]
HickeyMANewFibreOpticPulseOximeterProbeForMonitoringSplanchnicOrganArterial	Lit Review - Athena	[Remove]

At the bottom, there is a table with columns for 'Get', 'File', 'Folder', 'Date', and 'Delete'. The file listed is:

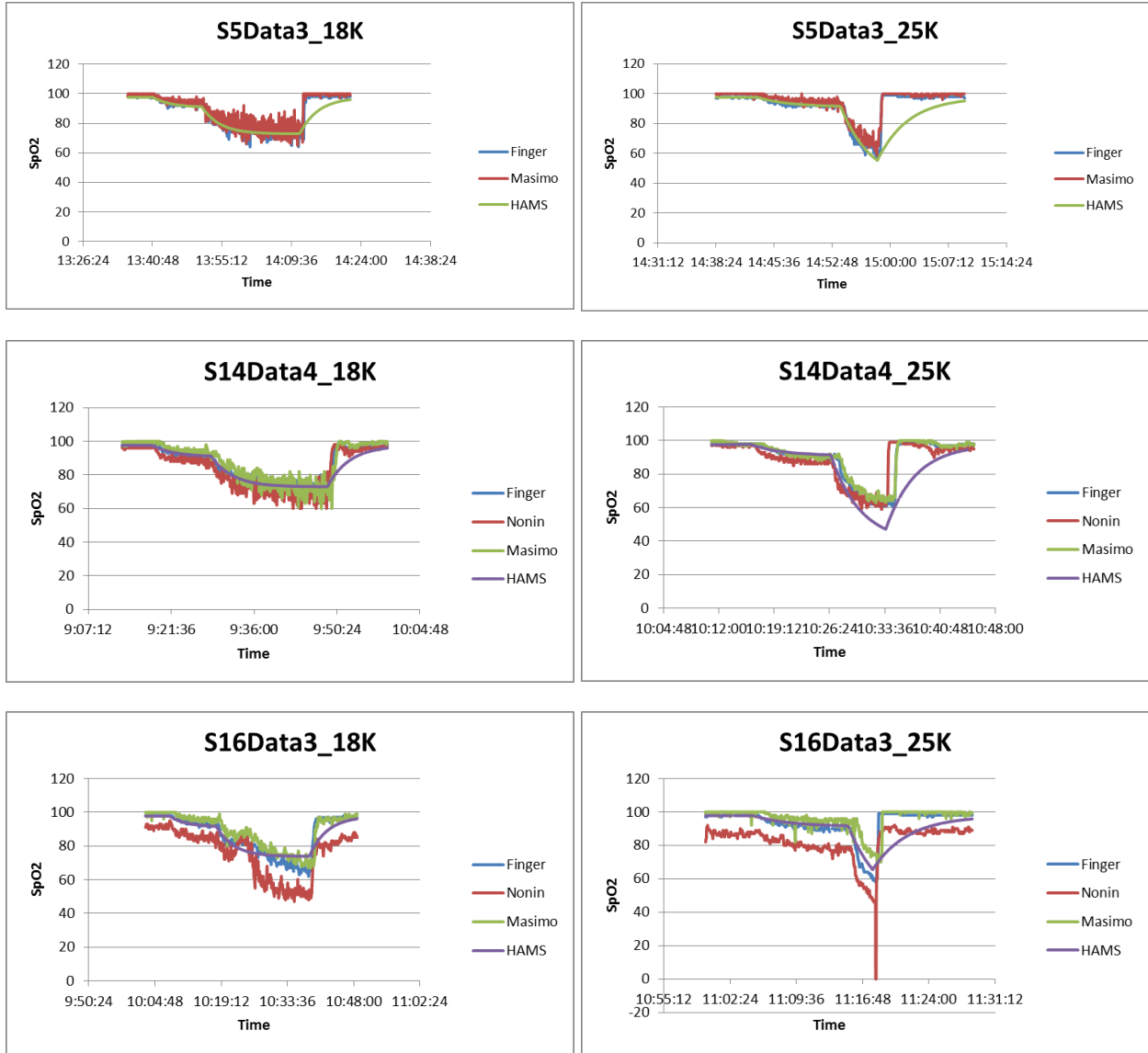
Get	File	Folder	Date	Delete
[Icon]	zzAbrairiJH Cognitive performance during a simulated climb of Mount Everest, implications for brain function and central processes under chronic hypoxic stress 1998.pdf	Lit Review - Athena	Sep 6, 2013	[Delete]

Note: To upload all the files into a single Folder, select the folder first then select the Choose Button. This will auto populate the folder field in the upload process. This field can be edited if one or more documents selected for upload are to go into a different folder.

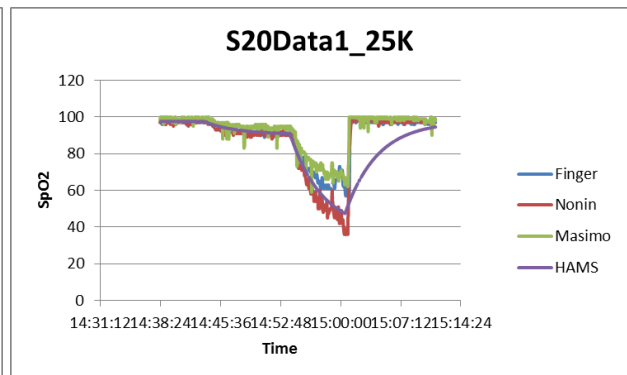
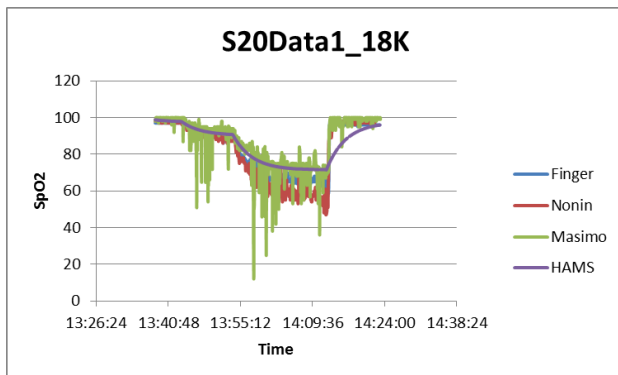
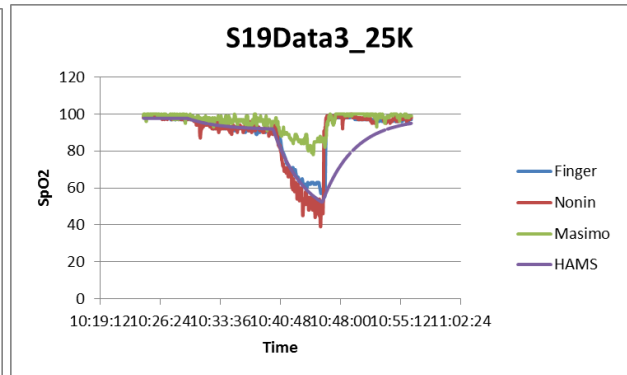
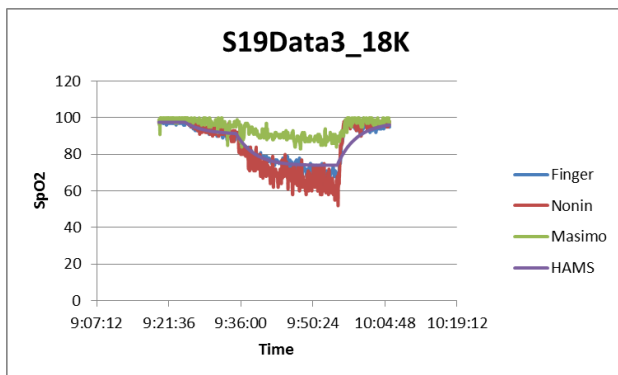
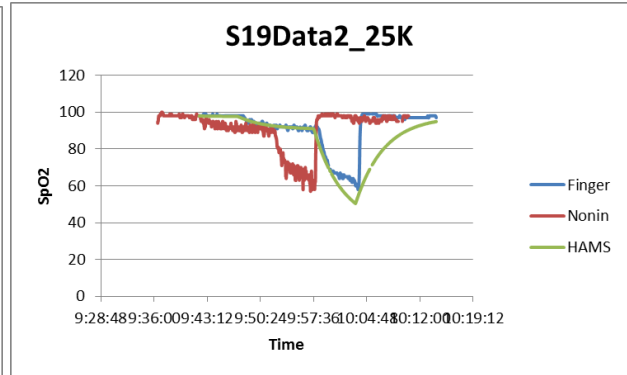
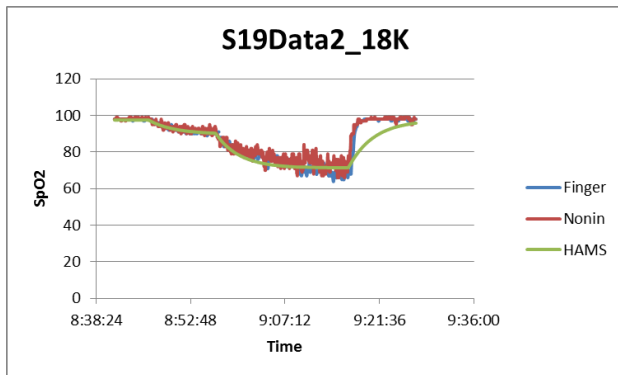
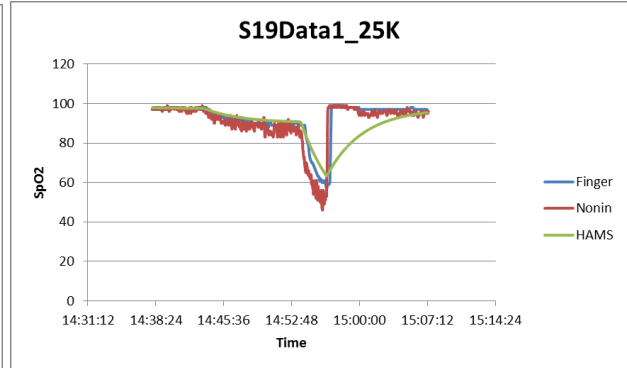
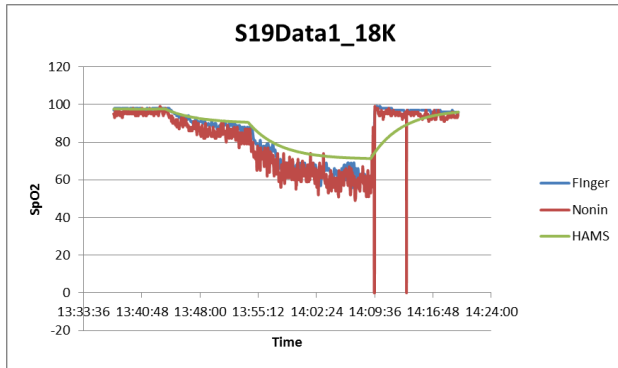
10.2 Task 4: BETA Model

10.2.1 Subject Hypoxia Simulation Runs-Parametric Model

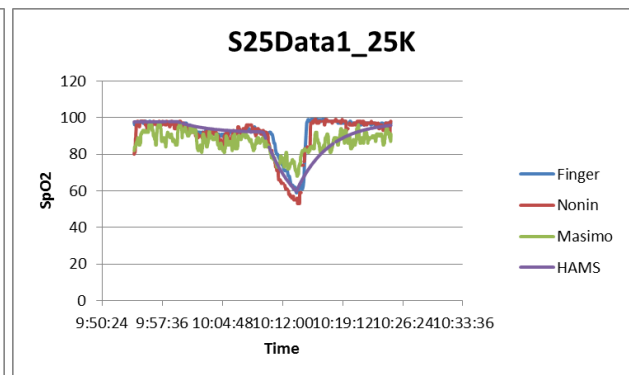
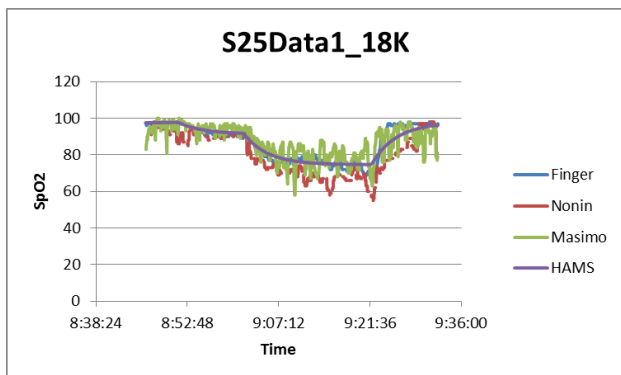
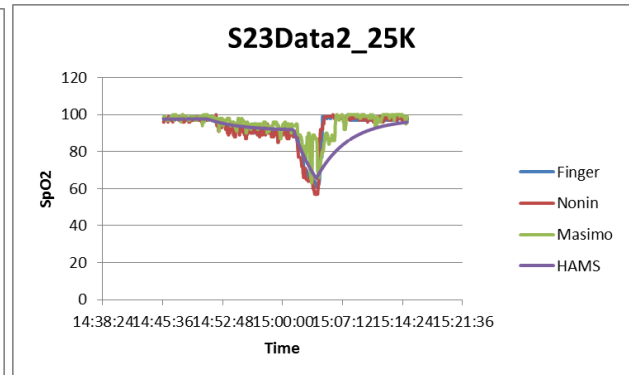
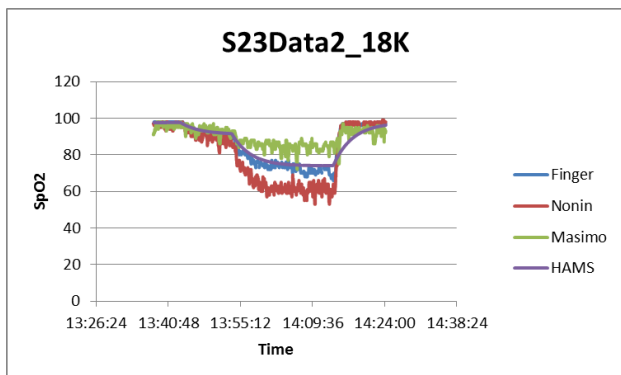
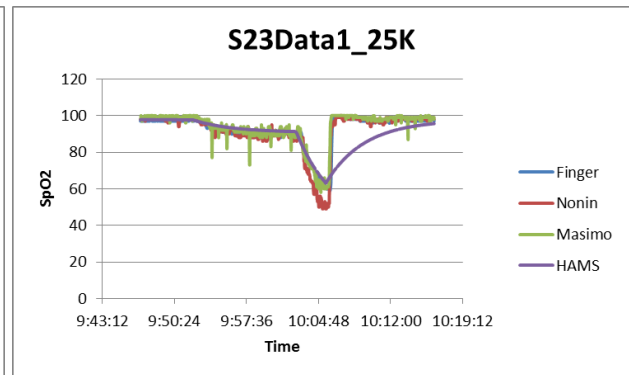
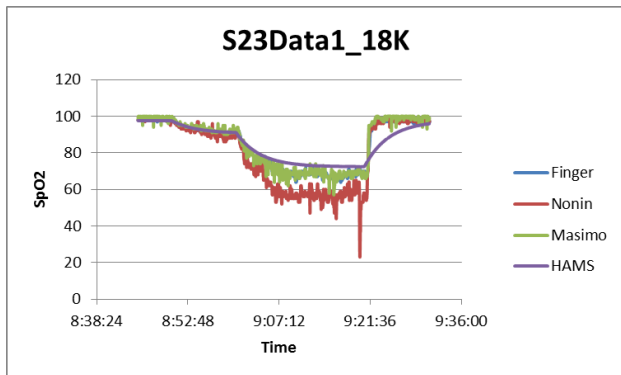
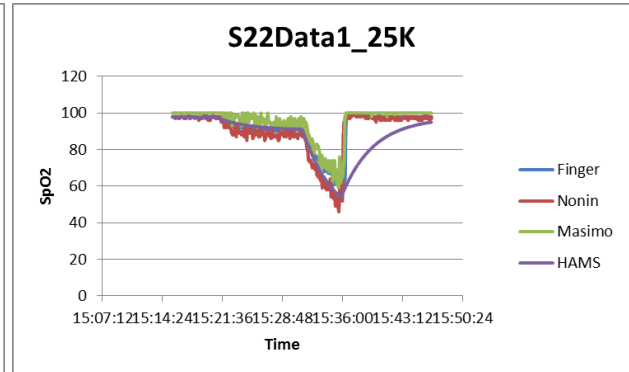
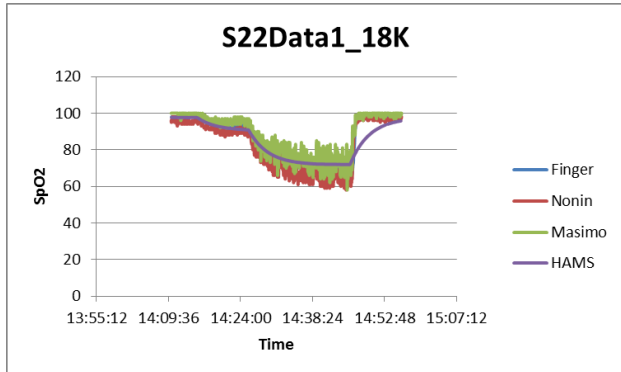
The data from "RawAmbientTempHypoxiaPhysiologicDatawithNIRSandO2" was used to generate the following data plots.



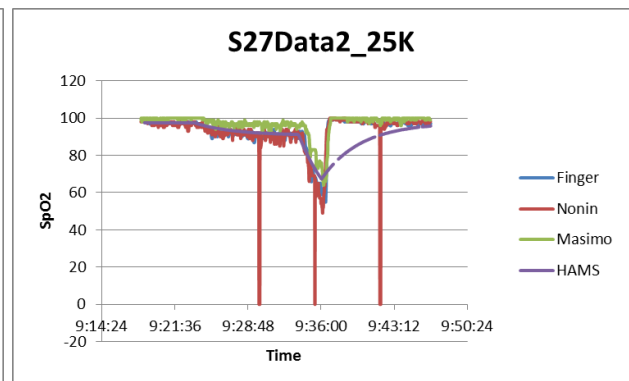
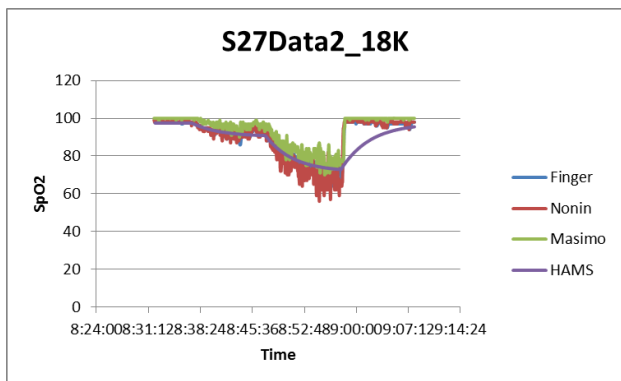
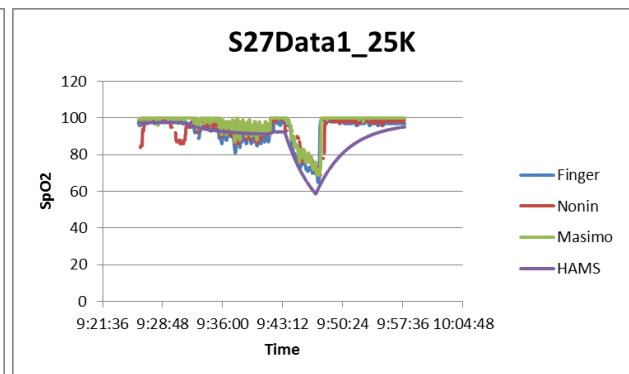
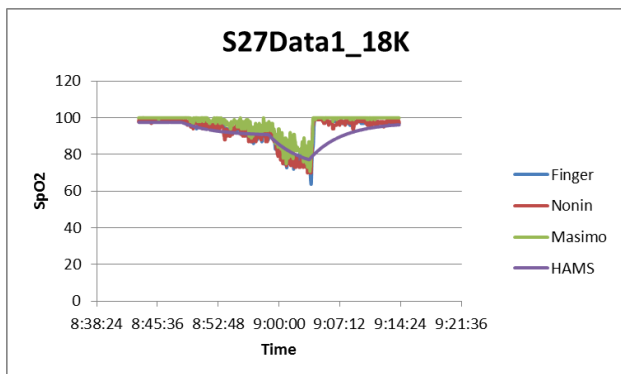
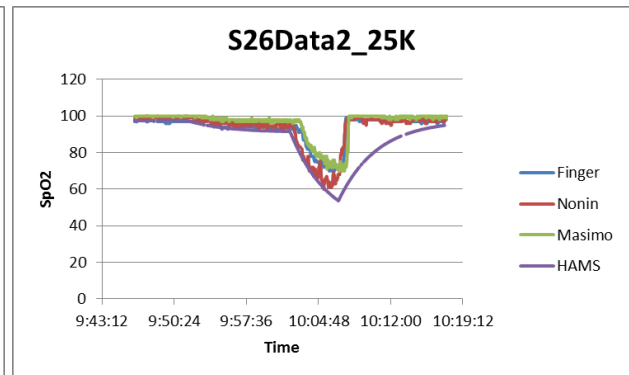
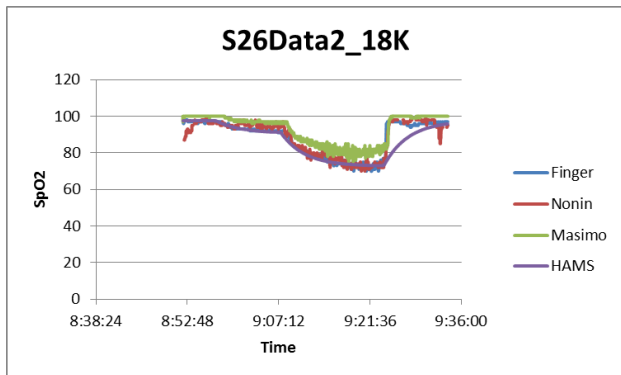
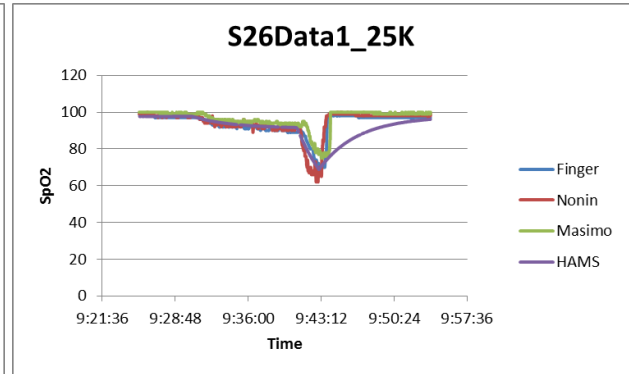
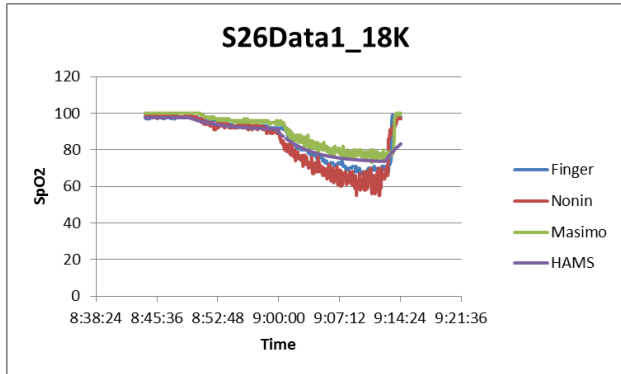
Document Title: HAMS Final Report (Technical and Financial)



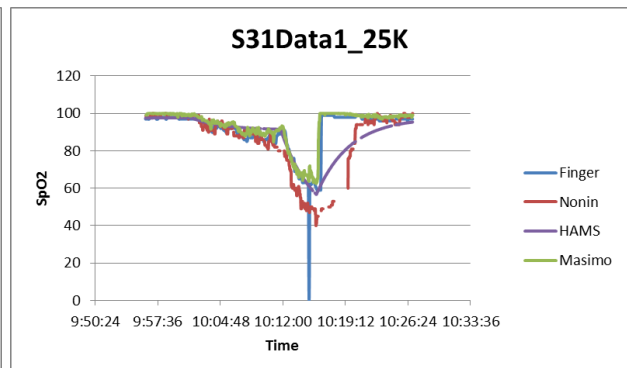
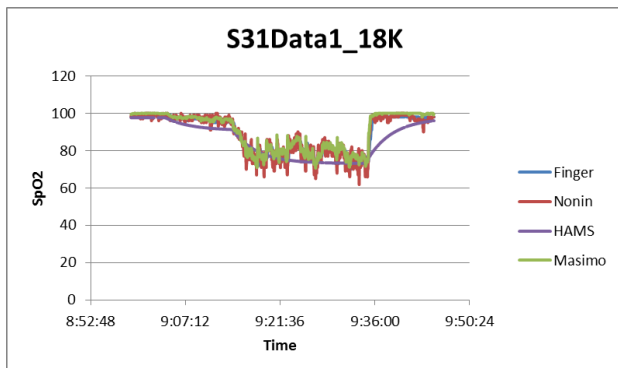
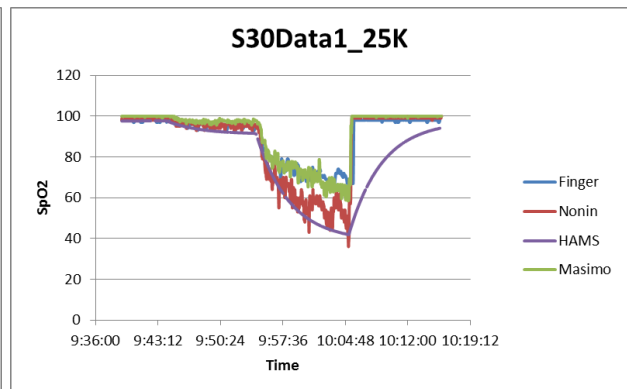
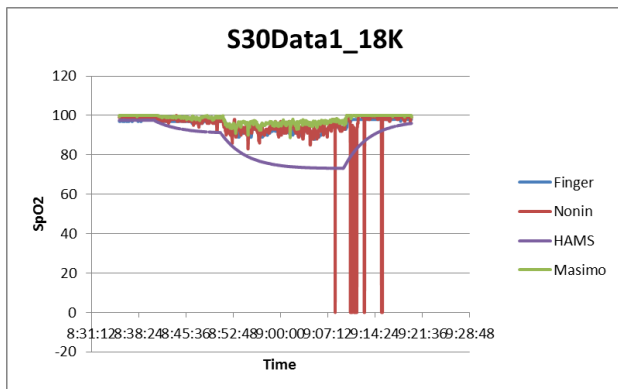
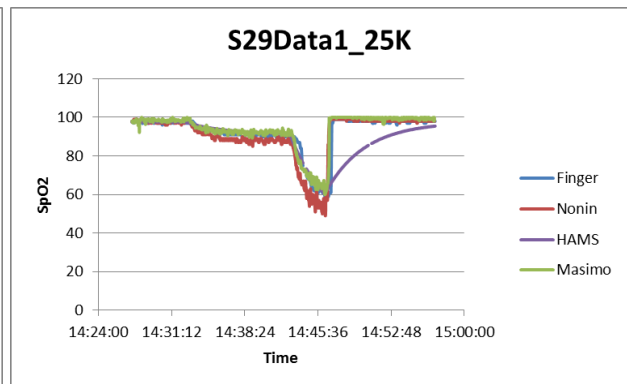
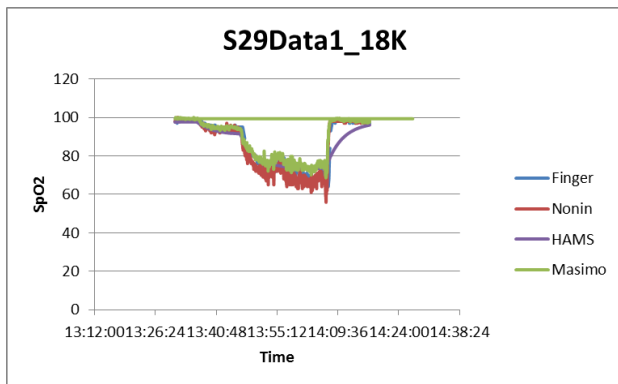
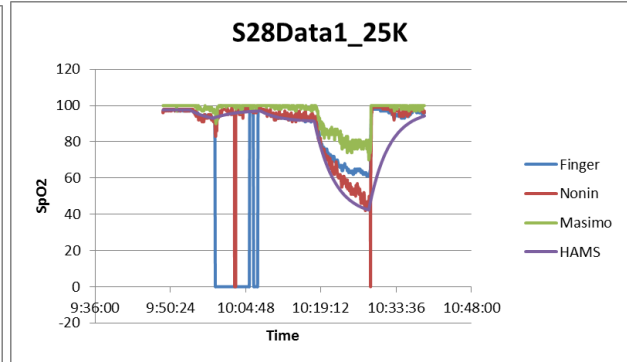
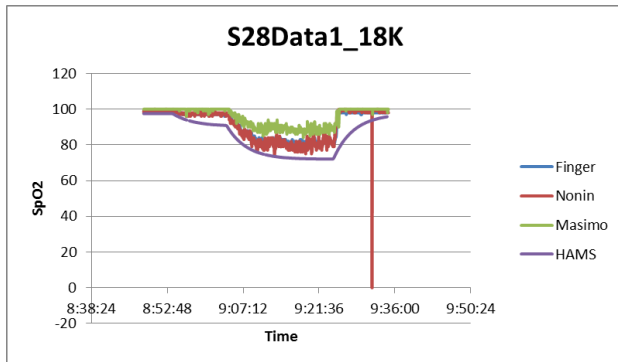
Document Title: HAMS Final Report (Technical and Financial)



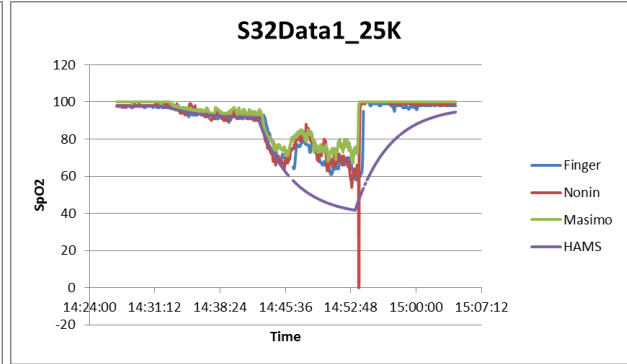
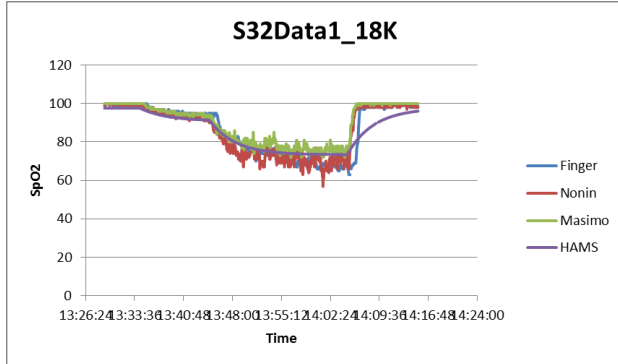
Document Title: HAMS Final Report (Technical and Financial)



Document Title: HAMS Final Report (Technical and Financial)

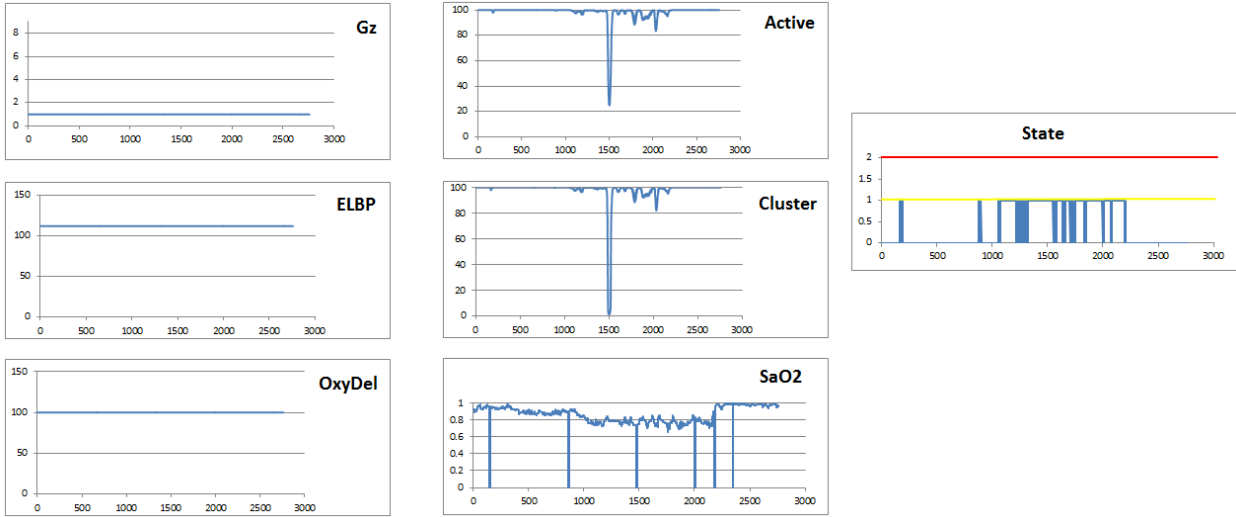


Document Title: HAMS Final Report (Technical and Financial)

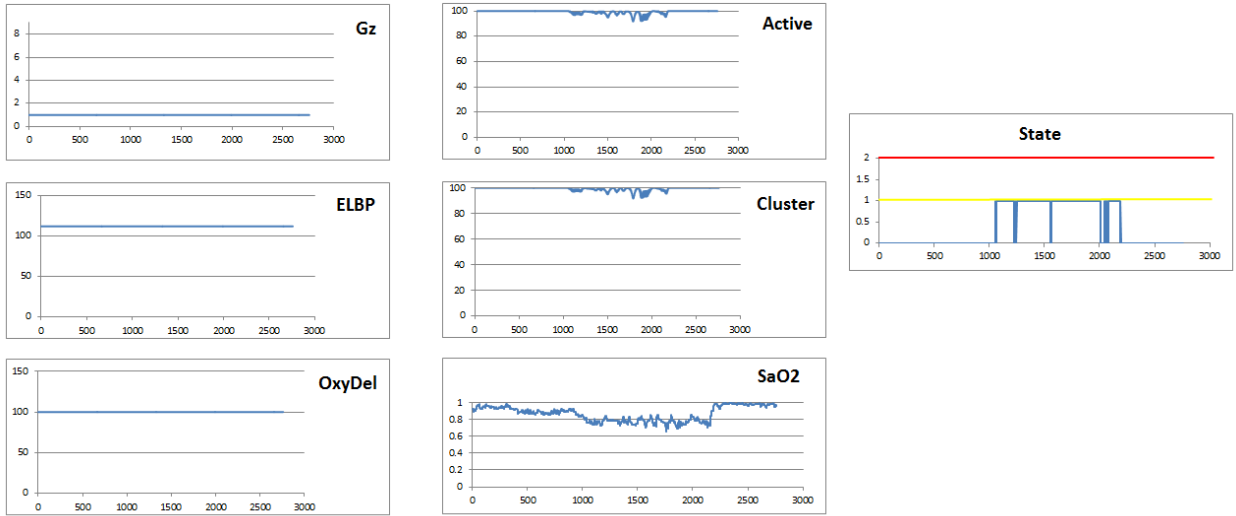


10.2.2 Subject Hypoxia Simulation Runs – Unconsciousness Model

S1 with dropouts at 18K



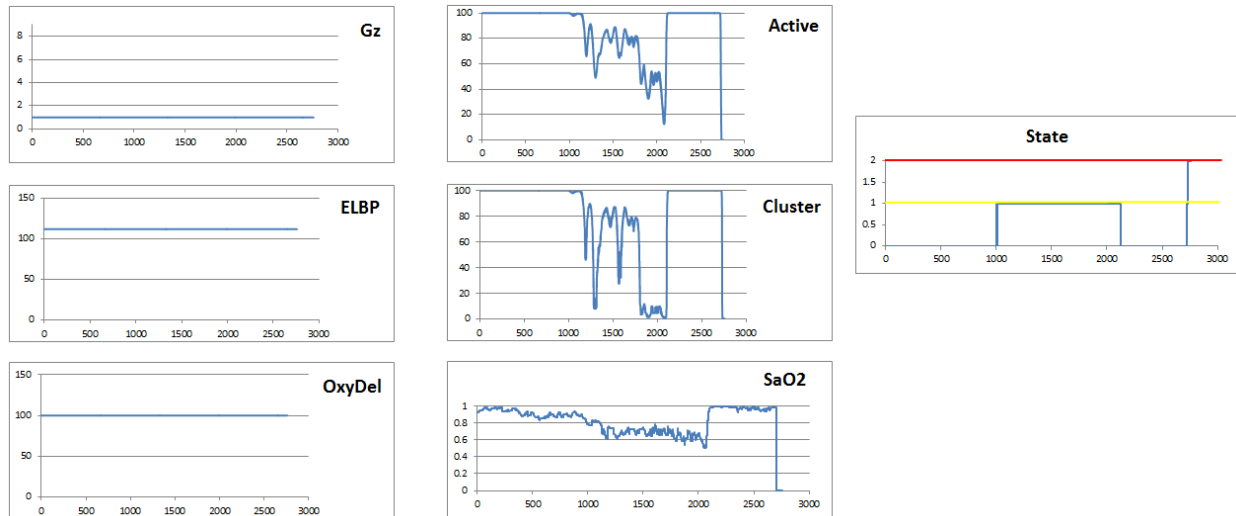
S1 at 18K with dropouts set to last value



S1-repeat



S1-1 25K



100% Oxygen given at 2082 sec

S3 – 18K



S3 – 18k - repeat

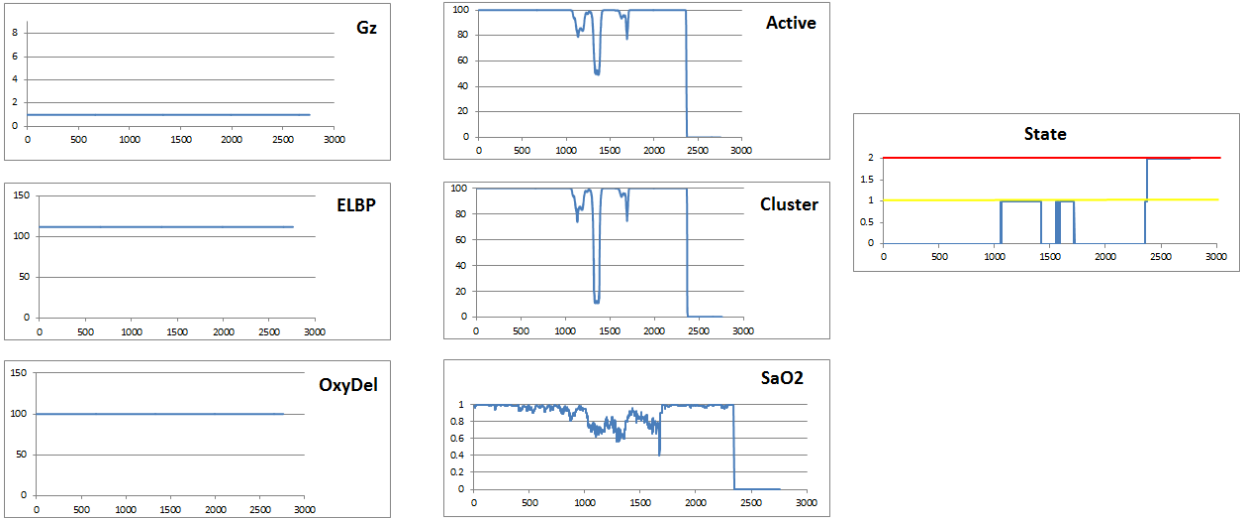


S3 – 25K



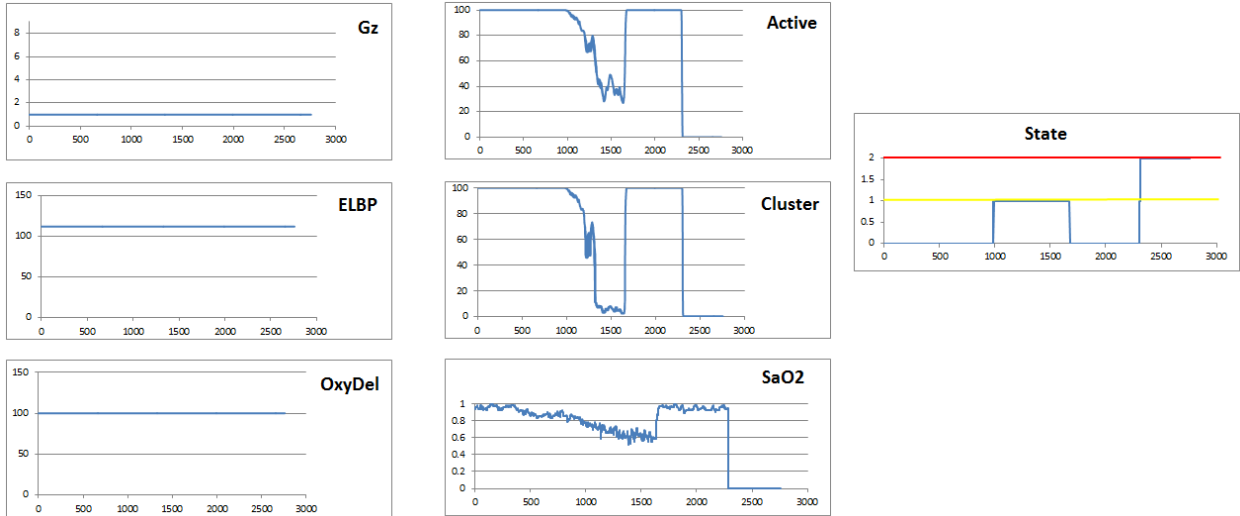
100% Oxygen given at 1696 seconds

S3 -25K - repeat



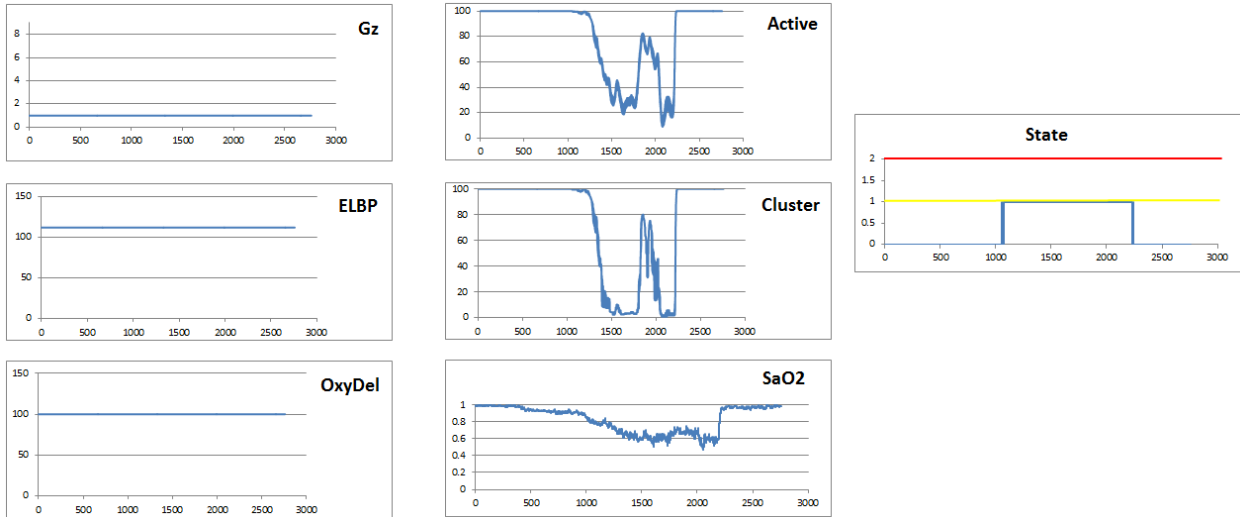
100% Oxygen given at 1660 seconds

S4 – 18K

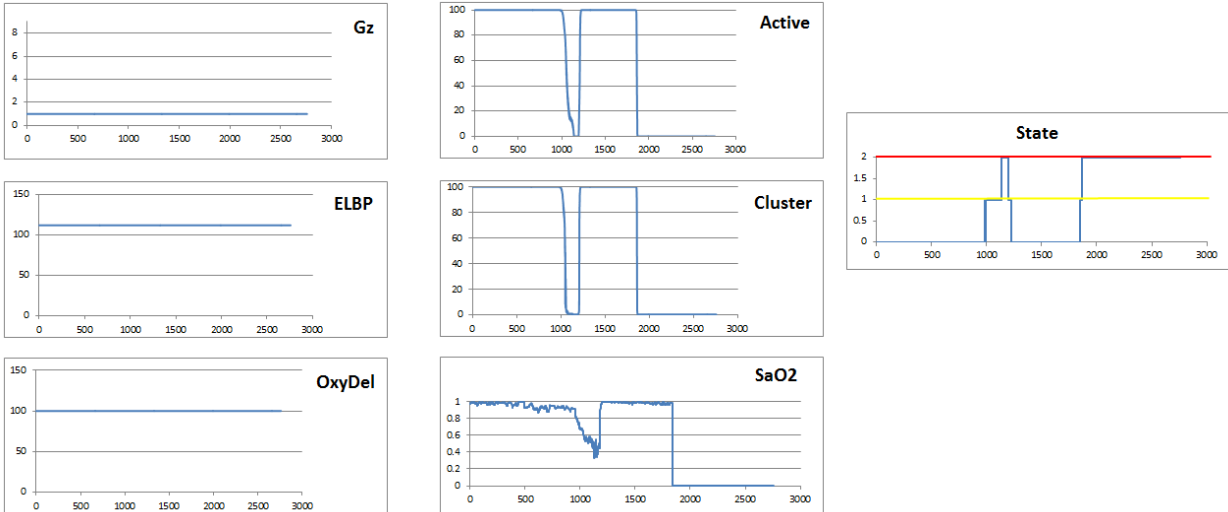


100% Oxygen given at 1645 seconds

S4 – 18K – repeat

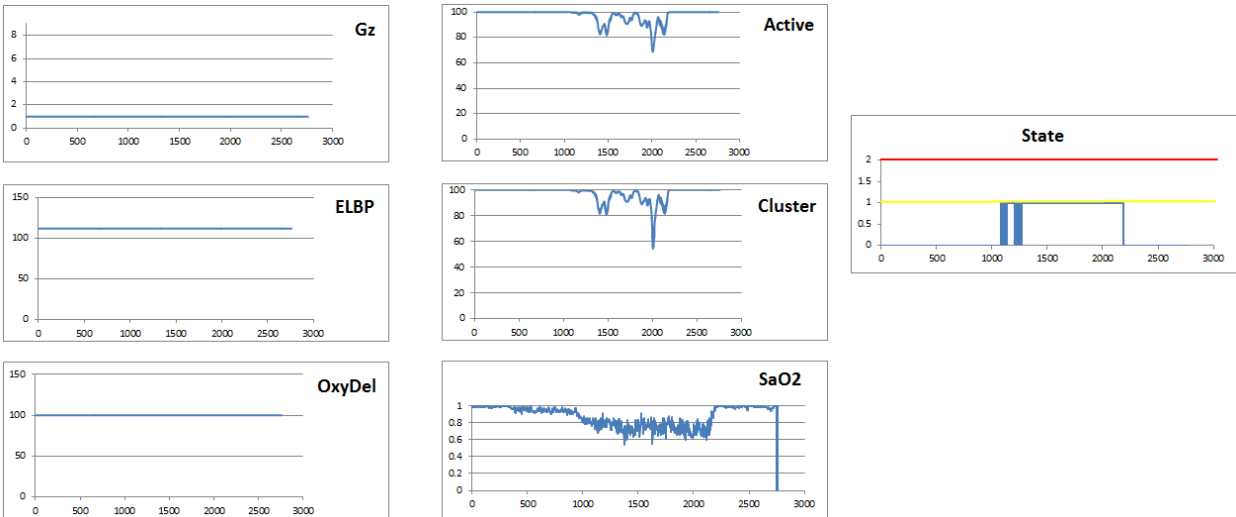


S4 – 25K

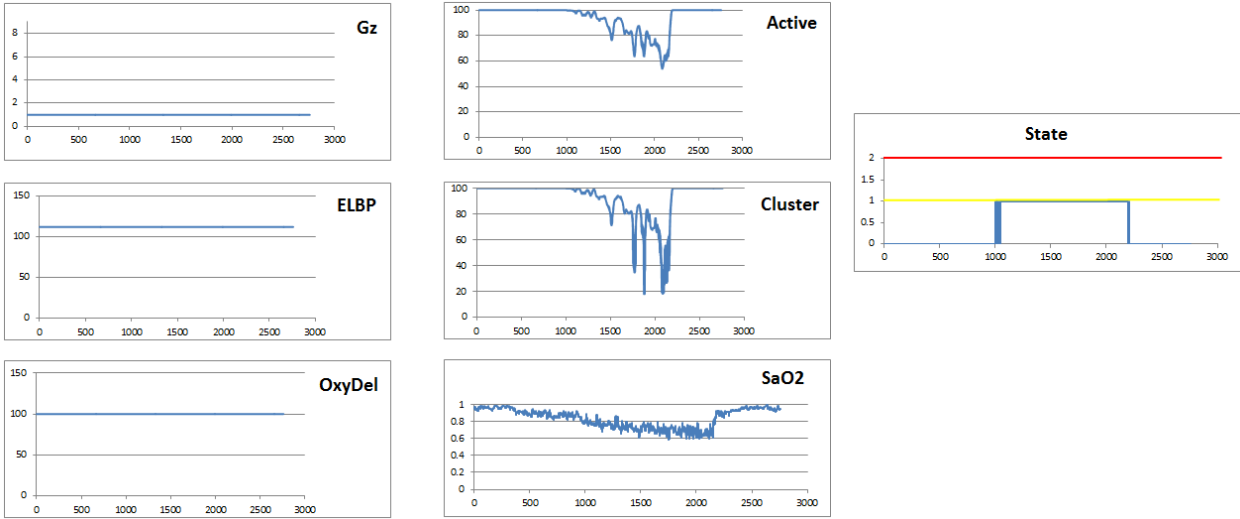


100% Oxygen given at 1177 seconds

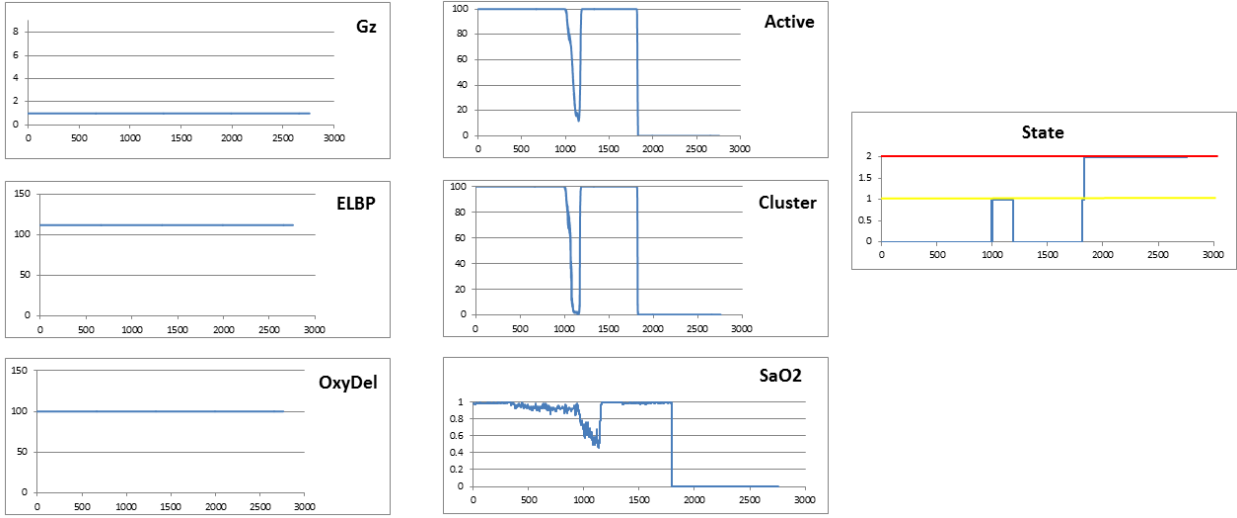
S5 – 18K



S5 – 18K – repeat



S5 – 25K



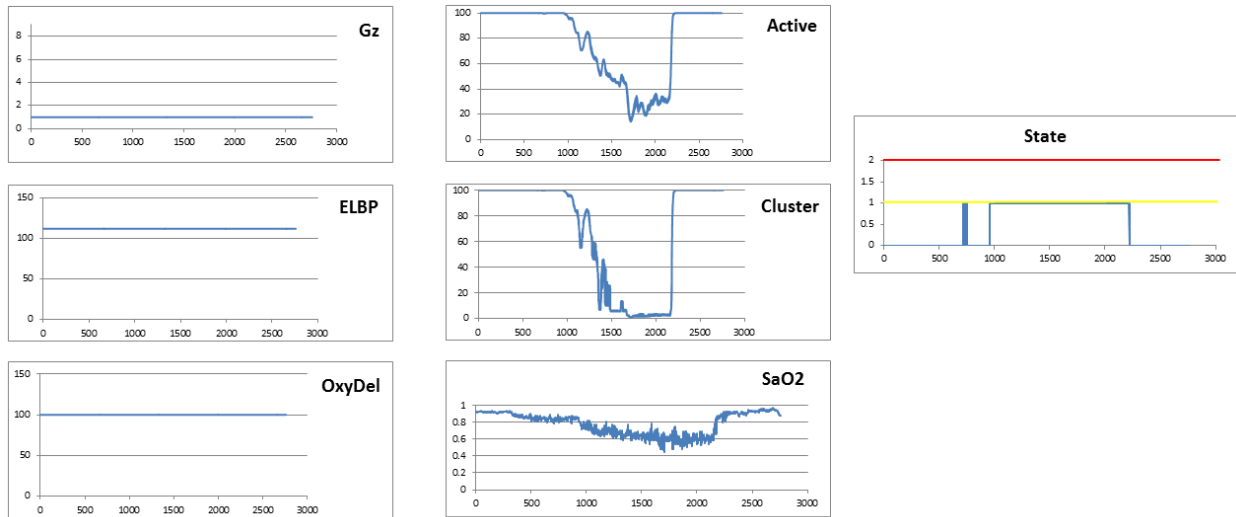
100% Oxygen given at 1145 seconds

S5 – 25K – repeat



100% Oxygen given at 1371 seconds

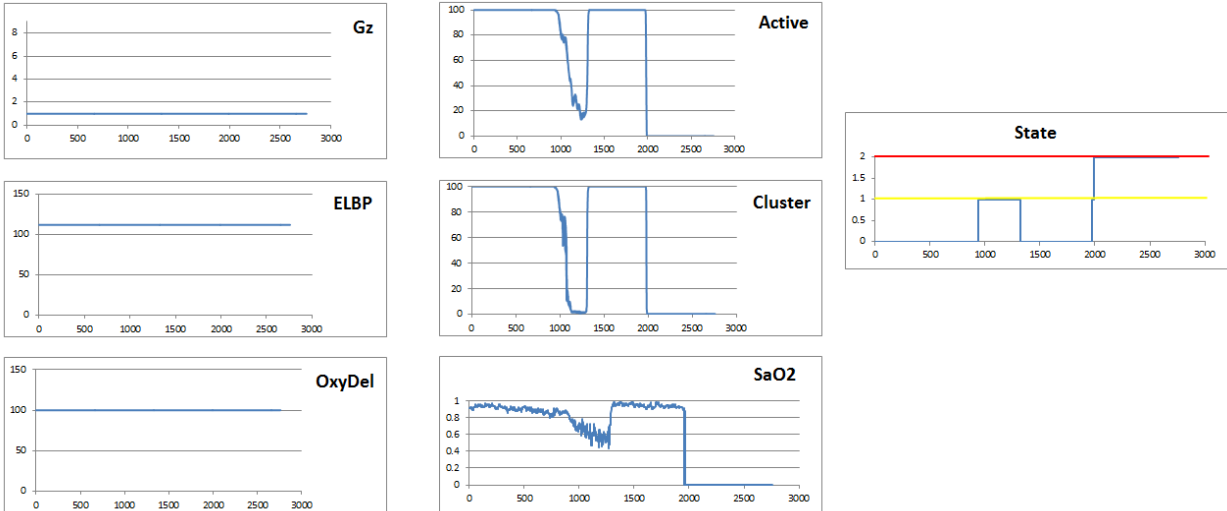
S7 – 18K



S7 – 18K – repeat



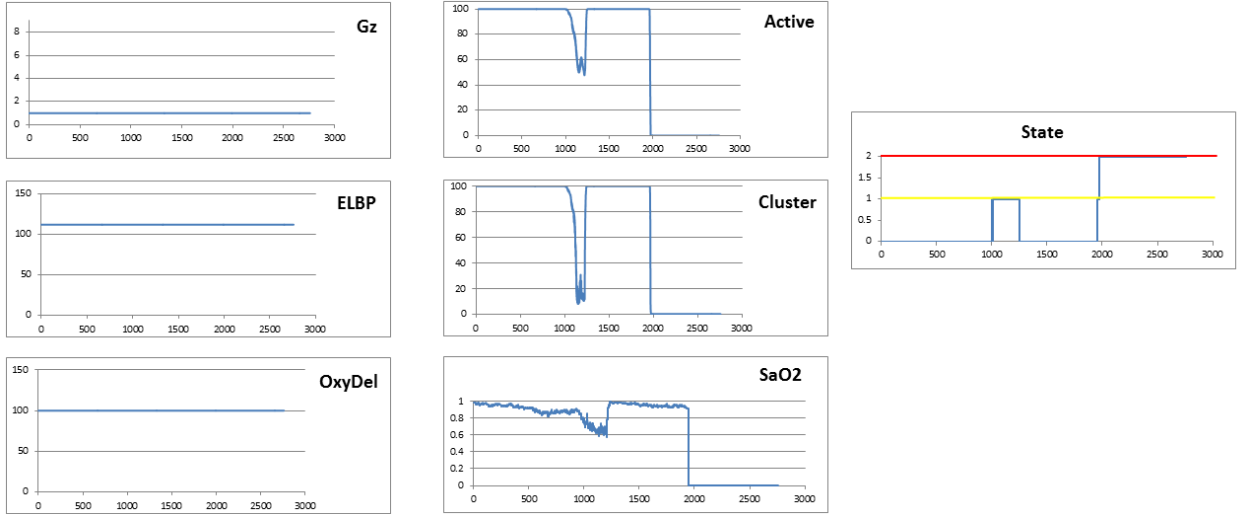
S7 – 25K



100% Oxygen given at 1308 seconds

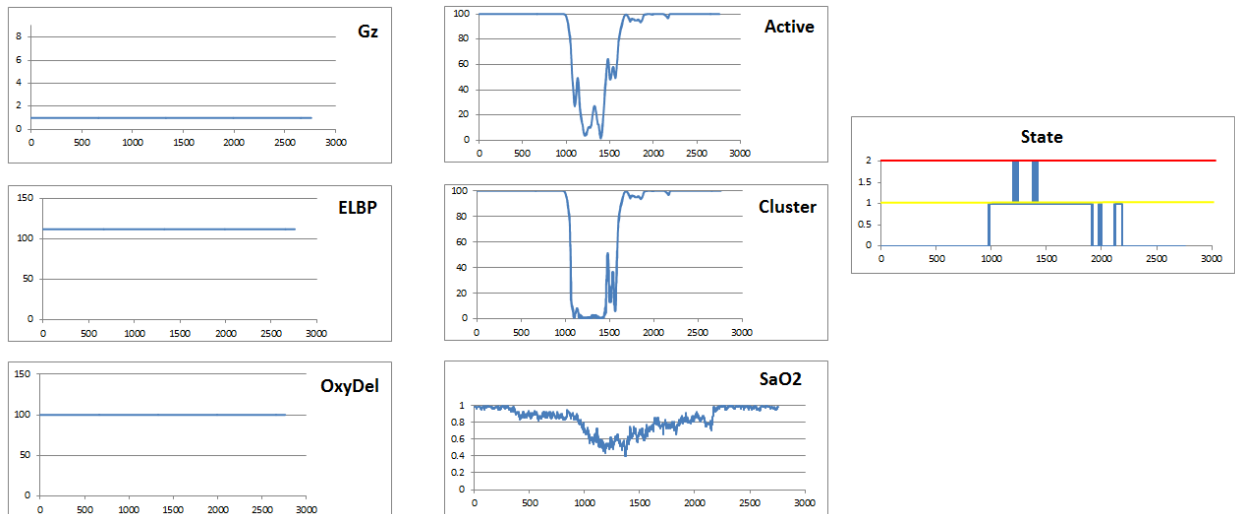
Document Title: HAMS Final Report (Technical and Financial)

S7 – 25K – repeat



100% Oxygen given at 1185 seconds

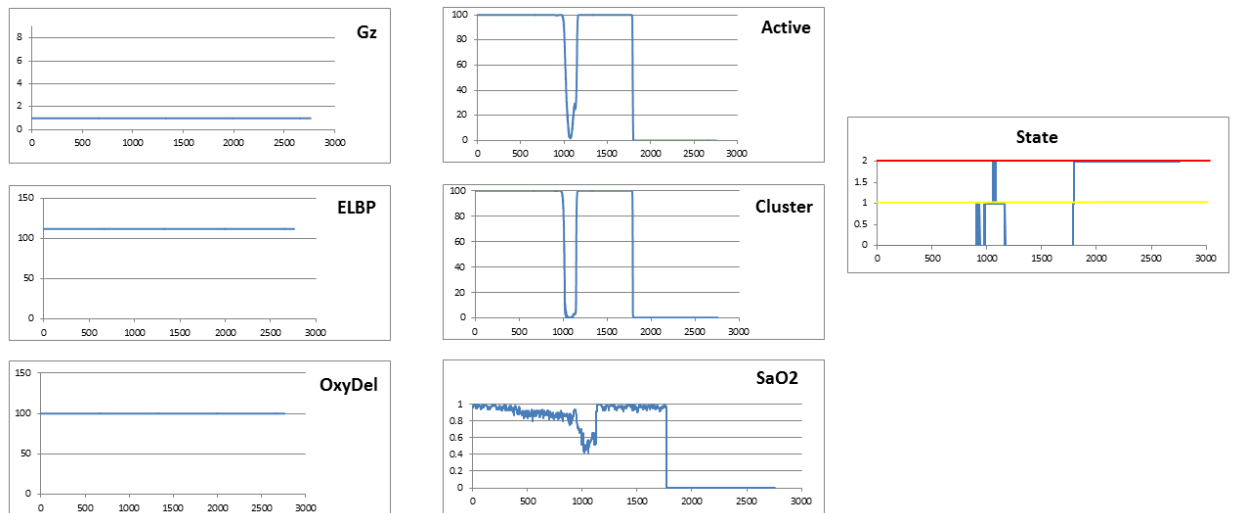
S8 – 18K



S8 – 18K – repeat

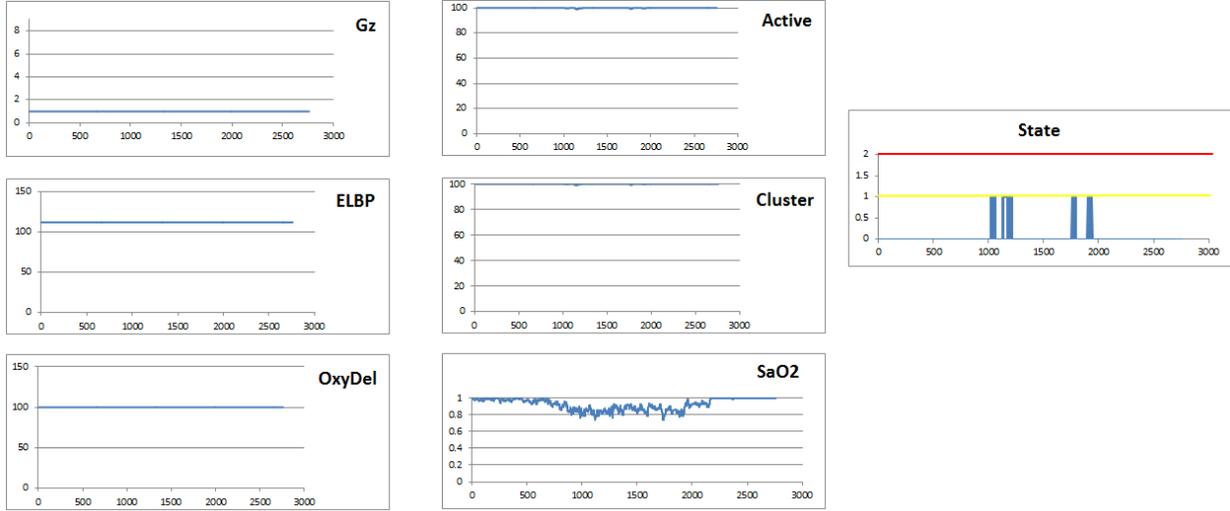


S8 – 25K

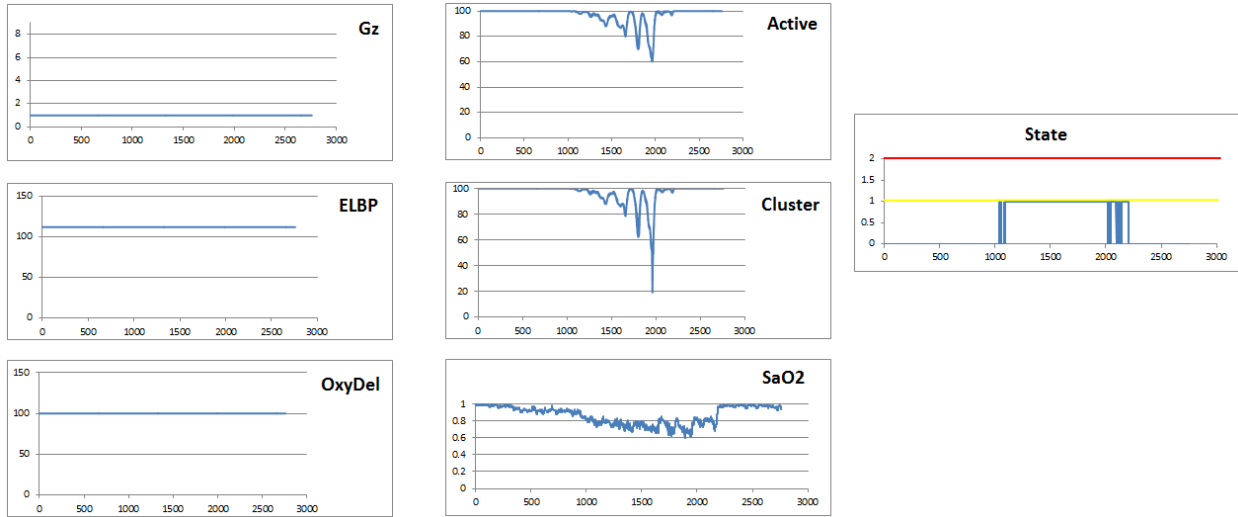


100% Oxygen given at 1117 seconds

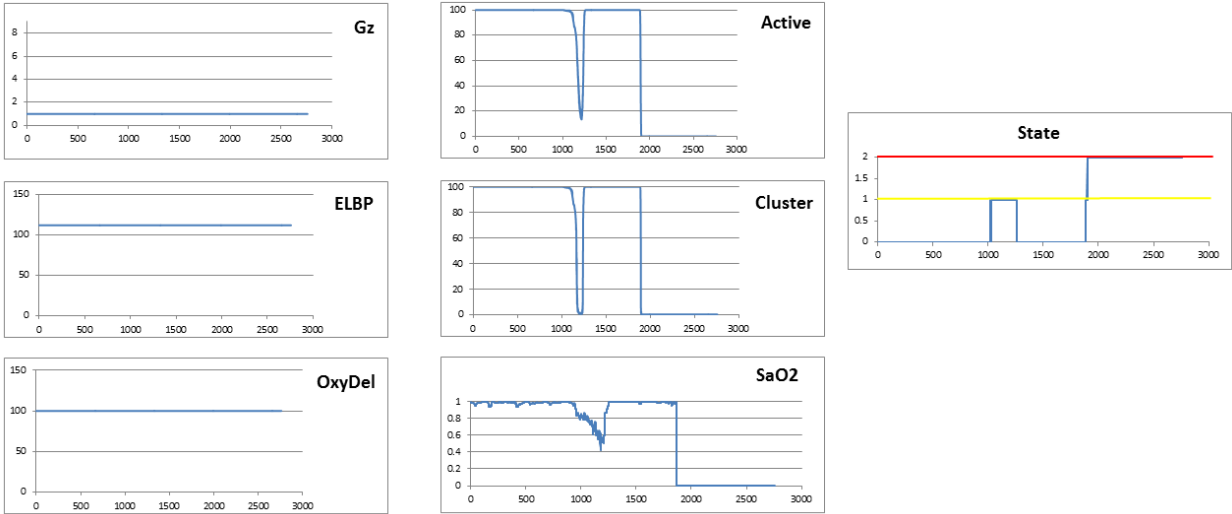
S9 – 18K



S9 – 18K - repeat

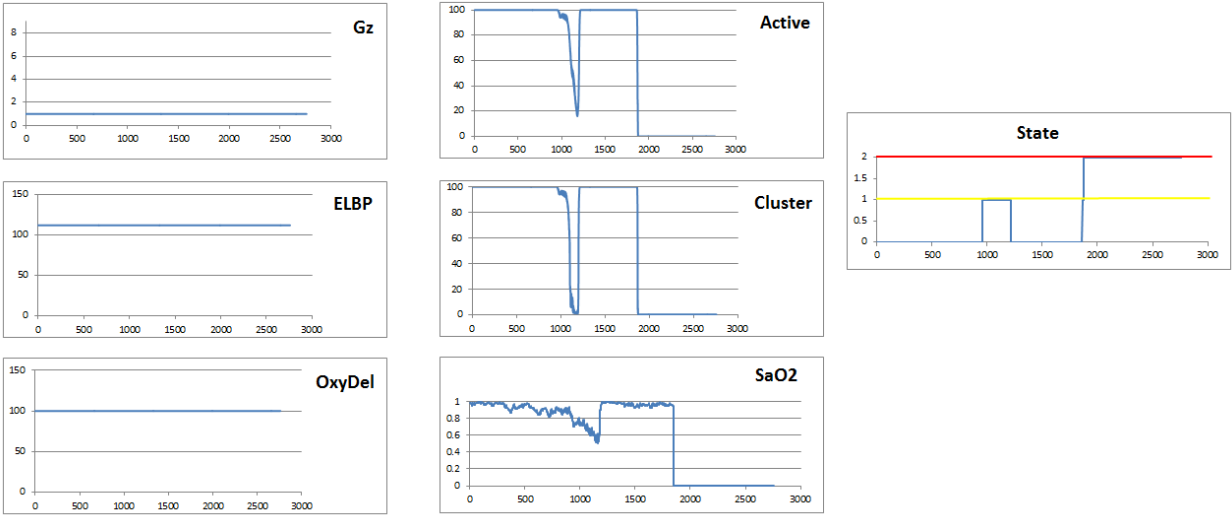


S9 – 25K



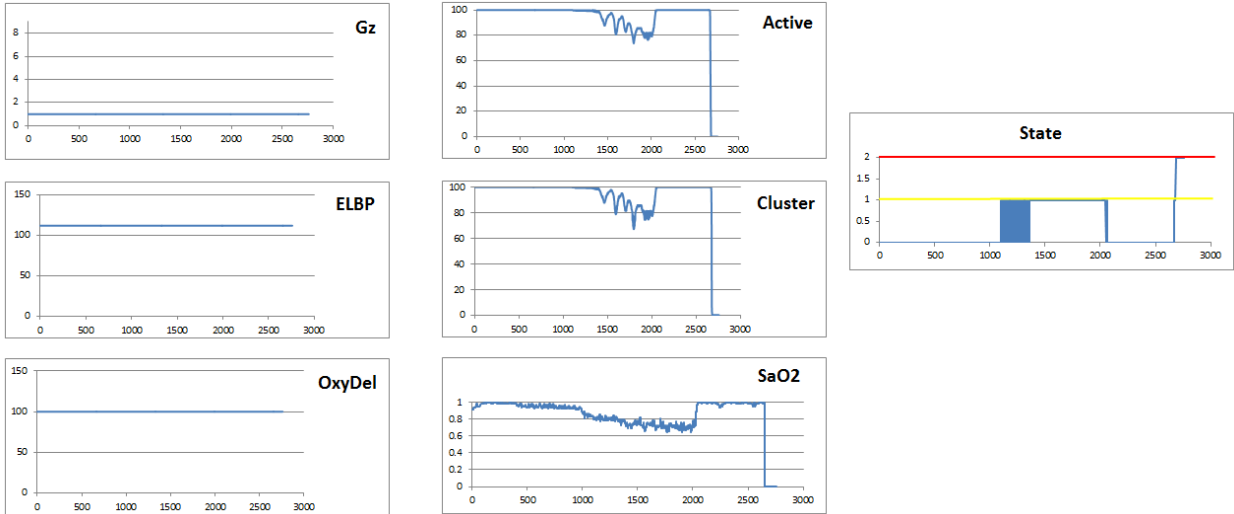
100% Oxygen given at 1212 seconds

S9 – 25K – repeat

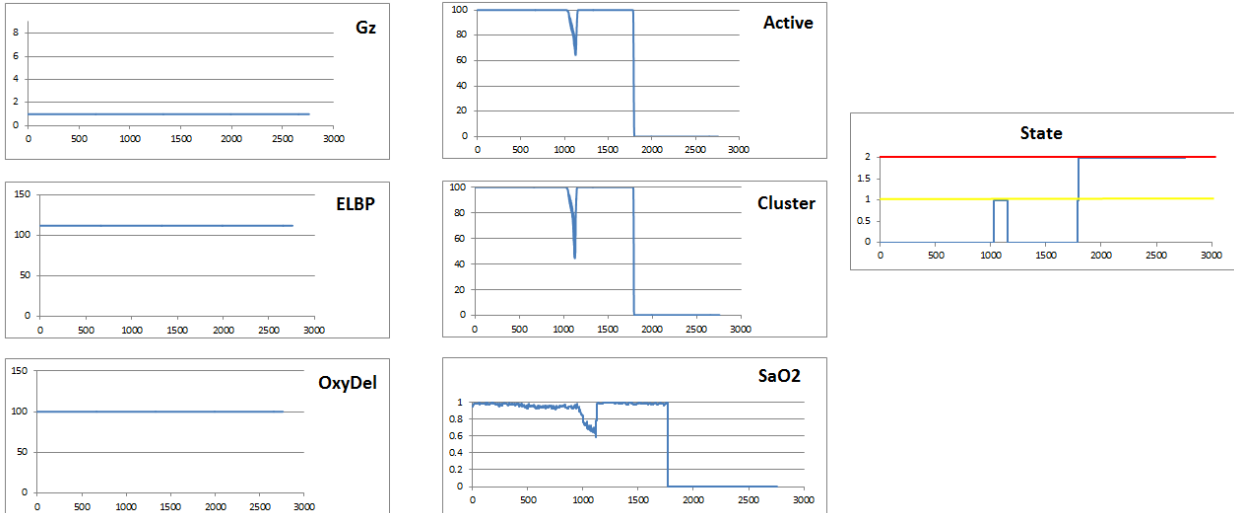


100% Oxygen given at 1208 seconds.

S10 – 18K



S10 – 25K



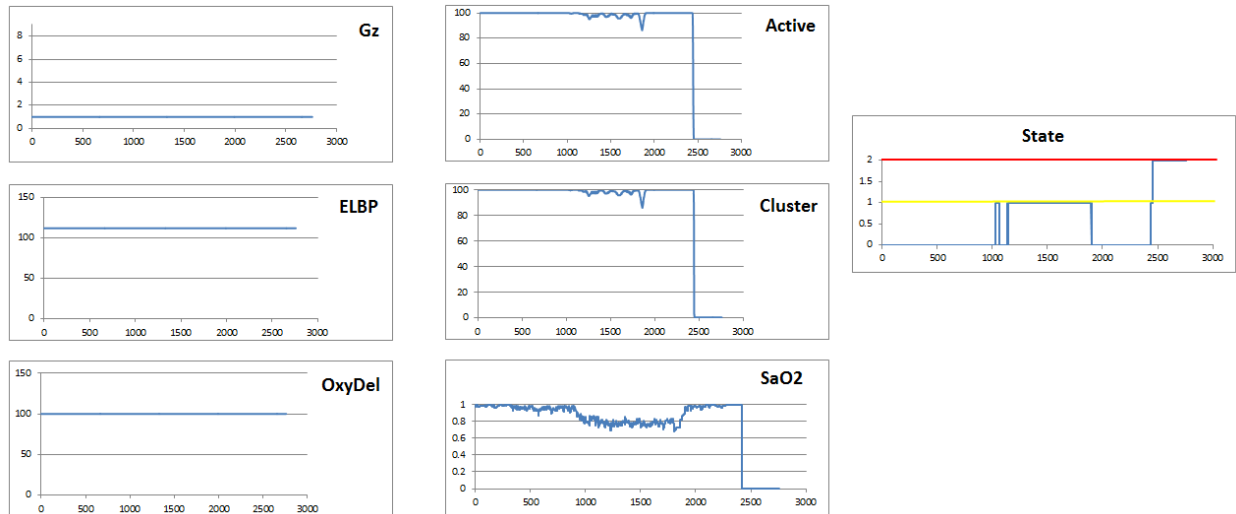
100% Oxygen given at 1208 seconds

S11 – 18K



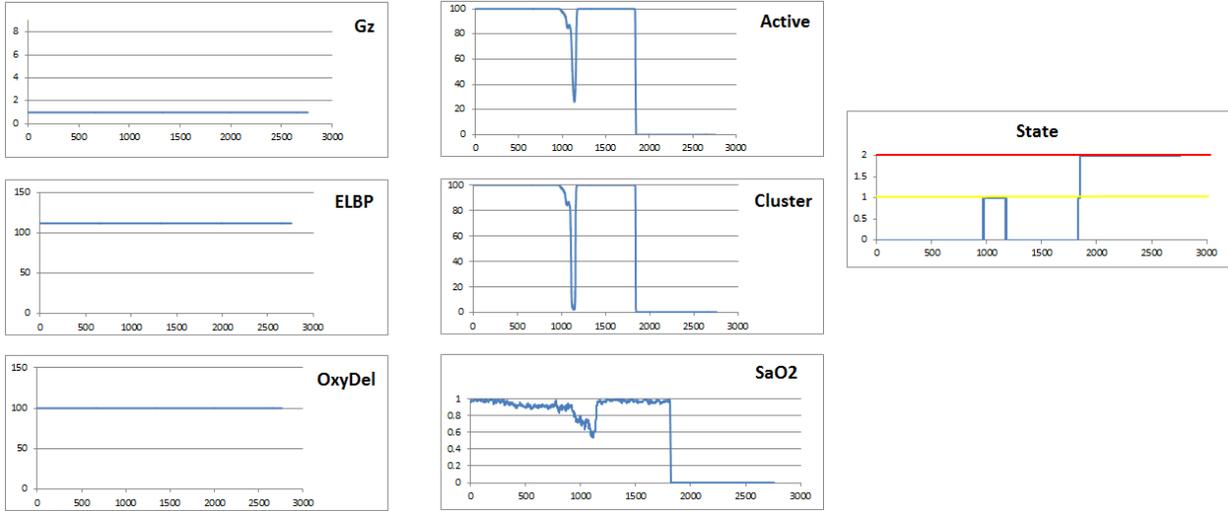
100 % Oxygen given at 1862 seconds

S11 – 18K - repeat



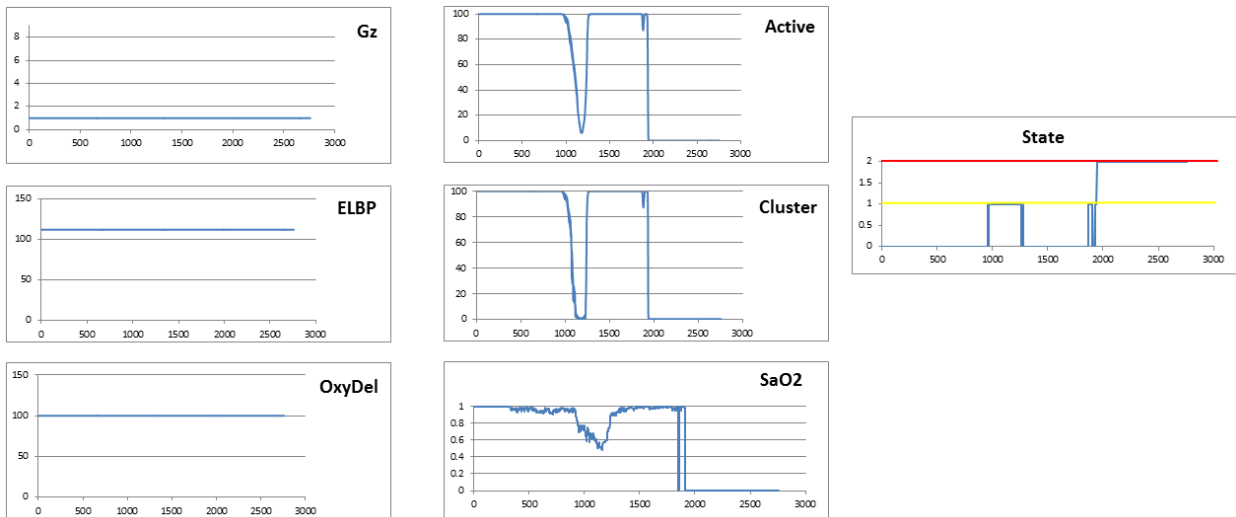
100% Oxygen given at 1855 seconds

S11 – 25K



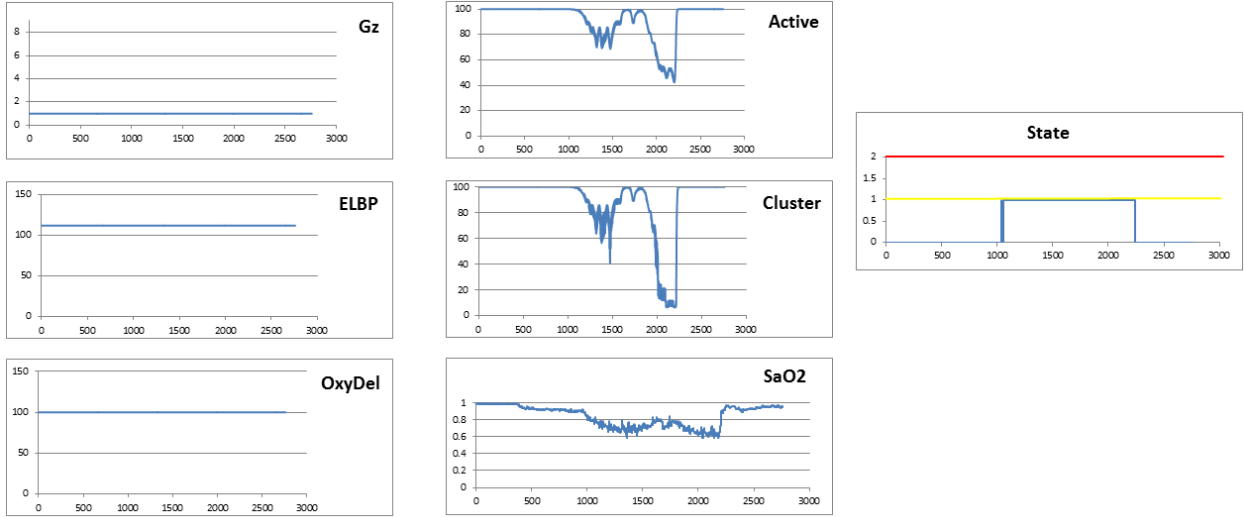
100% Oxygen given at 1152 seconds

S11 – 25K - repeat

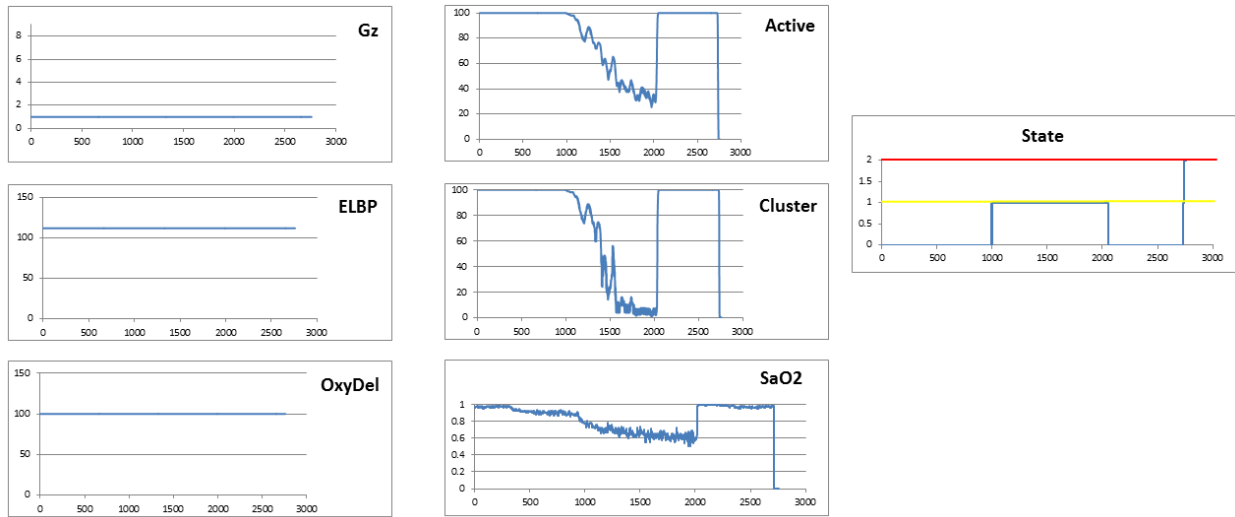


100% Oxygen given at 1185 seconds

S13 – 18K

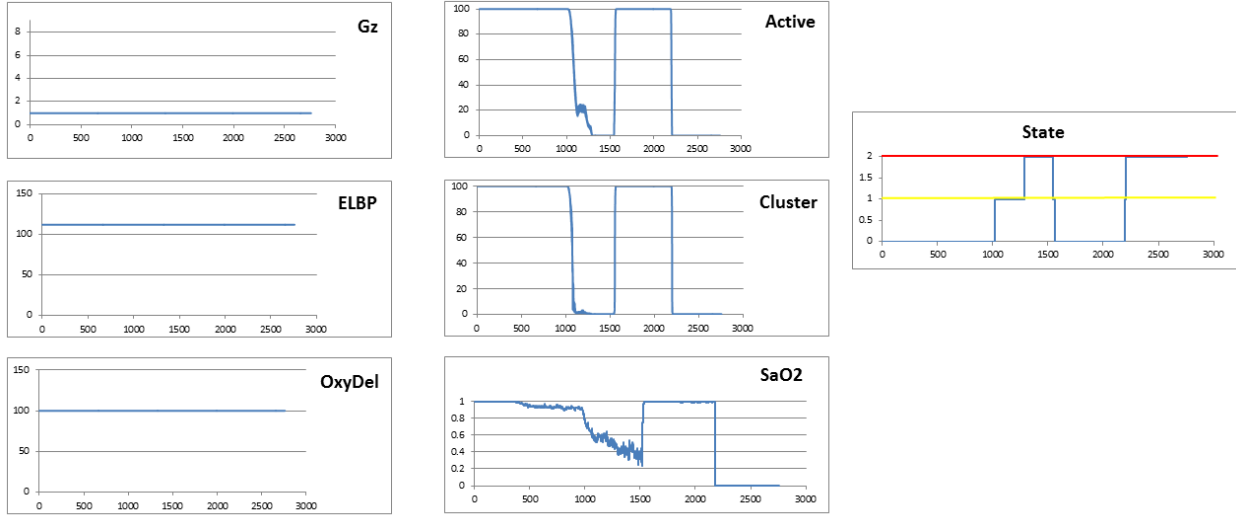


S13 – 18K – repeat



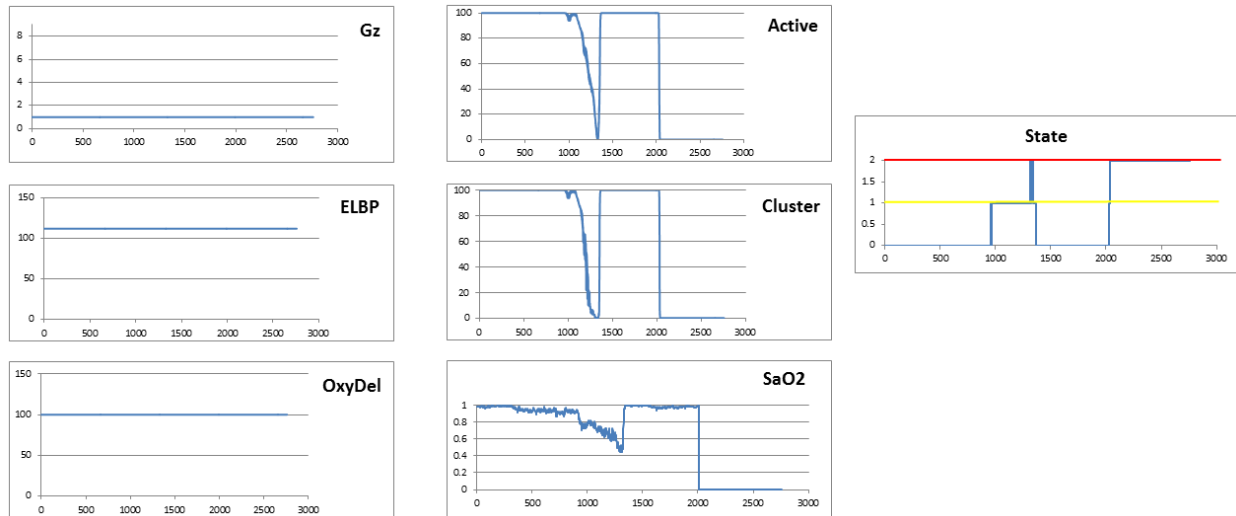
100% Oxygen given at 2017 seconds

S13 – 25K



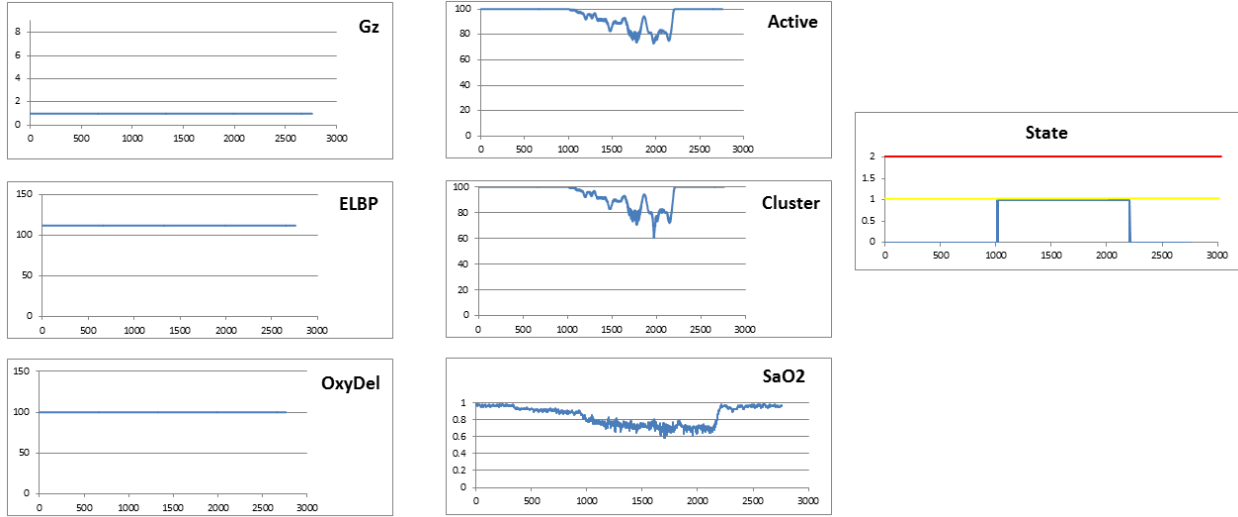
100% Oxygen given at 1486 seconds

S13 – 25K – repeat

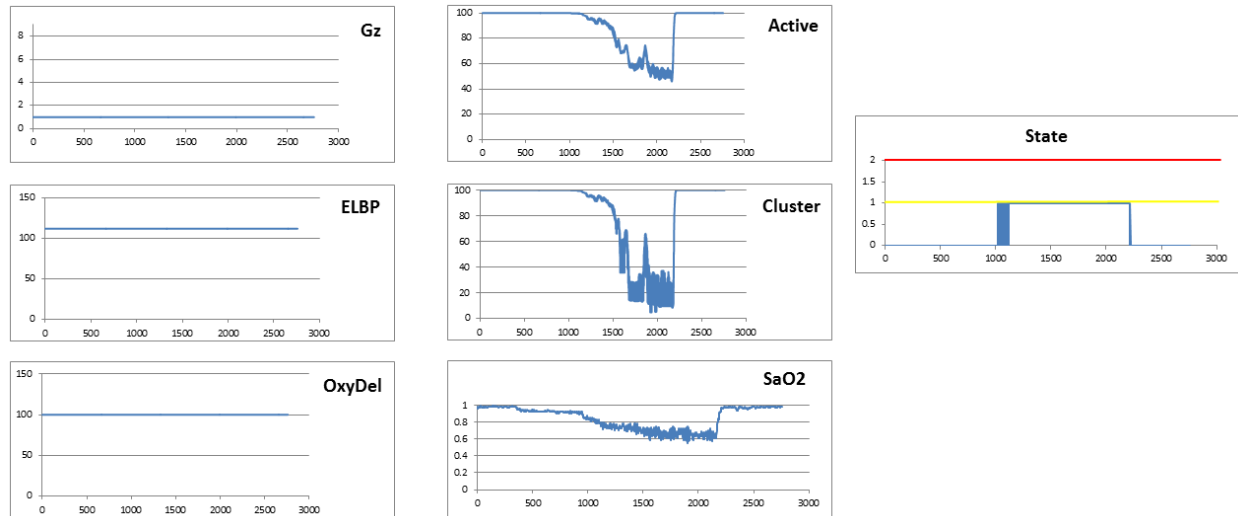


100% Oxygen given at 1350 seconds

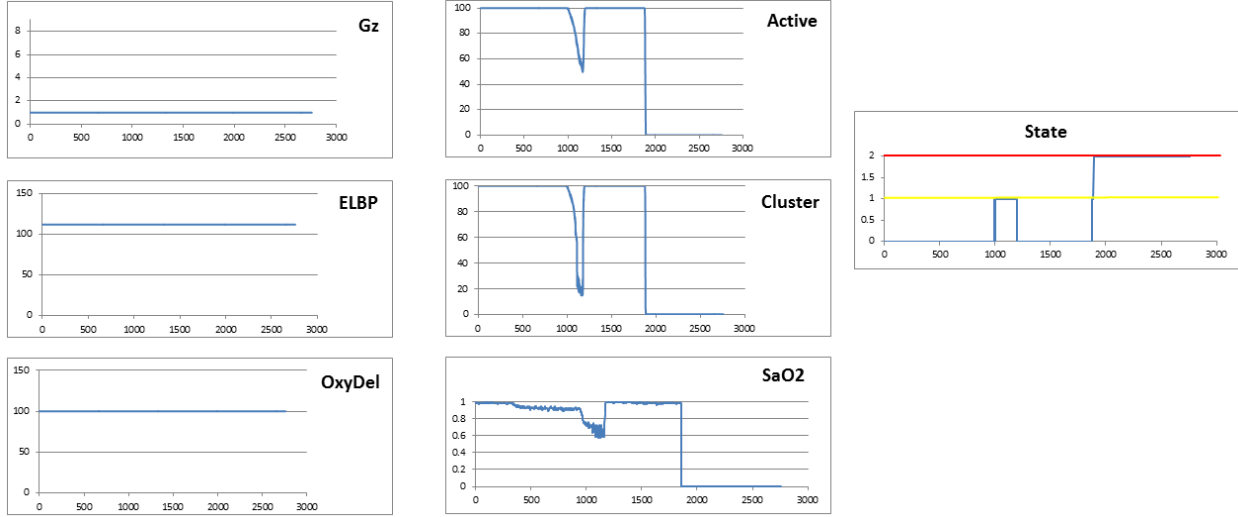
S14 – 18K



S14 – 18K – repeat

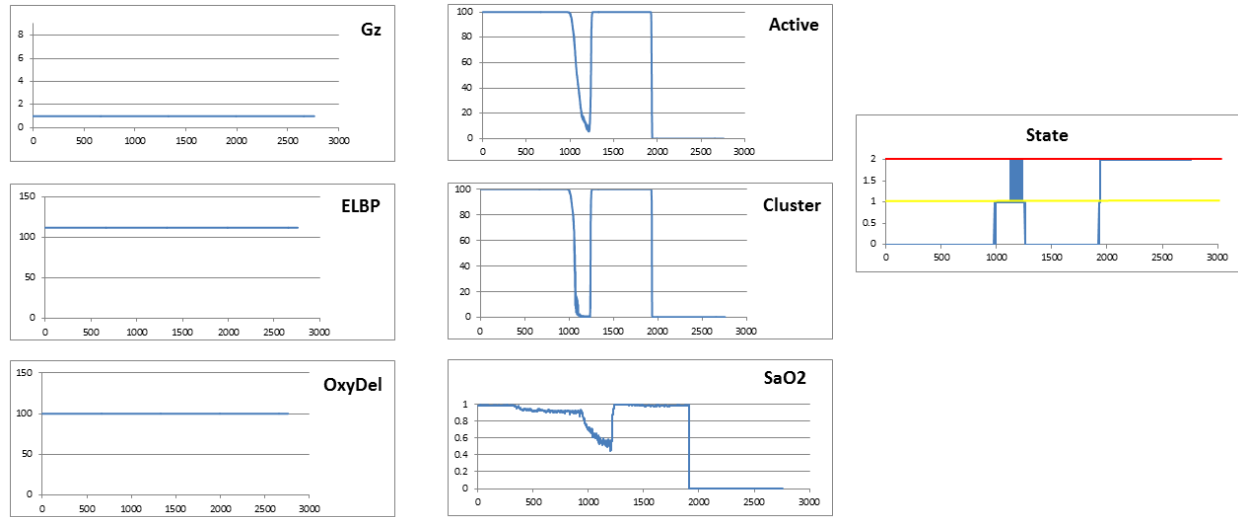


S14 – 25K



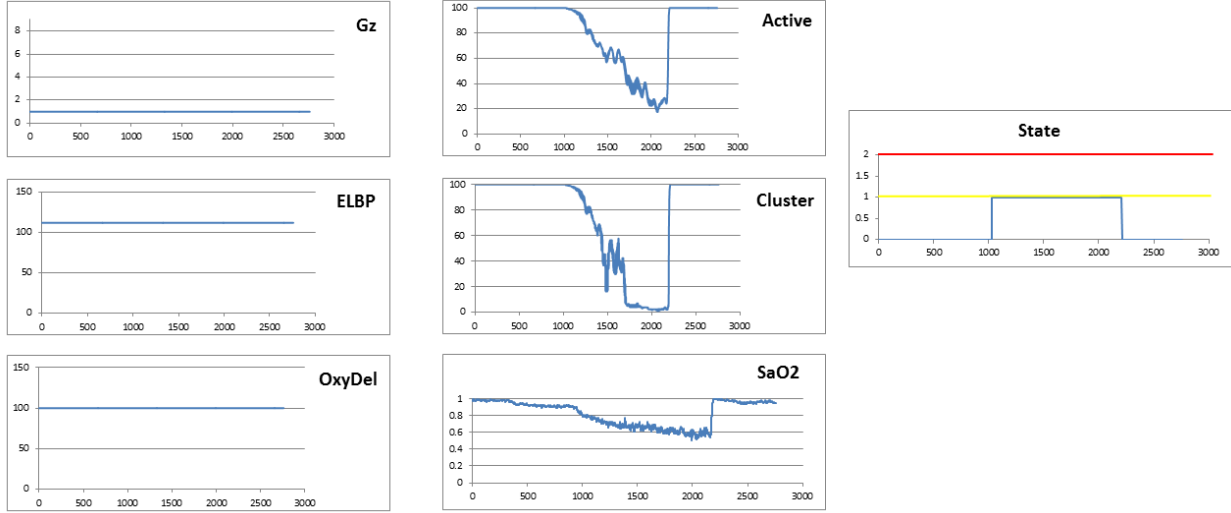
100% Oxygen given at 1157 seconds

S14 – 25K – repeat



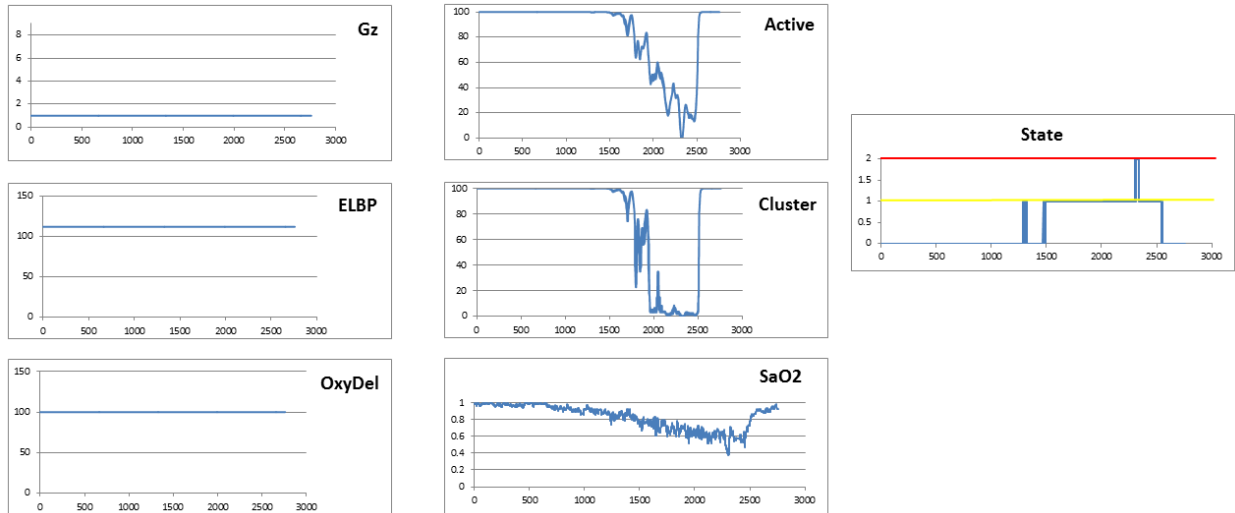
100% Oxygen given at 1212 seconds

S16 – 18K

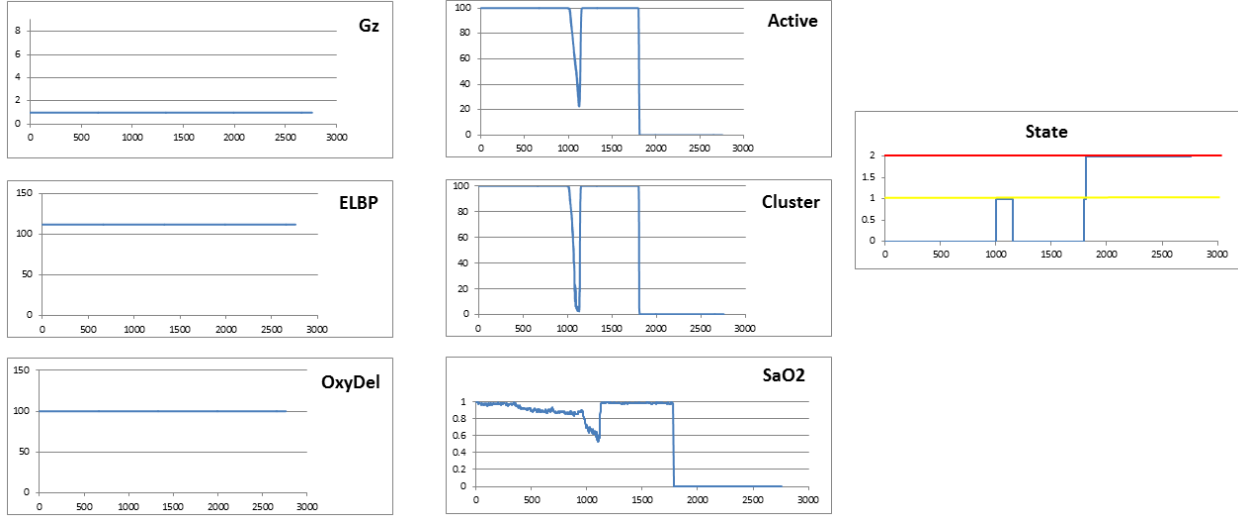


100% Oxygen given at 2150 seconds

S16 – 18K – repeat

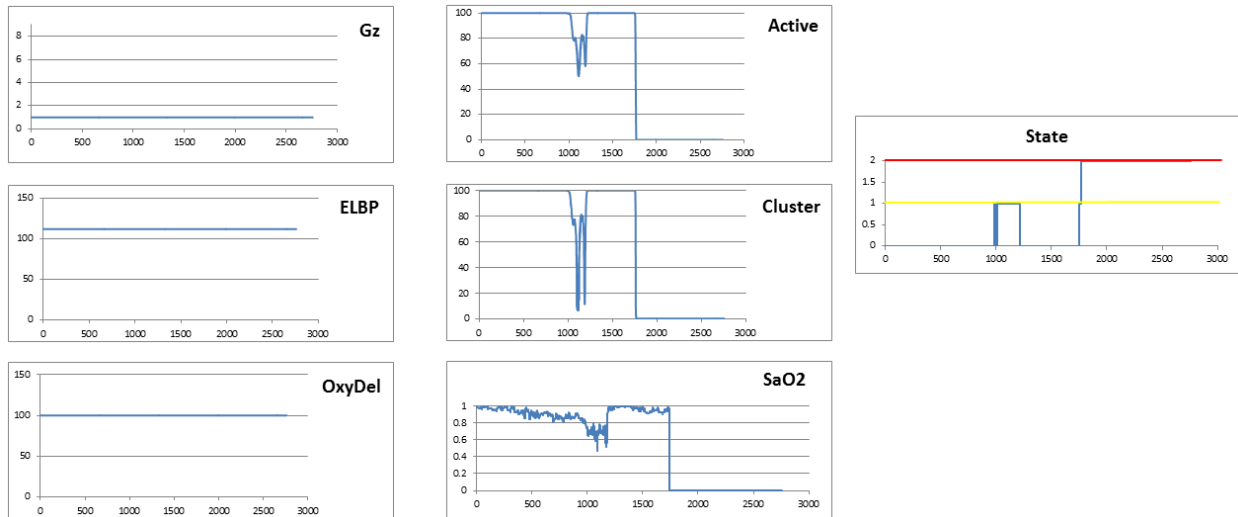


S16 – 25K



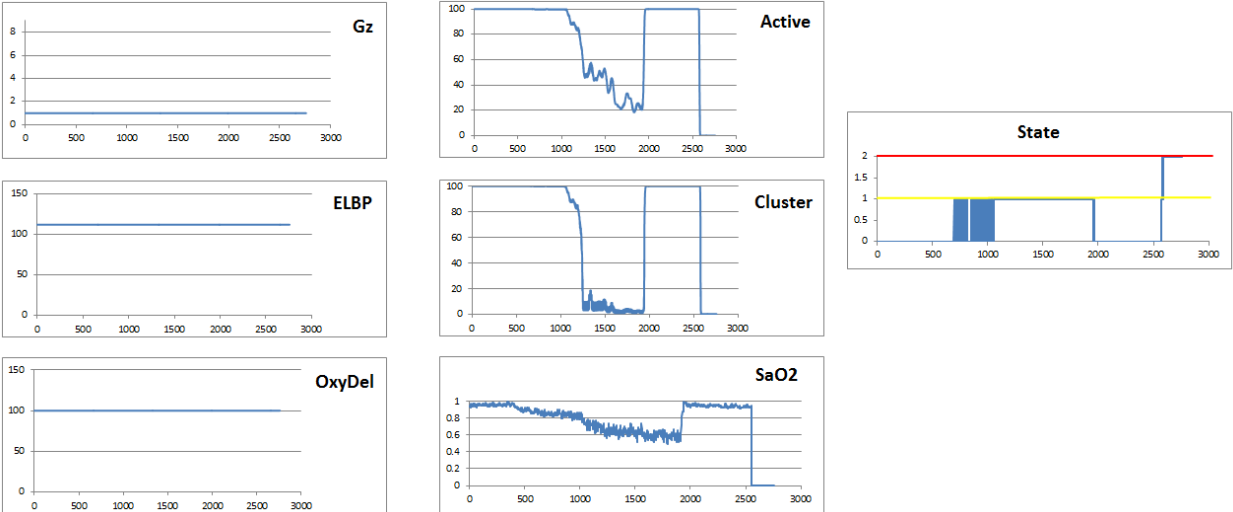
100% Oxygen given at 1096 seconds

S16 – 25K – repeat



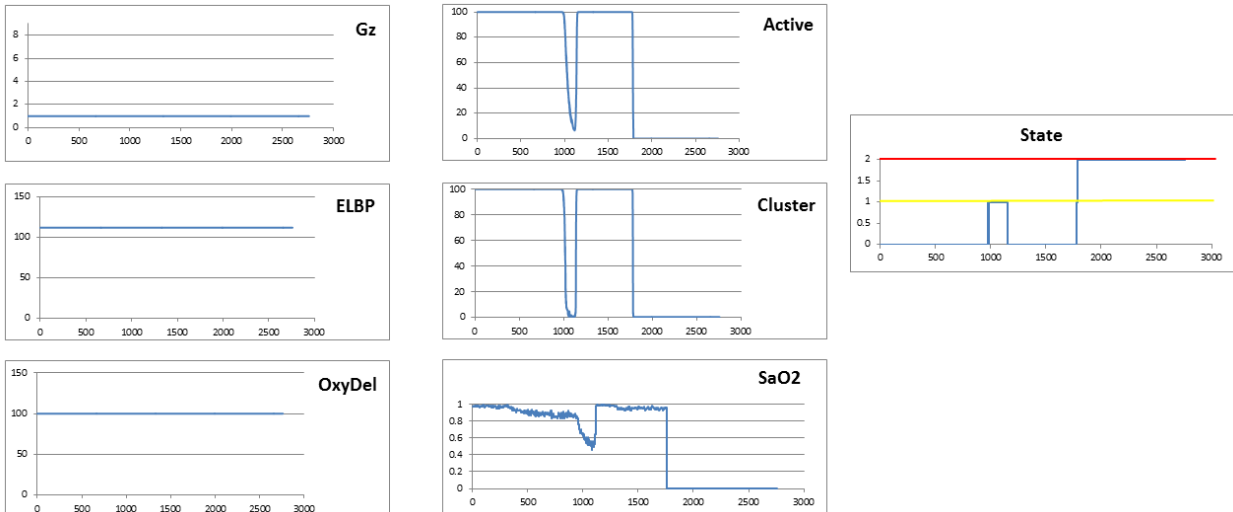
100% Oxygen given at 1155 seconds

S19 – 18K



100% Oxygen given at 1911 seconds

S19 – 25K



100% Oxygen given at 1114 seconds

10.3 Detailed Financial Spreadsheets (PDF)

H.A.M.S. FUND YEAR 2013															
CONTRACT# N00014-13-C-0323															
Begins July 24, 2013 - May 31, 2014															
ACTUAL EXPENDITURE % BY MONTH based on 170K															
58.69% 81.48% 93.81% 100.00% 100.00% 100.00% 100.00% 100.00% 100.00% 100.00%															
HAMS FY 2013	CUMULATIVE SPENT FY13 FUNDS	REMAINING BUDGET	% of Total FUNDS Expended	MO 1 - AUG	MO 2 - SEP	MO 3 - OCT	MO 4 - NOV	MO 5 DEC	MO 6 - JAN	MO 7 - FEB	MO 8 - MAR	MO 9 - APR	MO 10 - MAY	MO 11 - JUN	MO 12 - JUL
COST INCURRED	\$ 170,000.00	\$ 0.00	100%	\$ 99,767.22	\$ 38,756.79	\$ 20,956.96	\$ 10,519.03	\$ -	\$ -	\$ -	\$ -	\$ -	\$ -	\$ -	\$ -
				Benchmark FY13											
				49.07%	56%	57.87%	63.12%	67.67%	73.02%	76.04%					

H.A.M.S. FUND YEAR 2014															
CONTRACT# N00014-13-C-0323															
Begins Jul 24, 2013 - Jul 31, 2014															
ACTUAL EXPENDITURE % BY MONTH Based on 286K															
0.00% 0.00% 0.00% 0.20% 9.64% 20.90% 34.93% 49.33% 63.45% 73.46% 73.46% 73.46%															
HAMS FY 2014	CUMULATIVE SPENT FY14 FUNDS	REMAINING BUDGET	% of Total FUNDS Expended	MO 1 - AUG	MO 2 - SEP	MO 3 - OCT	MO 4 - NOV	MO 5 DEC	MO 6 - JAN	MO 7 - FEB	MO 8 - MAR	MO 9 - APR	MO 10 - MAY	MO 11 - JUN	MO 12 - JUL
TOTAL USED	\$ 210,214.12	\$ 75,946.88	73.46%	\$ -	\$ -	\$ -	\$ 560.08	\$ 27,023.01	\$ 32,216.03	\$ 40,167.74	\$ 41,186.33	\$ 40,403.31	\$ 28,657.62	\$ -	\$ -
				Task 1, 2, 3, 6 Task 1, 2, 3, 6 Task 2, 3, 6 Task, 3, 6 Task, 3, 6 Task, 3, 4, 6 Task, 4, 6 Task, 4, 6 Task, 4, 6 Task, 4, 6 Option task 5 option task 5											
HAMS FY 2014	BUDGET 2			MO 1 - AUG	MO 2 - SEP	MO 3 - OCT	MO 4 - NOV	MO 5 - DEC	MO 6 - JAN	MO 7 - FEB	MO 8 - MAR	MO 9 - APR	MO 10 - MAY	MO 11 - JUN	MO 12 - JUL
TOTAL BUDGET	\$ 286,161.00			\$ -	\$ -	\$ -	\$ -	\$ 44,196.87	\$ 53,243.55	\$ 34,325.33	\$ 30,929.78	\$ 24,021.05	\$ 28,388.41	\$ 37,392.10	\$ 33,663.91
				Projected expenditure % based on \$286K											
				0.00%	0.00%	0.00%	0.00%	15.44%	34.05%	46.05%	56.85%	65.25%	75.17%	88.24%	100.00%
				2014 Benchmarks											
				0.32%	1.34%	3.51%	6.25%	12.53%	20.00%	23.03%	29.22%	35.15%	42.12%		

11.0 List of Symbols, Abbreviations and Acronyms

[O ₂]	Concentration of Oxygen
AMS	Altitude Mountain Sickness
ANS	Autonomic Nervous System
COPD	Chronic Obstructive Pulmonary Disease
DSP	Digital Signal Processing
ECG	Electrocardiogram
EPO	Erythropoietin
FDA	Food and Drug Administration
FTP	File Transfer Protocol
HAMS	Hypoxia Monitoring, Alert and Mitigation System
HRV	Heart Rate Variability
ONR	Office of Naval Research
PaCO ₂	Alveolar Pressure of Carbon Dioxide
PaO ₂	Alveolar Pressure of Oxygen
RER	Respiratory Exchange Ratio
ROBD	Reduced Oxygen Breathing Device
SaO ₂	Arterial Oxygen Saturation Measured via CO-Oximeter
SpO ₂	Arterial Oxygen Saturation Measured via Pulse-Oximeter
TAILSS	Tactical Aircrew Integrated Life Support System
TUC	Time of Useful Consciousness
USN	United States Navy

12.0 Distribution List

ADDRESSEE	DODAAC CODE	NUMBER OF COPIES	
		UNCLASSIFIED/ UNLIMITED	UNCLASSIFIED/ LIMITED AND CLASSIFIED
Program Officer: : Christopher Steele ONR Code 342 E-Mail: christopher.steele4@navy.mil	N00014	1	1
Administrative Contracting Officer*	S2401A	1	1
Director, Naval Research Lab Attn: Code 5596 4555 Overlook Avenue, SW Washington, D.C. 20375-5320 E-mail: reports@library.nrl.navy.mil	N00173	1	1
Defense Technical Information Center 8725 John J. Kingman Road STE 0944 Ft. Belvoir, VA 22060-6218 E-mail: tr@dtic.mil	HJ4701	1	1